UNIVERSITY OF CALIFORNIA, MERCED

Wnt Antagonists Influence Cell Fate Decisions in Hematopoiesis

A dissertation submitted in partial satisfaction of the requirements for the degree of Doctor of Philosophy

in

Quantitative and Systems Biology

by

Corey Joseph Cain, B.S.

Committee in charge:

Dr. Michael D. Cleary, Chair
Dr. Marcos E. García-Ojeda
Dr. Maria G. Pallavicini
Dr. Jennifer O. Manilay

2012

DEDICATION

This dissertation is dedicated to my grandmothers Betty Ann Michael and Loraine Cain, who both encouraged me to press forward in life and to appreciate all that we have.

EPIGRAPH

The doubter is a true man of science; he doubts only himself and his interpretations, but he believes in science. ~Claude Bernard

TABLE OF CONENTS

LIST OF ABBREVIATIONS

AB – antibody
ALP – alkaline phosphatase
AML – acute myelocytic leukemia
APC – adenomatous polyposis coli
AXIN-1 – axis inhibition protein 1
BM – bone marrow
BMC – bone marrow cells
BMP– bone morphogenic protein
BMPR – bone morphogenic protein receptor
BSP – bone sialoprotein
CAR cell – CXCL12 abundant reticular cell
CCND1 – cyclin D1
CFU – colony forming units
CLP – common lymphoid progenitor
CMP – common myeloid progenitor
CRD – cysteine rich domain
DAG – diacylglycerol
DKK – dickkopf
DN – double negative
DSH – dishevelled
DP– double positive
ETP – early thymic progenitor
FACS – fluorescent activated cell sorting
FCM – flow cytometry
FCS – fetal calf serum
FL – fetal liver
FSC – forward scatter
GAPDH – glyceraldehyde 3-phosphate dehydrogenase
G-CSF – granulocyte colony stimulating factor
GMP – granulocytic monocytic progenitor
GSK3β – glycogen synthase kinase 3β
HSC – hematopoietic stem cell
HSPC – hematopoietic stem and progenitor cells
IL-6 – interleukin 6
IL-7 – interleukin 7
IP3 – inositol triphosphate
JNK – JUN N-terminal kinase
KB – kilobase
KO – knock out
LEF – lymphoid enhancer binding factor
LPS – lipopolysaccharide

LSK – lineage negative, Sca-1^{high}, c-Kit^{high} cell
LSK HSC – lineage negative, Sca-1^{high}, c-Kit^{high} hematopoietic stem cell
LT-HSC – long term hematopoietic stem cell
M-CSF – macrophage colony stimulating factor
MM – maintenance media
MIM – mineralization induction media
MMP-7 – matrix metalloprotease-7
MEP – megakaryocte erythrocyte progenitor
MPP – multipotent progenitor
MSC – mesenchymal stem cells
NK – natural killer cells
NFAT – nuclear factor of activated T cells
NFκB – nuclear factor kappa-B ligand
NTR – netrin like domains
OB – osteoblast
OC – osteoclast
OCY – osteocyte
OSX – osterix
PCP – planar cell polarity pathway
PCR – polymerase chain reaction
PI – phosphatidylinositol
PKC – protein kinase C
PLC – phospholipase C
qPCR – quantitative polymerase chain reaction
RANKL – receptor activator of nuclear factor kappa-B ligand
RT-PCR – reverse transcriptase polymerase chain reaction
RUNX – runt related transcription factor
RAD – radiation absorbed dose
ROR1/2 – receptor tyrosine kinase-like orphan receptor-1/2
Rpl-7 – ribosomal protein L7
SCF – stem cell factor
SCA – stem cell antigen
SD – standard deviation
SFRP – secreted frizzled related protein
SLAM – signaling lymphocyte activating molecule
SOST – sclerostin
ST-HSC – short term hematopoietic stem cell
SSC – side scatter
TCF – T cell factor
Tg – transgenic
VCAM – vascular cell adhesion molecule
WIF – Wnt inhibitory factor
Wnt – wingless and int
Wnt- Ca^{+2} – Wnt- calcium pathway
WT – wildtype

LIST OF FIGURES

LIST OF TABLES

ACKNOWLEDGEMENTS

I would like to thank my family, friends, and colleagues for all of their contributions to my dissertation and educational career. I am thankful for all of the positive influences I have had in my life and would be not been able to accomplish as much as I have without all of the connections I have made along the way. My parents, Koren Cain and Joseph Cain have never stopped believing in me, which allowed me to persist and complete this dissertation. As some may already know, my mother always thought I would become a doctor some day! My fiancé, Sarah Falls, is a continual source of inspiration and positive energy in my life and I am thankful for every day that I am able to spend with her.

I would especially like to thank Dr. Jennifer Manilay for her continued investment into this dissertation. Without her contributions, none of this work would have been possible. She is a wonderful mentor and friend. Every person that has worked with Dr. Manilay is truly better from the experience. She is a positive role model for all graduate students at UC Merced and I wish her the best of luck in her career, as I am sure it will be filled with success.

I have been fortunate to work with some very motivated and bright students here at UC Merced. Dean Santiago contributed to the MC3T3-E1 project and Randell Rueda dedicated much of his expertise to the Sclerostin project and I am thankful to both of them for the time and hard work that was invested into each project. I would also like to thank Dr. David Gravano and Mr. Bryce McLelland for helping me learn the techniques and experiments to answer the questions proposed in this dissertation, and also for the occasional thought provoking lecture that would stem from our conversations.

Additionally, I would like to thank the other members of the lab, Heather Thompson, Jesus Ciriza, Yvette Pellman for their support and guidance with this dissertation.

Other notable contributions to this dissertation are Roy Hoglund and the animal technicians Emily Werner and Megan Bevis, as well as the rest of the technicians in the UCM vivarium. Roy and the others continue to maintain an excellent mouse facility that helped us in our studies. I thank Dr. Andrea Mastro who provided us with the parental MC3T3-E1 cell line used in Chapter 2 as well as Dr. Gabriela Loots and Dr. Nicole Collette who both contributed significantly to Chapters 3 and 4 as well as provided the *Sost* knockout mice and *Lrp5* knockout mice. In addition, they were very helpful with my talk at ASBMR in Toronto and I thank them for their support. I would also like to thank my committee members, Dr. Mike Cleary, Dr. Marcos García-Ojeda and Dr. Maria Pallavicini for their guidance and advice on the projects that are presented in this dissertation.

VITA

2001-2004	Associate Degrees (2), Modesto Junior College, Modesto
2004-2007	Bachelor of Science, California State University, Stanislaus, Turlock
2007-2012	Graduate Student, Quantitative and Systems Biology Graduate Program, School of Natural Sciences, University of California, Merced
2007-2009	Teaching Assistant, School of Natural Sciences, University of California, Merced
2009-2012	Teaching Associate, School of Natural Sciences, University of California, Merced
2012	Doctor of Philosophy, University of California, Merced

PUBLICATIONS

Cain CJ**,** Conte DA, García-Ojeda, ME, Gómez Daglio L, Johnson J, Lau EH, Manilay JO**,** Phillips JB, Rogers NS, Stolberg SE, Swift HF, and Dawson MN (2008). What Systems Biology Is (Not, Yet). *Science* 320: 1013-1014

Cain CJ, Rueda R, McLelland B, Collette NM, Loots GG, Manilay JO (2012). Absence of sclerostin adversely affects B-cell survival. *J Bone Miner Res* 27: 1451-1461.

ABSTRACT OF THE DISSERTATION

Wnt Antagonists Influence Cell Fate Decisions in Hematopoiesis

by

Corey Joseph Cain

Doctor of Philosophy

University of California, Merced, 2012

Dr. Jennifer O. Manilay, Advisor

Dr. Michael D. Cleary, Chair

Dr. Marcos E. García-Ojeda

Dr. Maria G. Pallavicini

Sclerostin (SOST) and Secreted Frizzled Related Protein 2 (SFRP-2) are two Wnt antagonists that are important for maintaining bone homeostasis through different modes of regulation. Wnt signaling is an important regulator of hematopoietic stem cell and progenitor cells as well as lymphoid cells, but there are only a few studies that have investigated the influence of Wnt antagonists on hematopoiesis. In addition, Wnt signaling guides osteoblastic fate, in turn directing mineralization, which can also potentially influence hematopoiesis. Wnt antagonists are currently being targeted for treatments in osteoporosis, further demonstrating the importance of understanding how Wnt antagonists influence hematopoietic cell fate decisions. In this dissertation, I have shown that mineralization using *in vitro* mineralizing and non-mineralizing MC3T3-E1 osteoblast like cell lines display increased SFRP-2 expression, which correlated to a decrease in hematopoietic differentiation in mineralizing MC3T3-E1 co-cultures seeded with hematopoietic stem cells. We extended this study to an *in vivo* system using sclerostin knockout (*Sost*$^{-/-}$) mice that display overactive osteoblast and osteocytes populations. Sclerostin is secreted by osteocytes and mature osteoblasts transitioning to the osteocyte fate and blocks Wnt signaling by binding to Lrp4/5/6 receptors. Using *Sost*$^{-/-}$ mice, I observed decreased B cell survival in the bone marrow due to changes in the B cell microenvironment through alteration in CXCL12 and SCF. Interestingly, competitive and serial transplantation assays demonstrated that the absence of *Sost* resulted in increases in hematopoietic stem cell engraftment in the bone marrow. Taken together, our work demonstrates an underappreciated role of the Wnt antagonist Sclerostin, as well as the influence of osteoblast mineralization, on hematopoiesis.

Chapter 1: Wnt Antagonists and Hematopoiesis

1.1. Overview of Hematopoiesis:

The hierarchy of blood cell lineages that develop from hematopoietic stem cells (HSC) and their cell surface marker profiles in the mouse has been extensively reviewed [1], and is summarized in Figure 1.1. In the mouse, it is clear that critical relationships between hematopoietic cells in the bone marrow (BM) cavity and osteolineage cells, such as mesenchymal stem cells (MSCs), osteoblasts (OBs) and perhaps osteocytes (OCYs) exist. The generation of hematopoietic cells is tightly regulated by balancing the cell fate decisions of self-renewal, quiescence, differentiation and cell death through internal transcriptional programs and external cues from the environment that the stem cell resides [2]. Multiple BM stromal cell populations in the "stem cell niche," such as osteoblasts, perivascular CXCL12 abundant reticular (CAR) cells, endothelial cells, and nestin^{+} mesenchymal stem cells, support HSC self-renewal and other aspects of hematopoiesis [3,4,5,6,7,8,9]. For example, osteoblasts and BM stromal cells that remain close to the endosteum support B cell development by releasing interleukin-7 (IL-7), CXCL12 (SDF-1), and stem cell factor (SCF), all of which are required for B cell progenitors to mature into naïve B cells in the BM [6]. In addition, maturation of osteoclasts (OC, which are hematopoietic cells of the myeloid lineage) requires the secretion of the receptor activator of nuclear factor kappa-B ligand (RANKL) from OBs, highlighting the role of osteolineage cell to hematopoietic cell interactions in bone homeostasis [10]. Crosstalk between hematopoietic cells and the cells of the bone and bone marrow environment also requires Wnt signaling to facilitate proper development of hematopoietic stem and

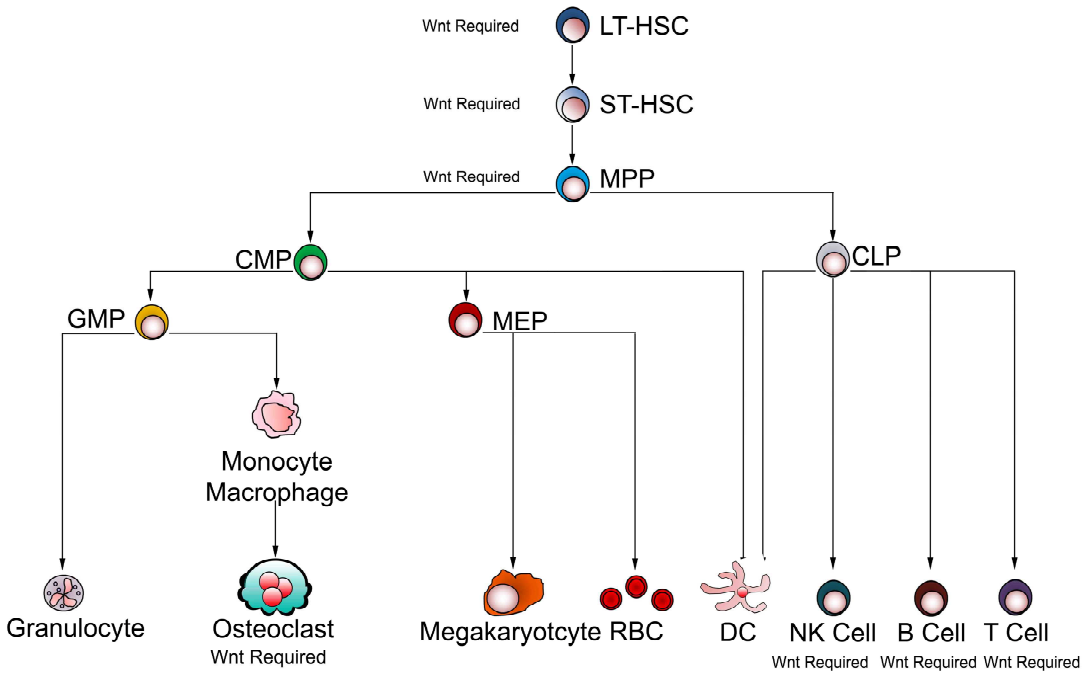

Figure 1.1: Wnt Requirements Along the Hematopoietic Lineage Hierarchy. A simplified schematic of the known hematopoietic cell hierarchy in the adult mouse is shown. The abbreviations for the distinct cell types and their identifying cell surface marker profile are listed as follows: LT-HSC (long-term hematopoietic stem cell) - Lineage (Lin)$^{-}$ c-Kit^{high} Sca-1^{high} FLK2^{-} CD34^{-} CD150^{+} CD41^{-} IL7Rα^{-}; ST-HSC (short term hematopoietic stem cell) - Lin^{-} c-Kit^{high} Sca-1^{high} FLK2^{-}CD34^{+} CD150^{+} CD41^{-} IL7Rα^{-}; MPP (multipotent progenitor) - Lin^{-} c-Kit^{high} Sca-1^{high} FLK2^{+} CD34^{+} CD150^{+} CD41^{-} IL7Rα^{-}; CMP (common myeloid progenitor) - Lin^{-} c-Kit^{high} Sca-1$^{lo/-}$ CD34^{+} IL7Rα^{-} CD16/32^{lo}; CLP (common lymphoid progenitor) - Lin^{-} c-Kit^{lo} Sca-1$^{lo/int}$ FLK2^{+} CD34^{+} IL7Rα^{+} CD16/32^{-} CD27^{+}; GMP (granulocytic/monocytic progenitor) - Lin^{-} c-Kit^{+} Sca-1^{-} CD34^{+} IL7Rα^{-} CD16/32^{hi}; MEP (myeloid/erythroid progenitor) - Lin^{-} c-Kit^{+} Sca-1^{-} CD34^{-} IL7Rα^{-} CD16/32^{-}. LT-HSC, ST-HSC, MPP, osteoclasts, B cells, T cells and NK cells rely on Wnt signaling during their development.

progenitor cells, as well as committed hematopoietic cells.

Once an HSC is removed from the "niche cell" in the bone marrow, differentiation into multipotent progenitors (MPPs) quickly occurs (Figure 1.1) [11]. MPPs are only capable of short bursts of proliferation and will differentiate into either common myeloid progenitors (CMPs) or common lymphoid progenitors (CLPs) (Figure 1.1) [1]. Differentiation into either the myeloid or lymphoid lineage occurs and the cell is irreversibly committed to that lineage. CMPs are also transit amplifying cells that will give rise to either the granulocyte macrophage progenitor (GMP) or a megakaryocyte erythroid progenitor (MEP) (Figure 1.1) [1]. The GMP produces innate immune cells such as granulocytes (eosinophils, basophils, neutrophils) along with monocytes and macrophages and myeloid derived dendritic cells. The MEP, on the other hand, produces red blood cells and megakaryocytes [1,11]. CLPs produce lymphoid derived dendritic cells, natural killer cells (NK cells), T cells and B cells of (Figure 1.1) [11].

HSC-enriched populations are commonly isolated from bone marrow suspensions by the depletion of committed hematopoietic lineages (i.e. positive cell surface expression of lineage-specific markers, such as CD3e, CD4, CD8, CD19, NK 1.1, CD11b, Gr-1, and Ter119, referred to as Lin^-) and then staining for c-Kit, Sca-1, often referred to as the LSK HSC population [1,11]. This population is still heterogeneous and further work has been performed to try to isolate and define the putative HSC from these enriched populations. Yang and colleagues used the LSK markers in addition with CD34 and FLK2 (Flt3) ligand to further delineate the LSK HSC population into long term (LT) HSCs and short term (ST) HSCs. LT HSCs lack the expression of CD34, and FLK2 while ST HSCs are transiently cycling and are positive for CD34 [12,13]. MPPs can also

be distinguished this way, having the LSK profile and positive expression of $CD34^{+}FLK2^{+}$. In a separate characterization study by Kiel and colleagues, the signaling lymphocyte activating molecule (SLAM) family proteins (specifically CD150) were used to enrich for long term hematopoietic populations [7]. Originally these markers consisted of CD150, CD48 and CD244, however, it was found that CD48 and CD41 (a megakaryocyte marker) better enriched for LT HSC populations [14]. Stringent isolation and characterization of LT HSCs is important to ensure that LT HSC populations are identical in each study. For murine LT HSC isolation, the most accepted definition uses Lin^{-} c-Kit^{high} Sca-1^{high} $FLK2^{-}$ $CD34^{-}$ $CD150^{+}$ $CD41^{-}$ IL7Rα^{-} (Figure 1) [15,16].

1.2. Canonical and non-canonical Wnt signaling:

Wnts are secreted glycoproteins that range in size from 350 to 400 amino acids [17]. Mutations in the *wingless* gene were first described in *Drosophila* [18,19]. It was later shown that the oncogene *Int* in *Drosophila* and *wingless* were orthologs and mapped to the same region as the *wingless* mutation [20]. The receptor for Wnt proteins remained unknown until the identification of Frizzled, a seven pass transmembrane G-coupled protein receptor [21]. Subsequently, disruption of *dishevelled* (DSH) definitively showed that Frizzled and Dishevelled proteins are regulated by Wnt proteins [22] (Figure 1.2A). At least 19 different Wnt molecules have been identified in humans and mice to date, as well as at least 10 Frizzled receptors. The diversity and complexity of the Wnt and Frizzled families makes the identification of Wnt-specific targets extremely challenging [23,24].

Activation of Frizzled receptors by the canonical Wnt signaling pathway triggers the release of β-catenin from the axis inhibition protein 1 (AXIN1), glycogen synthase kinase 3β (GSK3β), and adenomatous polyposis coli (APC) complex (Figure 1.2A). Migration of β-catenin to the nucleus results in its binding with the transcription factors T cell factor (TCF)/lymphoid enhancer binding factor (LEF), which together, activate an array of genes involved in proliferation and self renewal (e.g. c-Myc, n-Myc, Cyclin D1, Notch-1), tissue specific differentiation (e.g. CD44, matrix metalloprotease-7 (MMP-7)) or hematopoietic specification genes (e.g. runt related transcription factor-1 and -2 (RUNX1 and RUNX2), bone morphogenic protein 4 (BMP-4) and Jagged-1) [25,26,27]. Non-canonical Wnt signaling, in contrast to canonical Wnt signaling, is an alternative Wnt activation pathway that does not require β-catenin.

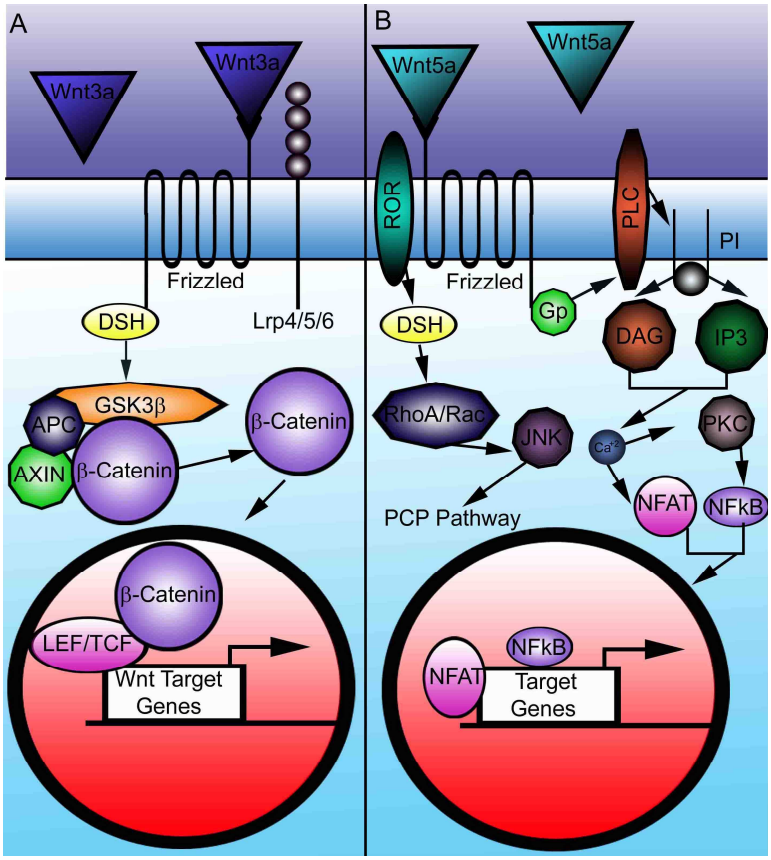

Figure 1.2: Canonical and Non-Canonical Wnt. (A) Canonical Wnt signaling utilizes Frizzled and Lrp4/5/6 receptors to transduce a signal to Dishevelled (DSH) protein. Dishevelled activation will signal the axis inhibition protein-1 (AXIN1), glycogen synthase kinase 3β (GSK3β), and adenomatous polyposis coli (APC) complex to release cytoplasmic β-catenin. Migration of β-catenin to the nucleus results in the activation of TCF and LEF-1 transcription factors and upregulation of Wnt target genes. (B) Non-canonical Wnt signaling pathways (which are β-catenin independent) have two pathways have been extensively described in hematopoiesis, the Planar Cell Polarity (PCP) Pathway and the Wnt-Ca^{+2} pathway. The PCP pathway (left) requires Wnt binding to Frizzled and/or the Receptor Tyrosine Kinase-like Orphan Receptor-1/2 (ROR1/2) binding. This involves the activation of DSH, RhoA/RAC family proteins culminating in the JUN N-terminal kinase (JNK) family proteins. The Wnt-Ca^{+2} (right) also requires Wnt and Frizzled binding but instead, G proteins are activated and go on to activate phospholipase C (PLC). Phospholipase C will hydrolyze a phosphotidyinositol (PI) to inositol triphosphate (IP3) resulting in the release of internal stores of Ca^{+2}. Diacyglycerol (DAG) is also released from PLC and will go on to activate Protein kinase C (PKC). Together with release of calcium, NFκB and NFAT will translocate to the nucleus and activate target gene expression of non-canonical Wnt target genes.

Non-canonical Wnt signaling was observed in studies that characterized Wnt signaling between Wnt5a and Frizzled in *Drosophila* [21,28]. Non-canonical Wnt signaling consists of at least 11 described pathways, but only a few have been extensively characterized in mice and humans [29,30,31]. The planar cell polarity (PCP) pathway and the Wnt-Ca^{+2} pathways are two non-canonical Wnt signaling pathways that are involved in hematopoiesis and are the best understood non-canonical Wnt pathways in mice and humans [29] (Figure 1.2B). Both of these pathways require Wnt/Frizzled binding for activation, and share some, but not all downstream targets [32]. The PCP pathway stimulates actin cytoskeletal rearrangement though the Receptor Tyrosine Kinase-like Orphan Receptor-1/2 (ROR1/2) and DSH proteins, which in turn upregulates Ras homolog gene family member A/ Ras related C3 Botulin Toxin (RhoA/RAC family) proteins resulting in the activation of JUN N-terminal kinase (JNK) family [29]. The Wnt-Ca^{+2} pathway utilizes G protein activation through the frizzled receptor, which will further signal the production of inositol triphosphate (IP3) and diacylglycerol (DAG). Phospholipase C (PLC) mediated degradation of phosphatidylinositol (PI) from the release of internal stores of Ca^{+2} will culminate in the activation the expression of Nuclear Factor of Activated T cells (NFAT) and Nuclear Factor kappa B (NFκB), that will then translocate to the nucleus for the upregulation of non-canonical Wnt target genes, which can also suppress canonical Wnt signaling [29,32].

1.3. Wnt Signaling in Hematopoietic Development:

Most studies on Wnt signaling in hematopoiesis have been performed in murine models. Wnt signaling facilitates cell fate decisions across all hematopoietic lineages, ranging from HSCs to myeloid cells (osteoclasts), and lymphoid lineages (NK, B, and T cells) [33]. The importance of Wnt signaling for HSC proliferation was first shown *in vitro* by the addition for soluble Wnt5a (a non-canonical Wnt) to HSC cultures [34,35]. Loss of Wnt5a signaling through the Ca^{+2} pathway resulted in the formation of B cell lymphomas, implying that non-canonical Wnt signaling normally down regulates proliferation in B cell precursors, in contrast to its activation of proliferation in HSCs [36]. In zebrafish (*Danio rerio*), Wnt signaling activates the BMP pathway, and in turn, the expression of *cdx-hox* pathway [37]. Recently, Wnt16, another non-canonical Wnt, was shown to be necessary for proper hematopoiesis in zebrafish, although the role of Wnt16 role in mammalian hematopoiesis is still unclear [38,39].

Canonical Wnt signaling is an important regulator of HSC homeostasis, lymphoid development and osteoclast maturation [33,40,41]. It is necessary for HSC self-renewal, as demonstrated through the injection of over expressing AXIN-1 HSCs into lethally irradiated mice [42]. Deletion of the Frizzled-9 receptor implicated Wnt signaling in the control of B cell development [43,44]. In support of this, *Lef-1*$^{-/-}$ mice display loss of B cell survival [45]. In addition, when Wnt signaling is excessively activated, Chronic lymphocytic leukemia can develop [43,44]. Surprisingly, conditional deletion of β-catenin (using Mx-Cre mice crossed with β-catenin$^{lox/lox}$ mice) did not alter the frequency of hematopoietic stem and progenitor cells or any other bone marrow derived hematopoietic cells. There was also no difference in committed T cell proliferation or

survival, although it should be noted that the functional redundancy of β-catenin with α- and γ-catenin is not well understood in hematopoietic cells [46,47].

Developing T cells are also reliant on Wnt signaling for normal development, as demonstrated by the blocks observed in the early transition of the $CD4^-$ $CD8^-$ (double negative, DN) thymocyte stage to the $CD4^+$ $CD8^+$ (double positive, DP) stage in knockout mice in which Wnt signaling pathway genes were targeted [41]. For example, conditional β-catenin knockouts display a pronounced block between the DN3 ($CD4^-$ $CD8^-$ $CD44^-$ $CD25^+$) to DN4 ($CD4^-$ $CD8^-$ $CD44^-$ $CD25^-$) stages [48], and *Tcf-1*$^{-/-}$ mice have an earlier thymocyte developmental defect, starting at the early thymic progenitor (ETP) or DN1a/DN1b stage of thymic development [33,48,49,50]. Germar and colleagues further demonstrated that TCF-1 was revealed to be a downstream target of Notch signaling (which is absolutely required for canonical T cell development), linking Wnt and Notch pathways in development of the T cell lineage [50]. No T cell developmental abnormalities were observed in *Lef-1*$^{-/-}$ mice [33,49], but *Lef-1* and *Tcf-1* double-deficient mice revealed a complete block at the Intermediate single positive stage of thymocyte development [51]. Natural killer (NK) cells, which also belong to the lymphoid lineage, require Wnt signaling. Specifically, the NK receptor Ly49A promoter contains a binding site for TCF-1, and *Tcf-1*$^{-/-}$ mice have a 2 fold reduction in the Ly49A subset of NK cells, although the NK cells that are present are still mature and functional [40]. Osteoclasts, which are cells of the myeloid lineage, are also sensitive to Wnt signaling. Secreted Frizzled related protein-1 (SFRP-1) was shown to reduce osteoclast development by binding to RANKL, presumably to prevent binding to the receptor [35]. Interestingly, Wnt signaling down regulation is required for the development of the

myeloid lineage and the dysregulation of Wnt signaling often results in myeloid-based leukemia [33,52,53].

1.4. Regulation of hematopoiesis by Wnt antagonists

Wnt signaling is tightly modulated by a multitude of soluble Wnt antagonists that vary in both function and structure. Some Wnt antagonists, such as Wnt inhibitory factor-1 (WIF-1) and SFRPs, bind to Wnt ligands directly and inhibit canonical Wnt signaling by preventing their interaction with Frizzled receptors[54] (Figure 1.3A). Other Wnt antagonists, such as Dickkopf (DKK) family proteins and Sclerostin (SOST), bind to Wnt co-receptors Lrp4, Lrp5 and Lrp6 and down regulate Wnt signaling [55] (Figure 1.3B). Below, we review the documented roles of SFRP and Sost Wnt antagonists on hematopoiesis (Table 1.1, and Figures 1.2 and 1.3).

Table 1: Wnt Antagonist Mouse Models that Display Altered Hematopoiesis

	Model	Is the Wnt antagonist expressed by hematopoietic cells?	Effect on HSC/HSPC numbers	Defect in HSC quiescence?	Alterations to Peripheral Blood Cells?	Alterations to Lymphoid Populations Defect?	Alterations to Bone Structure?	Non-Cell Autonomous Effect on Hematopoiesis?	Reference
Loss-of-function	*Sfrp-1*$^{-/-}$	No	None	Yes	Yes, increased B220+ B cells	Yes, B and T cell Defects	Yes	Yes	[56,57]
	Sfrp-2$^{-/-}$	unknown	unknown	unknown	unknown	unknown	unknown	unknown	[57]
	Sost$^{-/-}$	No	None	unknown	No	Yes, reduced B cells	Yes	Yes	[58]
Gain-of-function	*SFRP1 treatment in vitro*	No	decrease	unknown	n/a	n/a	n/a	Yes	[57,59]
	SFRP2 treatment in vitro	unknown	increase	unknown	n/a	n/a	Yes	Yes	[57,60]
	Wif-1 Tg	No	Increase[2]	yes	No	No	No	Yes	[61]
	Dkk-1 Tg	Yes	None	yes	No	No	Yes	Yes	[62]

1.4A. Secreted Frizzled Related Proteins

SFRPs bind to Wnt ligands directly via a cysteine rich domain (CRD) that is homologous to that of Frizzled transmembrane receptors [63] (Figure 1.3A). SFRPs can block both canonical and non-canonical Wnt signaling pathways [54] (Figure 2C). Currently, only five SFRPs have been identified. SFRP-1, SFRP-2 and SFRP-5 contain similar netrin like domains (NTR), which are distinct from the NTR domains in SFRP-3 and SFRP-4 [63]. The NTR is thought to bind Wnt proteins, although conclusive studies in mammalian models are lacking [64]. All SFRPs proteins contain a CRD that is used for binding both Wnt and Frizzled proteins [63]. To date, only SFRP 1 and SFRP 2 have been shown to influence hematopoiesis, which we will review below [56,57].

SFRP-1 is expressed by bone marrow stromal cells, and *Sfrp-1*$^{-/-}$ mice display increased trabecular bone formation due to reduced apoptosis in osteoblast and osteocyte populations [65]. As the osteoblast has been identified as a HSC niche cell, one might expect that HSCs would be increased in *Sfrp-1*$^{-/-}$ mice. In agreement with this, long-term (LT) HSCs (as defined by Lineage^{-} Sca1^{high} c-kit^{high} (LSK) CD34^{-} Flk2^{-}) were significantly increased, and cell cycle analysis showed that higher numbers of (LSK) HSCs and multipotent progenitors (MPP) were not actively cycling in *Sfrp-1*$^{-/-}$ mice compared to wild-type controls, demonstrating a more quiescent cell phenotype, which is typical of stem cells when they are in contact with their niche. Interestingly, the non-cell-autonomous effects of the *Sfrp-1* deficiency on HSCs were only revealed by serial bone marrow transplantation assays, which demonstrated that the maintenance of self

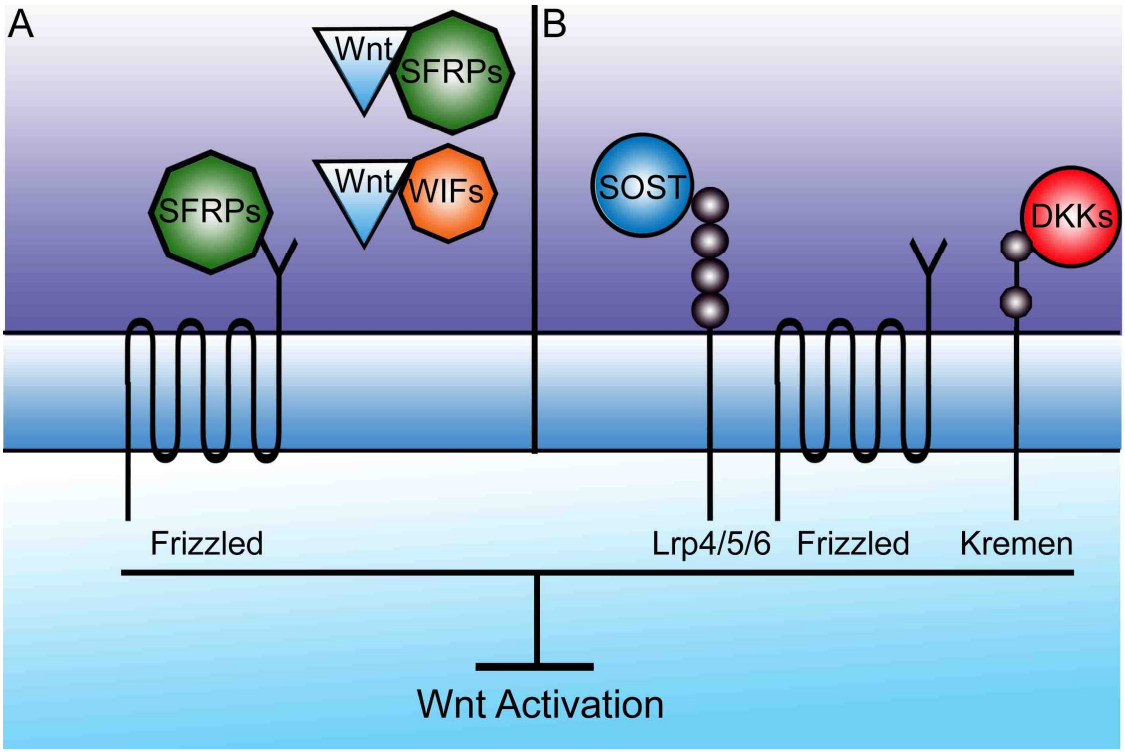

Figure 1.3: Wnt Antagonists in the Bone Marrow. (A) Wnt antagonists use a variety of mechanisms to block Wnt signaling transduction. SFRPs can bind both Wnt and Frizzled receptors to halt the Wnt activation whereas WIF-1 can only bind to Wnt proteins directly. (B) Dickkopf (DKKs) and Sclerostin (SOST) bind to Lrp family members that are Frizzled co-receptors. DKKs require another co-receptor, Kremen, to fully block Wnt signaling. It is not known if SOST requires a similar co-receptor.

renewing HSCs was negatively affected in the *Sfrp1*$^{-/-}$ bone microenvironment.

SFRP-1 can inhibit Wnt1, Wnt2, Wnt3a and Wnt7b-mediated signaling *in vitro* [63]. Exogenous SFRP-1 decreased hematopoietic forming colonies *in vitro*, and treatment of hematopoietic progenitors with SFRP-1 before transplantation resulted in decreased HSC engraftment efficiency [57], paradoxically similar to the HSC phenotype observed in the Sfrp1-deficient mice. In addition to the HSC phenotype, *Sfrp-1*$^{-/-}$ mice displayed increased numbers of white blood cells in the peripheral blood and a significant increase in B220^{+} B cells in the spleen, thymus, and bone marrow. Contrary to the known role of SFRP-1 as an antagonist of canonical Wnt signaling, *Sfrp-1*$^{-/-}$ mice displayed reduced β-catenin activation, but LSK HSCs contained higher levels of nuclear β-catenin indicating increased Wnt activation [56,63]. It has been suggested that the upregulation of non-canonical Wnt targets in the absence of SFRP-1 may be responsible for the diminished β-catenin stabilization observed in *Sfrp-1*$^{-/-}$ mice. For example, in *Sfrp-1*$^{-/-}$ mice, *Pparg*, a non-canonical Wnt target gene that can suppress β-catenin, is upregulated in MPPs [30,66,67].

SFRP-1 is estrogen-inducible and expressed by bone marrow stromal cells [59]. Both the injection of estrogen and natural pregnancy elevated the levels of SFRP-1, which resulted in reduced lymphoid cell production without influencing myeloid cell fate *in vivo*. Moreover, the exogenous addition of SFRP-1 reduced early B cell development *in vitro*. These studies demonstrate that SFRP-1 is an important mediator of early hematopoietic cell fate decisions, particularly those of LT-HSCs and early B cell precursors [57].

SFRP-1 and SFRP-2 and can stimulate CD34$^-$LSK HSC proliferation in a similar fashion, however, SFRP-2 appears to increase quiescence and engraftment of HSCs [57]. LT-HSCs treated with SFRP-2 also showed a subsequent increase in HSC engraftment in serial transplantation assays. *Sfrp-2*$^{-/-}$ mice are not embryonic lethal and are reproductively viable, but the analysis of HSC numbers and cell dynamics in these mice have not been reported [68,69].

It has been shown that SFRP-1 and SFRP-2 have redundant functions in embryonic development, but this redundancy does not appear to exist for adult hematopoiesis [68,69]. Given the observations that SFRP-1 and SFRP-2 mediate opposite effects on HSCs *in vitro*, it is possible that these two proteins also maintain distinctly different functions on hematopoiesis *in vivo*. It has been hypothesized that as osteoblasts mature and progress to the terminally differentiated osteocyte fate, that the expression of genes involved in hematopoietic support decreases [70]. SFRP-2 secretion from osteoblasts increases as a consequence of mineralization, in conjunction with the secretion of other Wnt antagonists (such as DKK-1 and Sclerostin, reviewed in later sections) [71]. The secretion of SFRPs in turn, could influence hematopoietic cell fate in the area where mature osteoblasts reside at the endosteum. In line with this, our laboratory has co-cultured HSCs with mineralizing osteoblasts, and observed a decrease in hematopoietic differentiation compared to co-cultures with non-mineralizing osteoblasts (described in detail in Chapter 2). SFRP-2 is upregulated in these cultures, although it does not seem to be the indicative factor for the hematopoietic reduction observed in our studies. Taken together, the SFRPs produced by bone marrow stromal cells, including osteoblasts, definitely can influence the behavior of their neighboring

hematopoietic cells in somewhat perplexing manners. A better understanding of how SFRPs control of canonical versus non-canonical Wnt signaling in HSC will help elucidate the molecular mechanisms that underlie their distinct effects on HSC cell fate decisions.

1.4B. Sclerostin

Sclerostin (*SOST*) is related to the differential screening-selected gene aberrant in neuroblastoma (DAN) family of BMP protein antagonists [72] (Figure 1.3B). SOST is a secreted protein that is encoded by the *Sost* gene, and is mainly restricted to mature osteocytes in its expression [72]. Initial studies described SOST's role in the regulation of bone development as a BMP antagonist, but later, it was shown that SOST was a more potent antagonist for Wnt signaling [73]. SOST is upregulated by BMP signaling, and may help in controlling osteoblast proliferation and differentiation through downregulation of Wnt signaling in these cells [74]. SOST binds directly to the Lrp4/5/6 co-receptor, effectively halting osteoblast differentiation into osteocytes [55,72,73]. There still exists some controversy as to whether or not SOST requires a co-receptor, (similar to DKK-1 co-receptor Kremen), although no such co-receptor has been identified [75]. *Sost* expression can be dampened by parathyroid hormone, a hormone that influences osteoblast growth and development, and stimulates genes involved in preserving HSC self-renewal [4].

The best known function of the *Sost* gene is to negatively reduce bone mass. In murine models, overexpression of the *Sost* gene results in marked defects in bone development and an osteoporotic phenotype [76,77]. Conversely, in $Sost^{-/-}$ mice, osteoblasts and osteocytes are increased seven-fold, resulting in osteopetrosis [78,79]. In humans, a 52 Kb deletion in the *Sost* enhancer region results in Van Buchem's disease, which presents with debilitating bone hardening [77]. Our laboratory has characterized the hematopoietic phenotype in $Sost^{-/-}$ mice and has observed that $Sost^{-/-}$ mice contain bones with severely reduced bone marrow cavities that contain hematopoietic

abnormalities [58] (described in detail in Chapter 3). Hematopoiesis and immune function in Van Buchem's patients has not been characterized, so it is still unclear whether the mouse *Sost*$^{-/-}$ phenotype is translatable to humans.

Previous descriptions of osteopetrotic mouse models have reported transient increases in HSCs [80]. In the *Sost*$^{-/-}$ mouse, LSK HSCs are largely unchanged, although further dissection of this population into LT-HSC versus ST-HSCs might reveal differences. The results of competitive co-transplantation of WT and *Sost*$^{-/-}$ bone marrow into WT recipients, serial transplantation assays, and HSC differentiation assays are presented in detail in Chapter 4.

1.5. Objective of study and hypothesis tested:

One of the most difficult questions to address in hematopoietic stem cell biology is the contribution of the microenvironment to hematopoietic cell fate decisions. Both Wnt signaling and Wnt antagonists have been shown to play a role hematopoiesis, however the direct contribution on Wnt signaling and mineralization is only beginning to be elucidated. In this dissertation, I aimed to study the role of Wnt signaling and mineralization by completing the following objectives:

1) Analyze the role of mineralization on hematopoiesis. I hypothesized that mineralization would reduce hematopoiesis *in vitro*. To test this hypothesis, I co-cultured MC3T3-E1 cells together with LSK HSCs under mineralizing or non-mineralizing conditions to determine what factors influence hematopoiesis. These results are discussed in Chapter 2.

2) Determine how the absence of Sclerostin alters B cell development. I hypothesized that the absence of sclerostin would influence B cell survival. I tested this hypothesis in *Sost*$^{-/-}$ mice by analyzing the B cell populations that are present in the bone marrow. These results are discussed in Chapter 3.

3) Determine if the absence of Sclerostin influences hematopoietic stem cell function in vivo. I tested this by using *Sost*$^{-/-}$ mice and distinct transplantation assays to see if there was a definitive connection between sclerostin and hematopoietic stem cell function. These results are discussed in Chapter 4.

Chapter 2: Mineralization and Differentiation of Osteoblast Cells Decreases Hematopoietic Support *In vitro*

2.1 Introduction:

In mammals, hematopoiesis is supported and maintained by a heterogeneous population of bone marrow (BM) stromal cell populations that control hematopoietic stem cell (HSC) fate decisions [81]. Among these BM stromal cells, the osteoblast (OB) has been primarily indicated as supporting both HSC self-renewal and differentiation [4,5,82,83]. OBs differentiate from MSCs and progress through several stages of differentiation until terminal differentiation into an osteocyte (OCY). Commitment to the osteoblast lineage requires the expression of the transcription factor Runx2, effectively diminishing the MSC capacities to form both the adipocyte and chondrocyte lineages [84]. Runx2 expression also confers commitment to the pre-osteoblast stage of development and signals the upregulation of mineralization genes such as osteopontin, osteocalcin and bone sialoprotein [84,85]. Non-mineralized OBs (also known as bone lining cells) are located along endosteal regions of the bone cavity of the long bones, subject to modifications by various cells and factors present in the bone marrow and are mostly quiescent [86,87]. As pre-osteoblasts mature, they upregulate Osterix and express genes involved in mineralization and bone matrix formation. The differentiation of a pre-osteoblast to a mature OBs happens at the endosteum, the interface of the bone and the bone marrow [84].

In addition to terminally differentiating into osteocytes and establishing bone matrix, OBs have been shown to express factors involved in myeloid differentiation such as Granulocyte colony-stimulating factor (G-CSF) and Macrophage colony-stimulating

factor (M-CSF) [82,83,88]. Distinct OB cell lines have been shown to express interleukin-7 (IL-7), c-Kit, and stem cell factor (SCF), all of which are factors involved in B cell maturation and differentiation, demonstrating the capacity of OBs to support both myeloid and lymphoid differentiation [89,90,91]. Zhang and colleagues utilized BMPR1a conditional knockout mice to analyze endosteal niche dynamics and observed that an increase in OB populations correlated with increased numbers of HSCs in the BM [5]. Similarly, Calvi *et al*. observed an increase in OBs in mice that express constitutively active parathyroid hormone-related receptor (Pthrp), as well as an increase in HSCs in the BM [4]. The same group recently observed that murine osteocytes that constitutively express the parathyroid receptor Pthrp also have a corresponding increase in HSCs [92]. Further confirming the role of osteoblasts in supporting HSC self renewal and differentiation, conditional ablation of OBs resulted in a marked decrease of HSCs from the BM and induction of extramedullary hematopoiesis [93]. Embryonically-derived OB progenitors can support the development of ectopic hematopoietic stem cell niches, further supporting the role of osteoblasts in maintaining hematopoietic stem cell populations [94]. Taken together, these data support the role of the OB in hematopoietic stem cell self renewal and differentiation.

OB development and maturation is tightly regulated by Wnt signaling. Runx2 contains binding sites for Wnt activated Lef-1 along with a number of other proliferation induced genes [95]. In addition, Wnt3a and Wnt10b have been shown to be important for early osteoblast development and pre-osteoblast survival [96]. OBs themselves can serve as a source of Wnt signaling in the bone marrow, regulating proliferation of osteoblasts that have been exposed to mature hematopoietically derived osteoclasts [97]. Wnt

activation can upregulate other mineralization genes such as osteocalcin and alkaline phosphatase [97]. Mice that lack Lrp5, the Frizzled co-receptor, have severe osteoporosis, while mice that have Sclerostin deleted have high bone mass phenotypes, further implicating the role of Wnt signaling in OB development and mineralization [98,99].

Wnt signaling also plays a primary role in hematopoietic development, in the regulation of self renewal of hematopoietic stem cells and control of cell fate decisions of committed progeny [41]. B cells also rely on Wnt signaling, as Frizzled 9 knock-out mice lack mature B cell populations and Lef-1 knockout mice display reductions in Pro-B cells [44,45]. Myeloid progenitor proliferation is reliant on canonical Wnt signaling and the dysregulation of Wnt signaling can result in the development of Acute Myeloid Leukemia (AML) [53,100]. It has also been established that osteoblasts that are exposed to Wnt signals can better facilitate osteoclast differentiation, demonstrating the importance of Wnt signaling in bone homeostasis [101]. Wnt signaling can also modulate blood cell adhesion through VCAM-1 and CXCL12 that is secreted from stromal cell populations, further supporting hematopoietic development [102,103].

Wnt antagonists are important for regulating Wnt signals during hematopoiesis, by preventing Wnt binding to its receptors or by affecting Wnt co-receptors. DKK-1 transgenic mice show subtle hematopoietic phenotypes [62]. SFRP-1 knock-out mice have reduced LT HSC, while SFRP-2 promotes hematopoiesis *in vitro* [57,62]. Sclerostin alters B cell development in a non cell autonomous manner [58]. In another study that examined Wnt Inhibitory Factor 1 (WIF-1) expression, there was an overt depletion of

quiescent hematopoietic stem cells [61]. Together, these studies indicate an important role of Wnt antagonists in hematopoiesis.

In this study, we utilized the osteoblast-like cell line, MC3T3-E1 to address the question of how mineralization influences hematopoietic cell fate decisions. Under inducing conditions, MC3T3-E1 can be differentiated into mineralizing OBs [104,105]. We confirmed similarities in gene expression between MC3T3-E1 cells and primary OBs. We then co-cultured sorted HSCs with MC3T3-E1 cells under mineralizing and non-mineralizing conditions and investigated how Wnt signaling pathway genes changed upon mineralization of MC3T3-E1 cells. In particular, we identified SFRP-2 as differentially expressed in the mineralizing MC3T3-E1 subclone 4 and tested its role on HSC differentiation *in vitro.*

2.2 Methods:

Cell Culture. MC3T3-E1 "bulk" cells were a generous gift from Professor Andrea Mastro (Pennsylvania State University, State College, PA). MC3T3-E1 Subclone 4 (mineralizing), and MC3T3-E1 Subclone 24 (non-mineralizing) [106] were purchased from ATCC (Manassas, VA). MC3T3-E1 cells were grown in "maintenance media (MM)" consisting of αMEM (Invitrogen, Carlsbad, CA) supplemented with 10% FCS (Atlanta Biologicals, Lawrenceville, GA) and 1X penicillin/streptomycin (Invitrogen). For induction of mineralization, basal media was replaced with "mineralization induction media (MIM)" consisting of αMEM supplemented with 10% FCS 1X Penicillin/ Streptomycin (Invitrogen), 10 mM ascorbic acid (Fisher Scientific, Atlanta, GA) and 10 mM glycerol-2-phosphate (Sigma, St. Louis, MO). The OP9 cell line was purchased from ATCC and was maintained in αMEM supplemented with 20% FCS and 1x Penicillin/ Streptomycin, as described [107,108].

Mice. C57BL/6J (B6) mice were purchased from The Jackson Laboratory (Bar Harbor, ME) and housed in sterile microisolator cages with autoclaved feed and drinking water. Mice were used between 4 to 12 weeks of age and were all sex matched. Mice were euthanized by CO_2 asphyxiation followed by cervical dislocation before dissection. All animal procedures were approved by the UC Merced Institutional Animal Care and Usage Committee (IACUC).

Von Kossa Staining. Von Kossa staining was modified and performed as described [109]. Briefly, MC3T3-E1-Bulk and MC3T3-E1 subclones 4 and 24 were grown to confluency in 60 mm^2 tissue culture dishes in MM as described above. At day 0, the media was replaced with MIM, and cultures maintained for 10 or 20 days. At each

time point, the media was aspirated and cells were fixed in 4% paraformaldehyde diluted in Phosphate Buffered Saline (PBS). Cells were then treated with 1% silver nitrate (Fisher Scientific) and sodium thiosulfulate (Fisher Scientific) to remove nonspecific mineralization and counterstained with Nuclear Fast Red stain (Fisher Scientific). Cultures were photographed at 100X magnification on a BX51 microscope and DP70 digital camera (Olympus, Central Valley, PA) using ImagePro Plus 5.1 software (Silverspring, MD).

RNA extraction, cDNA synthesis and RT-PCR. MC3T3-E1 cell lines and OP9 cells were cultured to confluency and then cells were treated with 0.25% Trypsin-EDTA (Invitrogen) then placed in Trizol (Invitrogen) for RNA extraction. For bone preparations, whole bones were isolated by flushing the marrow then putting the remaining empty bone in Trizol. mRNA was isolated via phenol-chloroform extraction (Fisher Scientific) and cDNA was synthesized using the Superscript III kit (Invitrogen) with oligo-dT as the primer for the reaction, as described [108]. Conventional reverse transcriptase PCR (RT-PCR) was performed using gene-specific primers with the following thermocycler conditions: 90°C for 5 minutes (min), then 35-40 cycles of 95°C for 1 min, 55-60°C for 30 seconds and 72°C for 1 min, followed by a 5 min 72°C extension. PCR products were visualized by electrophoresis on a 1.5% agarose gel in 1x Tris base, Acetic acid and EDTA (TBA) buffer.

Quantitative real time PCR (qPCR). RNA extraction and cDNA synthesis were performed as described above. qPCR was performed using SYBR Green PCR Master Mix (Applied Biosystems, Foster City, CA). All primer efficiencies were validated by using serial dilutions and standard slope method of quantification using gene specific

PCR primers) [108]. Mouse Wnt Signaling Pathway PCR arrays were purchased from SA Biosciences (Frederick, MD). When using the arrays, cDNA was synthesized using the RT^2 First Strand Kit, and qPCR was performed using RT^2 SYBR Green/ROX qPCR Master Mix. All qPCR was run on the Applied Biosystems 7300 Real-Time System and the double delta C_t method was used to compare gene expression between samples.

Antibodies. Purified anti-CD16/32 (clone 93), biotinylated anti-CD8 (clone 53-6.7), anti-c-Kit-eFluor-780 (ACK2), IL7Rα-PECy7 (A7R34), were all purchased from eBioscience (San Diego, CA). Biotinylated anti-CD3ε (clone 145-2C11), biotinylated anti-CD4 (clone GK1.5), biotinylated anti-CD19 (clone 6D5), biotinylated anti-CD11b (clone M1/70), biotinylated NK1.1 (clone PK136), biotinylated Gr-1 (clone RB6-8C5), biotinylated Ter119 (clone Ter119), and anti-Sca-1-APC (clone E13-161.7), anti-CD45.2 APC-Cy7 (clone 104), anti-CD105-PE (clone MJ7/18), anti-VCAM-1-FITC (clone 429 (MVCAM.A)) were all purchased from Biolegend (San Diego, CA). Antibody titrations were performed to determine the for optimal antibody dilution to use for flow cytometry (FCM).

FCM analysis and cell sorting. To isolate HSCs, BM cells were sterilely obtained by flushing the marrow from the hind limbs of six C57BL/6 mice with Medium 199 (Invitrogen) media contained 2% FCS [108,110]. Cells were then passed through a 70-micron mesh and red blood cells were lysed with ACK lysis buffer. BM cells were then incubated with anti-CD16/32 to block Fc receptors γII/III, and then stained with biotinylated antibodies specific for CD3ε, CD4, CD8, CD19, CD11b, NK1.1, Gr-1, and Ter119 (to identify "lineage (Lin) positive" cells) for 30 minutes at 4^oC, and washed in MACS buffer containing 1X PBS, 2 mM EDTA and 0.5% BSA. Cells were then stained

with 20 μl of streptavidin (SA)-conjugated magnetic beads (Miltenyi Biotec, Auburn, CA) per 10^7 cells for 15 minutes, and washed. Magnetic-activated cell sorting (MACS) was then performed to deplete Lineage-positive ($Lin^{+)}$ cells using the DepleteS program on the AutoMACS (Miltenyi Biotec). Lineage negative (Lin^-) cells were then stained with antibodies for c-kit (CD117), IL7Rα (CD127) and Sca-1, as well as SA-Pacific Blue and DAPI. HSCs were purified on the FACS Aria IIu or FACS Aria III flow cytometric sorters (BD Biosciences, San Jose, CA) by gating on Lin^- $DAPI^-$ $CD117^{high}$ $Sca1^{high}$ $CD127^-$ cells.

MC3T3-E1 bulk cells were harvested from MM and stained with anti-CD16/32, anti-CD45.2, anti-Ter119, anti-CD105, and anti-VCAM-1. Identification of specific hematopoietic lineages after MC3T3-E1/HSC co-cultures was performed by staining with anti-CD16/32, anti-CD45, anti-CD19, anti-Gr-1, anti-CD11b, anti-Ter119 and anti-CD3e. All FCM analysis was performed on the BD FACS Aria IIu, FACS Aria III, or BD LSR II (BD Biosciences, San Jose, CA) and analyzed with Flowjo software version 7.6.1 (Treestar, Ashland, Oregon, USA).

HSC co-culture conditions. For co-cultures with non-mineralized cells, sorted HSCs were cultured on monolayers of MC3T3-E1 bulk, MC3T3-E1 Subclone 4, MC3T3-E1 Subclone 24, or OP9 cells for two weeks in αMEM, 20% FCS, 1x Pen/Strep, 5 ng/ml Flt3 ligand and 5 ng/ml interleukin-7 (both from Peprotech, Rocky Hill, NJ). For co-cultures with mineralized cells, MC3T3-E1 differentiation was induced by first culturing cells in MIM for 10 days, as described above. After these 10 days, sorted HSCs were added to the mineralized cells, and cultured for an additional two weeks in MIM

containing 5 ng/ml Flt-3 ligand, and 5 ng/ml interleukin-7. Two weeks were allowed for HSC differentiation in both MM and MIM conditions.

For co-cultures with SFRP-2, we added 10, 20 or 100 ng/ml of recombinant SFRP-2 (RD Biosystems, Minneapolis, MN) to the non-mineralized MC3T3-E1 bulk cells seeded with HSCs. After two weeks, cells were harvested by gently disrupting the monolayer with a pipette and running them through a 70-micron mesh, and then analyzed for the presence of committed hematopoietic lineages by FCM as described above.

Statistical Analysis. Differences between the means of biological replicates for all samples were calculated using two-tailed T-test (GraphPad Prism, La Jolla, CA, USA). The two tailed T-test was justified by the assumption that all samples follow a Gaussian distribution even though sample sizes are small, and are not paired samples. All samples were considered statistically significant if $*p<0.05$, $**p<0.01$, and $***p<0.001$.

2.3 Results:

Characterization of hematopoietic gene expression in MC3T3-E1 mineralizing and non-mineralizing cell lines

MC3T3-E1 cells were originally derived from neonatal calvaria and have been used to study the dynamics of osteoblastic and hematopoietic development [82,104]. Wang and colleagues isolated specific subclones of MC3T3-E1 cells by their capacity to mineralize *in vitro* and *in vivo* [106]. Of these cell lines, we used MC3T3-E1 subclone 4 (mineralizing) and subclone 24 (non-mineralizing) in addition to the parental MC3T3-E1 cell line (herein referred to as "MC3T3-E1 bulk") [104,106]. Although osteoblasts have been shown to support hematopoietic stem cell self renewal, investigation into whether or not MC3T3-E1 cells could provide an *in vitro* support model for HSC self renewal has not yet been performed [10]. Additionally, the effect of mineralization on hematopoietic co-cultures has yet to be assessed and how osteoblast mineralization influences hematopoiesis is still widely debated [70].

In order to see if MC3T3-E1 cells could support hematopoietic co-cultures, we examined the expression of factors involved in hematopoietic stem cell self renewal and hematopoietic differentiation. Using RT-PCR, we confirmed the expression of *osteopontin*, *N-Cadherin*, stem cell factor (*Scf*), *CXCL12* (*Sdf-1*) and Bone Morphogenic Protein Receptor 1a (*Bmpr1a*) in all MC3T3-E1 bulk, Subclone 4 and Subclone 24 cells grown under MM (Figure 2.1A and Figure 2.2). *Osterix* and *Runx2* were also expressed in MC3T3-E1 cells, indicating that the osteoblast populations within the cultures were heterogeneous (Figure 2.1A and 2.2) [81,111]. MC3T3-E1 cells also expressed genes involved in hematopoietic differentiation such as *Jagged-1*, *Interleukin-6* (*IL-6*),

Macrophage colony-stimulating factor (*M-csf*), and *Vascular Adhesion Marker 1* (*Vcam-1*) (Figure 2.2) [112,113,114]. The expression of genes involved in hematopoietic stem cell self renewal and differentiation indicated that MC3T3-E1 cells could possibly support hematopoietic stem cell self renewal and differentiation together *in vitro*.

We next characterized osteoblast-enriched populations within MC3T3-E1 cells, using FCM and previously described cell marker profiles [115]. MC3T3-E1 bulk cells expressed VCAM-1 but did not express the hematopoietic markers CD45, Gr-1, CD11b, Ter119 or CD19 (Figure 2.1B). In addition, CD105, a marker for mesenchymal stem cells, was not expressed by MC3T3-E1 cell lines (Figure 2.1B) [116]. Taken together, these data demonstrated that MC3T3-E1 cells express a similar cell surface profile to that of osteoblastic enriched populations that are freshly isolated from bone.

Kinetics of mineralization in MC3T3-E1 subclones

As osteoblasts mature, the upregulation of genes involved in the production of mineralizing matrix proteins increases. We used Von Kossa staining to examine the kinetics of MC3T3-E1 cell mineralization over a 20 day period. Under mineralizing conditions, MC3T3-E1 Subclone 4 cultures showed pronounced dark areas (indicating active mineralization) by Day 20, whereas markedly less mineralization was observed in Subclone 24 and MC3T3-E1 bulk cultures at the same time point. This indicated that the MC3T3-E1 bulk cells behaved more like the non-mineralizing subclone 24 (Figure 2.1C and Figure 2.2) [106]. The difference in mineralization kinetics was also confirmed by qPCR for *osteocalcin* and bone sialoprotein (*Bsp*) (Figure 2.1D-E). Both MC3T3-

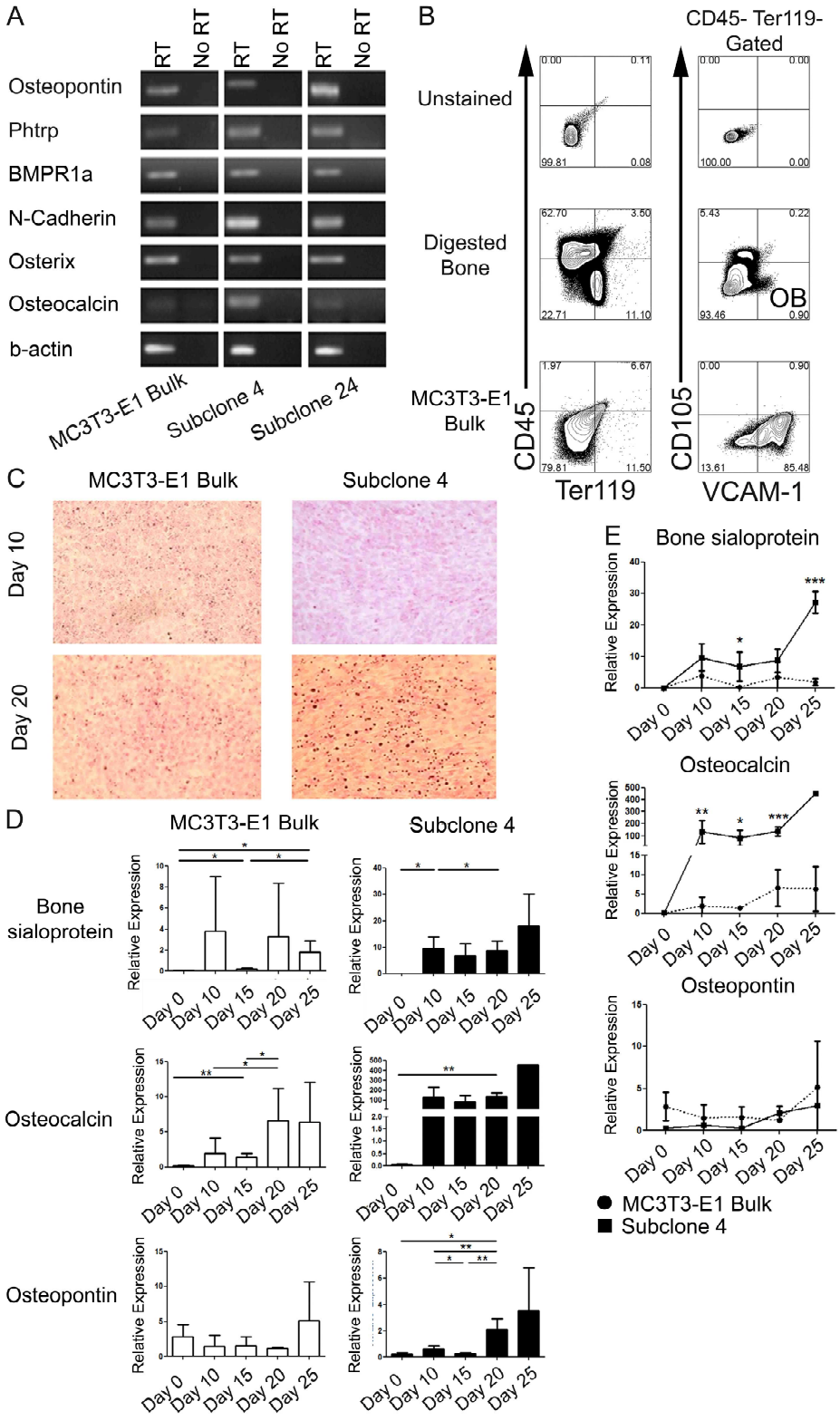
A
RT
No RT
RT
No RT
RT
No RT
Osteopontin
Phtrp
BMPR1a
N-Cadherin
Osterix
Osteocalcin
b-actin
MC3T3-E1 Bulk
Subclone 4
Subclone 24
B
CD45- Ter119- Gated
Unstained
Digested Bone
MC3T3-E1 Bulk
CD45
Ter119
CD105
VCAM-1
OB
C
MC3T3-E1 Bulk
Subclone 4
Day 10
Day 20
D
MC3T3-E1 Bulk
Subclone 4
Bone sialoprotein
Osteocalcin
Osteopontin
Relative Expression
Day 0
Day 10
Day 15
Day 20
Day 25
E
Bone sialoprotein
Osteocalcin
Osteopontin
Relative Expression
MC3T3-E1 Bulk
Subclone 4

Figure 2.1: The MC3T3-E1 cell line as a model of primary osteoblasts in culture. (A) RT-PCR was performed on MC3T3-E1 bulk, Subclone 4, and Subclone 24 for genes involved in osteoblast differentiation (*Osteopontin, Osterix*), mineralization (*Osteocalcin*) and the hematopoietic stem cell "niche" (*N-Cadherin, BMPR1a, Pthrp*), using *β-actin* as the positive control. Positive control tissue: collagenase digested bone. (B) Representative FACS plots showing the expression of VCAM-1, and lack of the mesenchymal stem cell marker CD105 on MC3T3-E1 bulk cells. Digested bone cells highlighting osteoblast populations show that MC3T3-E1 cells show a similar profile that of MC3T3-E1 bulk cells. (C) Von Kossa staining at Days 10 and 20 showing progressive mineralization in culture (black regions), with Subclone 4 displaying high mineralization compared to the MC3T3-E1 bulk cell line. (D) Real time PCR of *bone sialoprotein* (top panel), *osteocalcin* (middle panel), and *osteopontin* (bottom panel), at Days 0, 10, 15, 20 and 25 after the addition of MIM in MC3T3-E1 and Subclone 4. (E) Real time PCR comparing MC3T3-E1 and Subclone 4 of *bone sialoprotein* (top panel), *osteocalcin* (middle panel), and *osteopontin* (bottom panel), at Days 0, 10, 15, 20 and 25 after the addition of MIM. Samples were considered significant by a Student's T-test if *$p<0.05$, **$p<0.01$, ***$p<0.001$.

E1 bulk and subclone 4 showed significant increases in *osteocalcin* and *bone sialoprotein* from Day 0 to Day 25. When we compared the bulk to the subclone 4, there was a highly significant difference in the fold expression of *osteocalcin* and *bone sialoprotein* (Figure 2.1E). Interestingly, *osteopontin* expression increased significantly from Day 0 to Day 25 in the mineralizing subclone 4, but the level of *osteopontin* expression was not significantly different between MC3T3-E1 bulk and Subclone 4 from Day 0 to Day 25 within each cell line (Figure 2.1D-E). These results verified that MC3T3-E1 subclone 4 could be induced to mineralize *in vitro*, and that the MC3T3-E1 subclones could be utilized to examine how osteoblast mineralization influences hematopoiesis.

MC3T3-E1 cells support hematopoiesis towards myeloid differentiation

The expression of hematopoietic niche related genes suggested that MC3T3-E1 cells might be able to support hematopoietic development within an *in vitro* co-culture. To investigate whether or not MC3T3-E1 cells could support *in vitro* hematopoiesis, we co-cultured LSK HSCs (Lin^- ,$Sca\text{-}1^{high}$,$c\text{-}Kit^{high}$,$IL7R\alpha^-$) on MC3T3-E1 monolayers for 14 days using the OP9 cell line as a positive control (Figures 2.3A-G). LSK HSCs were assessed by looking at the numbers of LSK HSC and CLP present after 2 weeks. We saw no evidence of self renewal in our co-cultures (data not shown). We also analyzed MC3T3-E1 co-cultures for the presence of committed hematopoietic lineages. $CD45^+$ hematopoietic cells were present in MC3T3-E1 cultures, and the majority of these cells were either monocytes ($CD11b^+$ $Gr\text{-}1^-$) while there was also a population of granulocytes present ($CD11b^+$ $Gr\text{-}1^+$) (Figure 2.3A, 2.3E and 2.3F). No evidence for lymphoid development was observed on MC3T3-E1 co-cultures even with the addition of Flt-3

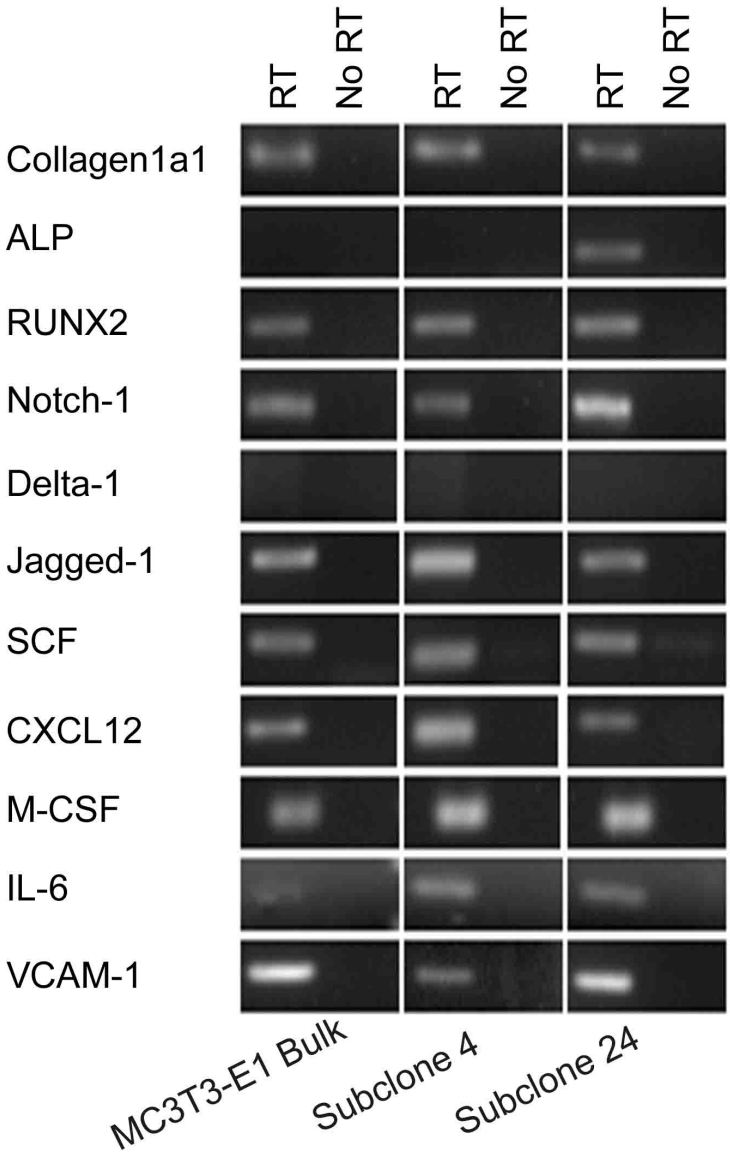
RT
No RT
RT
No RT
RT
No RT
Collagen1a1
ALP
RUNX2
Notch-1
Delta-1
Jagged-1
SCF
CXCL12
M-CSF
IL-6
VCAM-1
MC3T3-E1 Bulk
Subclone 4
Subclone 24

Figure 2.2: Expression of genes involved in osteoblast development and the hematopoietic stem cell niche. RT-PCR from mRNA isolated from MC3T3-E1 Bulk, MC3T3-E1 Subclone 4, and MC3T3-E1 Subclone 24. Genes involved in osteoblast development and maturation (collagen1a1, Runx2, Notch-1), hematopoietic stem cell niche and hematopoietic development (Notch-1, Jagged-1, Stem cell factor (SCF), CXCL12, M-CSF, and VCAM-1) were expressed in the cell lines used. Alkaline phosphatase (ALP) was expressed in only Subclone 24, while interleukin 6 (IL-6) was expressed in both subclones. *Delta-1* was not expressed in any MC3T3-E1 cell line. β-actin was used as a housekeeping gene control. The positive control tissue sample is bone that was flushed of bone marrow.

and IL-7, as compared to HSC co-cultures with OP9 BM stromal cell line monolayers prepared in the same experiment (Figures 2.3A, 2.3B and 2.3G). Quantification of the hematopoietic cells from the co-cultures also validated the flow cytometry results (Figures 2.3D-G). Although our co-cultures did not support HSC self renewal, these data demonstrated that MC3T3-E1 cells efficiently supported the differentiation of monocytes and granulocytes *in vitro* and could thus be used to see how mineralization affects monocyte and granulocyte populations *in vitro*.

Osteoblast mineralization decreases their ability to support hematopoiesis

Osteoblasts are important for supporting HSCs, B cells, and OC development [9,81,117]. The endosteum does not only contain one population of osteoblasts, rather it is a dynamic environment that is constantly changing from differentiation and osteoclast resorption activity [9,118]. While it does not appear that MC3T3-E1 subclones can generate self renewing HSCs, they do influence proliferation of monocytes and *in vitro*. MC3T3-E1 cells support myeloid differentiation through secretion of M-CSF and GM-CSF, however, the effect of mineralization on the generation of $CD11b^+$ monocytes and $CD11b^+$, $Gr\text{-}1^+$ granulocytes has not been investigated [82,88,119].

In order to assess how mineralization affects monocyte/macrophage generation *in vitro*, we induced mineralization in MC3T3-E1 bulk, MC3T3-E1 subclone 4 and MC3T3-E1 subclone 24 by the addition of 2-glycerophosphate and ascorbic acid to the culture media for 10 days, a time point when mineralization has clearly begun (Figures 2.1C-E). Ten-day cultures of MC3T3-E1 monolayers in which mineralization

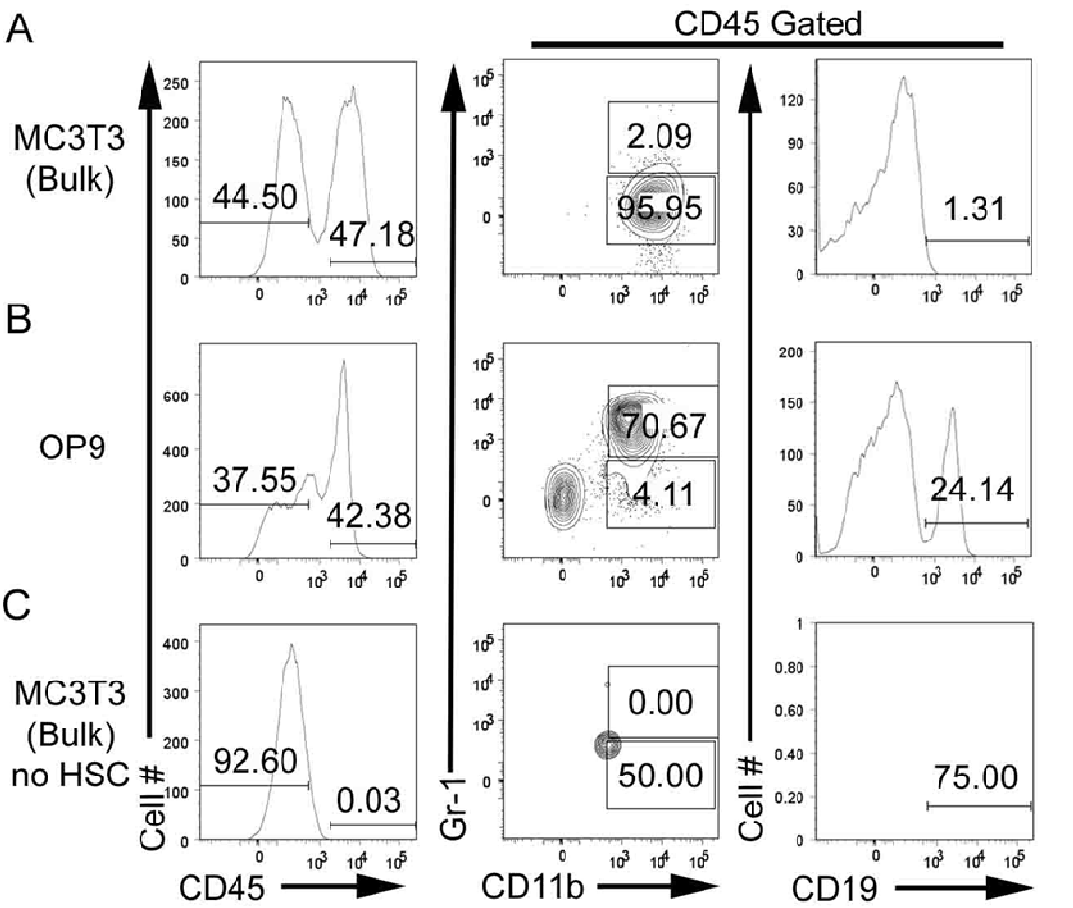
A
CD45 Gated
MC3T3 (Bulk)
44.50
47.18
2.09
95.95
1.31
B
OP9
37.55
42.38
70.67
4.11
24.14
C
MC3T3 (Bulk) no HSC
92.60
0.03
0.00
50.00
75.00
Cell #
Gr-1
Cell #
CD45
CD11b
CD19

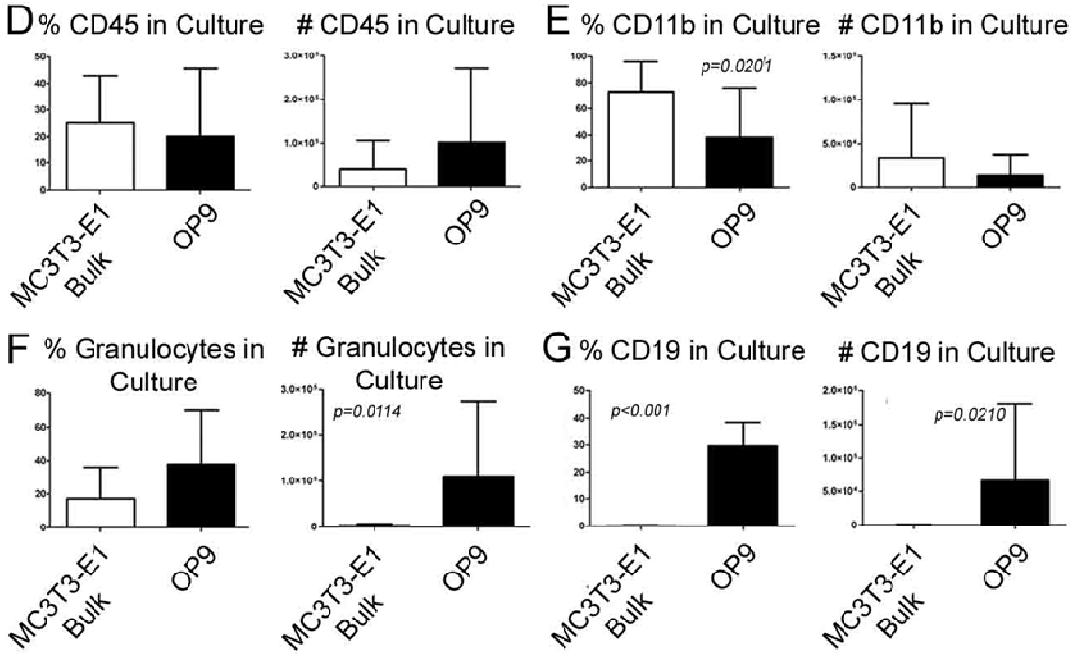
D % CD45 in Culture
CD45 in Culture
E % CD11b in Culture
p=0.0201
# CD11b in Culture
MC3T3-E1 Bulk
OP9
F % Granulocytes in Culture
p=0.0114
# Granulocytes in Culture
G % CD19 in Culture
p<0.001
# CD19 in Culture
p=0.0210

Figure 2.3: Co-culture of non-mineralized MC3T3-E1 cells supports myelopoiesis. (A) Representative FACS plots showing $CD45^+$ cells after culturing HSCs on MC3T3-E1 bulk cells for 14 days in culture. (B) Representative FACS plots showing $CD45^+$ cells after culturing HSCs on OP9 cells for 14 days in culture. (C) Representative FACS plots showing $CD45^+$ cells on MC3T3-E1 bulk cells with no HSCs for 14 days in culture. (D-G) Graphs showing the percentage (left) and cell number (right) of the CD45+ hematopoietic cells (D), CD11b+ monocytes (E), CD11b+ Gr-1 granulocytes (F), and CD19+ B cells (G) from MC3T3-E1 and OP9 co-cultures. Samples were considered significant by a Student's T-test if $*p<0.05$, $**p<0.01$, $***p<0.001$.

was not induced were also prepared as controls. On Day 10, HSCs were plated on both control and mineralizing MC3T3-E1 monolayers, and co-cultures were allowed to progress for an additional 14 days in MIM (Figure 2.4A). After this time, all cells were then harvested from each co-culture and the presence of differentiated hematopoietic cells was assessed by FCM.

Under mineralizing conditions, the mean numbers of $CD45^+$ and $CD11b^+$ cells were decreased in all co-cultures, but only significantly in the subclone 4 cultures (Figure 2.4B-I). As described above, MC3T3-E1 cells were first cultured in MIM for 10 days before seeding with HSC, and one interpretation of these results is that the decrease in hematopoiesis in all cultures was due to the sensitivity of the HSCs to the differentiation media. To rule out that HSCs were not sensitive to the MIM, we directly co-cultured HSCs and MC3T3-E1 cells in either MM or MIM for 14 days. In this case, the percentages of $CD45^+$ cells observed were not different between cultures in MM or MIM, demonstrating that HSCs were not adversely affected by the components of the MIM (Figure 2.4J). Statistical analysis revealed that only co-cultures of HSCs and the mineralization-prone subclone 4 produced statistically significantly lower percentages and numbers of CD45+ cells in MIM compared to MM (Figure 2.4E and 2.4F). Therefore, the data presented here indicates that mineralization alters the ability of MC3T3-E1 cells to decrease myeloid differentiation and/or proliferation *in vitro*. We next performed studies to identify the molecular mechanisms behind this decreased support.

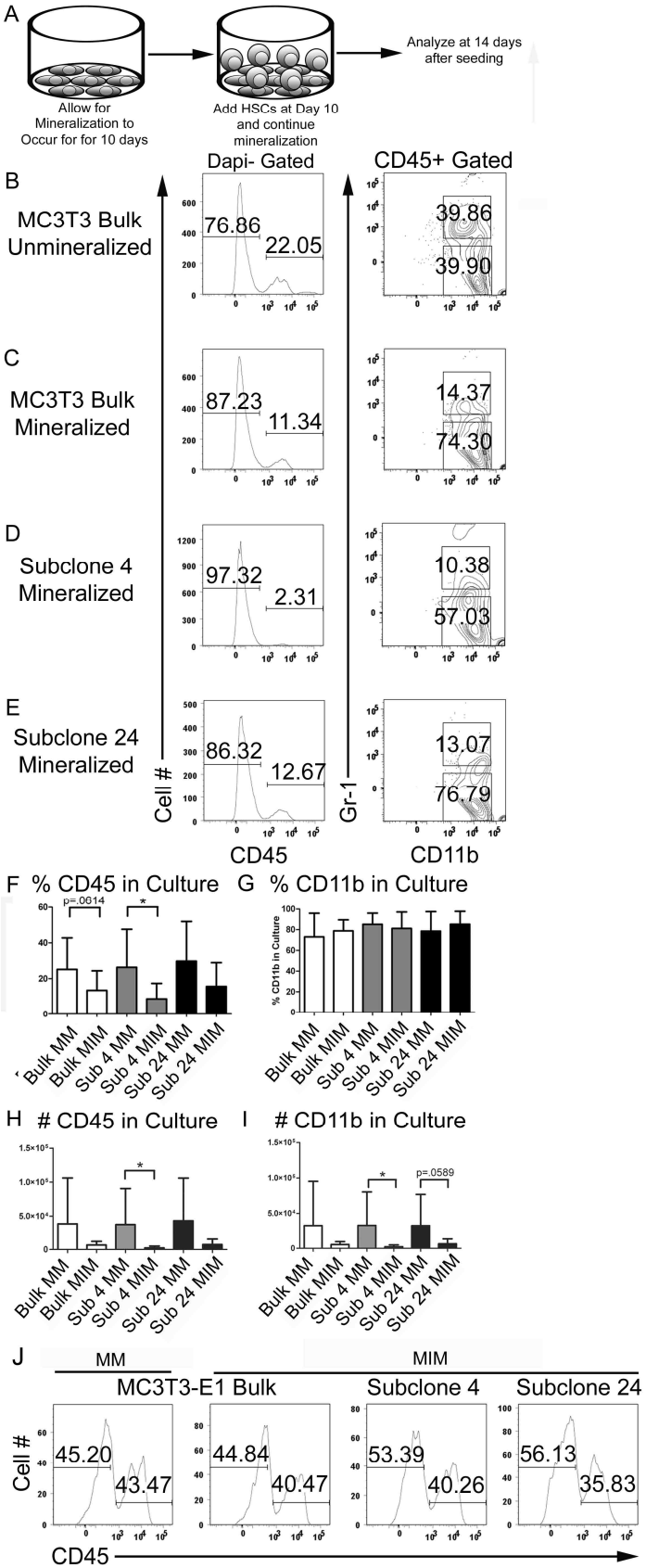
A
Allow for Mineralization to Occur for for 10 days
Add HSCs at Day 10 and continue mineralization
Analyze at 14 days after seeding
B
MC3T3 Bulk Unmineralized
C
MC3T3 Bulk Mineralized
D
Subclone 4 Mineralized
E
Subclone 24 Mineralized
Dapi- Gated
CD45+ Gated
76.86
22.05
39.86
39.90
87.23
11.34
14.37
74.30
97.32
2.31
10.38
57.03
86.32
12.67
13.07
76.79
Cell #
Gr-1
CD45
CD11b
F % CD45 in Culture
G % CD11b in Culture
p=.0614
*
% CD11b in Culture
Bulk MM
Bulk MIM
Sub 4 MM
Sub 4 MIM
Sub 24 MM
Sub 24 MIM
H # CD45 in Culture
I # CD11b in Culture
p=.0589
J
MM
MIM
MC3T3-E1 Bulk
Subclone 4
Subclone 24
45.20
43.47
44.84
40.47
53.39
40.26
56.13
35.83
Cell #
CD45

Figure 2.4: Induction of MC3T3-E1 mineralization results in a dramatic decrease of hematopoietic support. (A-D) Representative FCM plots of co-culture experiments in which HSCs were added to (A) Non-mineralized MC3T3-E1 cells, (B) Mineralized MC3T3-E1 bulk cells, (C) Mineralized MC3T3-E1 Subclone 4 cells and (D) Non-mineralized Subclone 4 cells. Staining for CD45+ cells, CD11b monocytes and $CD11b^+$ $Gr\text{-}1^+$ granulocytes are shown. (E-F) Percentage of $CD45^+$ (E) and $CD11b^+$ monocytes (F) on mineralized and non-mineralized MC3T3-E1 co-cultures. (G-H) Cell numbers of $CD45^+$ (G) and $CD11b^+$ monocytes (H) on mineralized and non-mineralized MC3T3-E1 co-cultures. (I) MC3T3-E1 cells were grown in basal media (left) and mineralization media for 14 days without the 10 day mineralization step. Samples were considered significantly different if $p<0.05$ by Student's T-test if $*p<0.05$, $**p<0.01$, $***p<0.001$.

Wnt Signaling Molecules Involved in Hematopoietic Development are Decreased upon Mineralization

Wnt 3a, 5a, 5b, 7b, 9b, and 10b are expressed by osteoblasts as they develop and are particularly important in the differentiation of early osteoblastic progenitors to mature osteoblasts, resulting in upregulation of Runx2 and other osteoblast-specific transcription factors [96,118]. At the mature osteoblast stage, downregulation of Wnt signaling is required for terminal differentiation into the osteocyte [84]. In a similar fashion, Wnt signaling has been implicated in HSC maintenance in the bone marrow niche, and can also facilitate proliferation in myeloid subsets and regulation of B cell development [42,120].

We hypothesized that the decrease in myelopoiesis observed under mineralizing conditions might result from alterations in Wnt signaling in the MC3T3-E1 cells. Alterations in Wnt signaling could then, in turn, have an adverse effect on myeloid proliferation. Myeloid cells are influenced by Wnt signaling to regulate their proliferation, and dysregulation of Wnt signaling can result in AML [53,100]. Additionally, increased Wnt3a can decrease myeloid proliferation through stromal cell interactions [24]. We hypothesized that alterations in Wnt signaling occurred upon the induction of mineralization, which in turn, resulted in altered hematopoiesis. To test this idea, we performed qPCR analysis of Wnt pathway-specific genes in MC3T3-E1 bulk and MC3T3-E1 subclone 4 cells before Day 0 and ten days after induction of mineralization. There were only a few genes that were significantly up- or down-regulated after induction of mineralization of the MC3T3-E1 bulk cells such as *Ccnd2, Fbxw4, Dixdc1, Csnk1a2, Tcf7, Wnt4, Wnt5b, and Wnt7b* (Tables 2.1-2.2). We also

examined Wnt antagonist genes in MC3T3-E1 cells by qPCR and observed that *Wif-1* and *Sfrp-2* were differentially expressed (Tables 2.3-2.4).

Examination of the Wnt target genes using qPCR

Preliminary investigation of MC3T3-E1 bulk and subclone 4 gene expression changes allowed us to determine which genes are altered upon induction of mineralization. We next wanted to examine Wnt target gene expression over the course of mineralization in MC3T3-E1 cells. Wnt activation in osteoblast cells results in the upregulation of numerous target genes that are involved in both proliferation and survival. Of these target genes, we examined *Lef-1* and *c-Myc* by qPCR at Days 0, 10, and 24 in MC3T3-E1 bulk and subclone 4 to assess Wnt activation in our cultures (Figure 2.5A and 2.5B).

Interestingly, *c-Myc* showed high expression at Day 10, but dropped significantly at Day 24 to the levels observed at Day 0 (Figure 2.5A). Subclones 4 displayed a higher level of expression of *c-Myc* compared to MC3T3-E1 bulk at Day 10, but then dropped to the Day 0 levels at Day 24. *Lef-1* showed no significant difference in expression from Days 0-24, however, at Day 24, *Lef-1* expression was significantly higher in subclone 4 compared to MC3T3-E1 bulk cultures (Figure 2.5B). The continued expression of Wnt target genes indicated that Wnt signaling was still active at the endpoint of our cultures, and that this could potentially alter myeloid proliferation in our cultures. Another interesting finding from the qPCR screen was the upregulation of *Sfrp-2* in subclone 4 at day 24 (Figure 2.5A and 2.5B). *Sfrp-2* levels remained unchanged at Days 0 and 10, but drastically increased at day 24 in culture. We hypothesized that the increase in *Sfrp-2*

Table 2.1: Relative Expression of Selected Genes from PCR Array for MC3T3-E1 Bulk and MC3T3-E1 Subclone 4.

Gene Symbol	Gene Name	Bulk Day 0	Bulk Day 10	Sub 4 Day 0	Sub 4 Day 10
CCND2	Cyclin D2	1.28 (n=3)	3.53 (n=4)	1.50 (n=2)	8.40 (n=2)
Fbxw4	F-box/WD repeat-containing protein 4	1.43 (n=3)	3.35 (n=3)	0.38 (n=2)	1.38 (n=2)
DIXDC1	DIX Domain Containing 1	1.65 (n=3)	2.63 (n=3)	0.83 (n=2)	7.29 (n=2)
CSNK1a2	Casein kinase 1, alpha 1	1.74 (n=3)	2.50 (n=3)	0.29 (n=2)	1.63 (n=2)
TCF7	T-cell-specific transcription factor 7	1.22 (n=3)	1.45 (n=3)	0.14 (n=2)	3.70 (n=2)
Wnt 4	wingless-type MMTV integration site family, member 4	1.057 (n=3)	2.05 (n=4)	6.19 (n=2)	9.22 (n=2)
Wnt5b	wingless-type MMTV integration site family, member 5b	5.980 (n=3)	28.546 (n=4)	2.944 (n=2)	26.78 (n=2)
Wnt7b	wingless-type MMTV integration site family, member 7b	1.71 (n=3)	25.12 (n=4)	3.22 (n=2)	43.01 (n=2)

Table 2.2: p values of Selected Genes from PCR Array of MC3T3-E1 Bulk and MC3T3-E1 Subclone 4.

Gene Symbol	Gene Name	Bulk Day 0 vs. Bulk Day 10	Sub 4 Day 0 vs. Sub 4 Day 10	Bulk Day 0 vs. Sub 4 Day 0	Bulk Day 10 vs. Sub 4 Day 10
CCND2	Cyclin D2	0.2290	0.0009	0.8027	0.0694
Fbxw4	F-box/WD repeat-containing protein 4	0.2544	0.0169	0.4041	0.3049
DIXDC1	DIX Domain Containing 1	0.4957	0.0353	0.5058	0.0441
CSNK1a2	Casein kinase 1, alpha 1	0.1962	0.0226	0.0652	0.3473
TCF7	T-cell-specific transcription factor 7	0.7110	0.0710	0.2359	0.0396
Wnt 4	wingless-type MMTV integration site family, member 4	0.4788	0.6246	0.2100	0.0114
Wnt5b	wingless-type MMTV integration site family, member 5b	0.1107	0.0444	1.000	0.9006
Wnt7b	wingless-type MMTV integration site family, member 7b	0.0215	0.7156	0.3663	0.3882

Table 2.3: Relative Expression of Wnt Antagonists from Gene Array of MC3T3-E1 Bulk and MC3T3-E1 Subclone 4.

Gene Symbol	Gene Name	Bulk Day 0	Bulk Day 10	Sub 4 Day 0	Sub 4 Day 10
DKK-1	Dickkopf-1	N.D.	N.D.	N.D.	N.D.
SFRP-1	Secreted Frizzled Related Protein 1	1.00 (n=2)	2.03 (n=4)	19.05 (n=2)	1.84 (n=2)
SFRP-2	Secreted Frizzled Related Protein 2	2.87 (n=3)	14.66 (n=4)	31.61 (n=2)	44.92 (n=2)
SFRP-3 (FRZB)	Secreted Frizzled Related Protein 3	3.51 (n=2)	39.20 (n=4)	45.06 (n=2)	31.83 (n=2)
SFRP-4	Secreted Frizzled Related Protein 4	1.26 (n=3)	0.86 (n=4)	1.77 (n=2)	N.D (n=1)
WIF-1	Wnt Inhibitory Factor 1	1.00 (n=1)	3.63 (n=4)	1.32 (n=2)	18.45 (n=2)

*N.D. Not determined

Table 2.4: p values of Wnt Antagonists from Gene Array of MC3T3-E1 Bulk and MC3T3-E1 Subclone 4.

Gene Symbol	Gene Name	Bulk Day 0 vs. Bulk Day 10	Sub 4 Day 0 vs. Sub 4 Day 10	Bulk Day 0 vs. Sub 4 Day 0	Bulk Day 10 vs. Sub 4 Day 10
DKK-1	Dickkopf-1	N.D	N.D	N.D	N.D
SFRP-1	Secreted Frizzled Related Protein 1	0.3995	N.D	0.2279	0.2436
SFRP-2	Secreted Frizzled Related Protein 2	0.2200	0.5764	0.2297	0.0445
SFRP-3 (FRZB)	Secreted Frizzled Related Protein 3	0.2511	0.9829	0.3650	0.7956
SFRP-4	Secreted Frizzled Related Protein 4	0.6051	0.5055	N.D.	N.D.
WIF-1	Wnt Inhibitory Factor 1	N.D.	0.7795	N.D.	0.0317

*N.D. Not determined

could potentially explain the decrease in myeloid cells in the highly mineralizing subclone 4.

Co-culture of MC3T3-E1 cells and hematopoietic stem cells with exogenous *Sfrp-2*

The finding that *Sfrp-2* expression was significantly upregulated at the end of our co-culture experiment indicated that this Wnt antagonist might be acting on myeloid cells to reduce hematopoiesis. We hypothesized that the increase in *Sfrp-2* at Day 10 may reduce the myeloid progenitors in our co-cultures. To test this hypothesis, we co-cultured LSK HSCs with MC3T3-E1 bulk and subclones for 14 days in co-culture under non mineralizing conditions with the addition of exogenous SFRP-2 (Figure 2.6A).

The addition of exogenous SFRP-2 at 10, 20, and 100 μg/μl did not result in any observable differences $CD45^+$ populations compared to the untreated control (Figure 2.6A-D). There were also no observable differences in $CD11b^+$ monocyte populations, both in percentage and cell number (Figure 2.6A, 2.6C and 2.6D). There was a significant increase in granulocytes cultured with 100 μg/μl SFRP-2 when compared to the untreated control, but no other observable differences in the cultures. Although it seems that there are Wnt signaling changes at Day 24, the cause of the decrease in myeloid cells we observed in culture is not due to decreases in *Sfrp-2* expression.

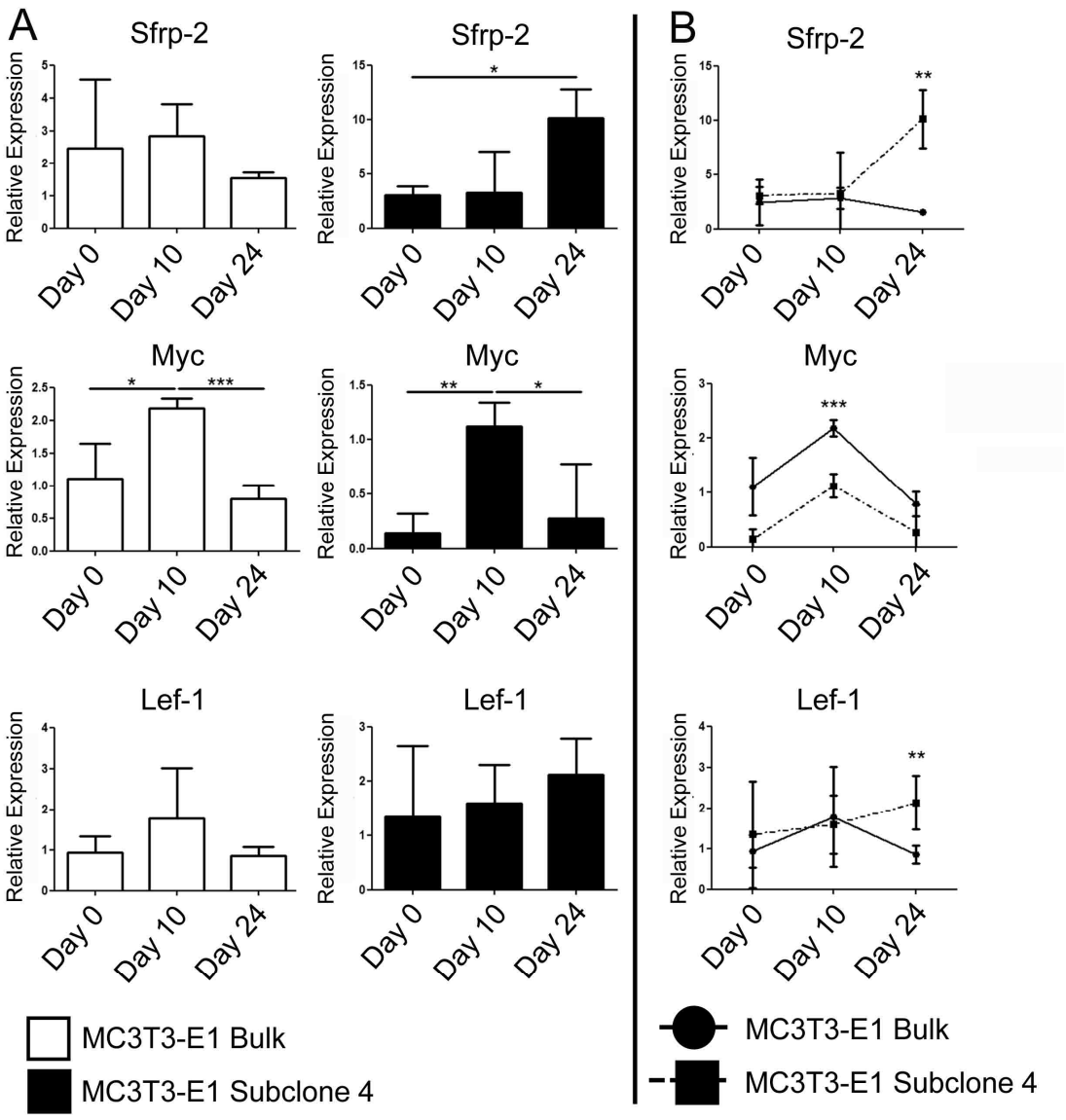

Figure 2.5: Differential Expression of Wnt target genes in MC3T3-E1 Bulk and Mineralizing MC3T3-E1 Subclone 4. (A) qPCR analysis of *Secreted Frizzled Protein 2* (*Sfrp-2*), *c-Myc* and *Lef-1* on MC3T3-E1 Bulk (left, n=3) and MC3T3-E1 Subclone 4 (right, n=3). (B) Comparison of *Sfrp-2* (top panel), *c-Myc* (middle panel) and *Lef-1* (bottom panel) expression in MC3T3-E1 Bulk and MC3T3-E1 Subclone 4 at days 0, 10 and 24. Mean ± SD are shown and were considered to be statistically significant Student's T-test if *p<0.05, **p<0.01, ***p<0.001.

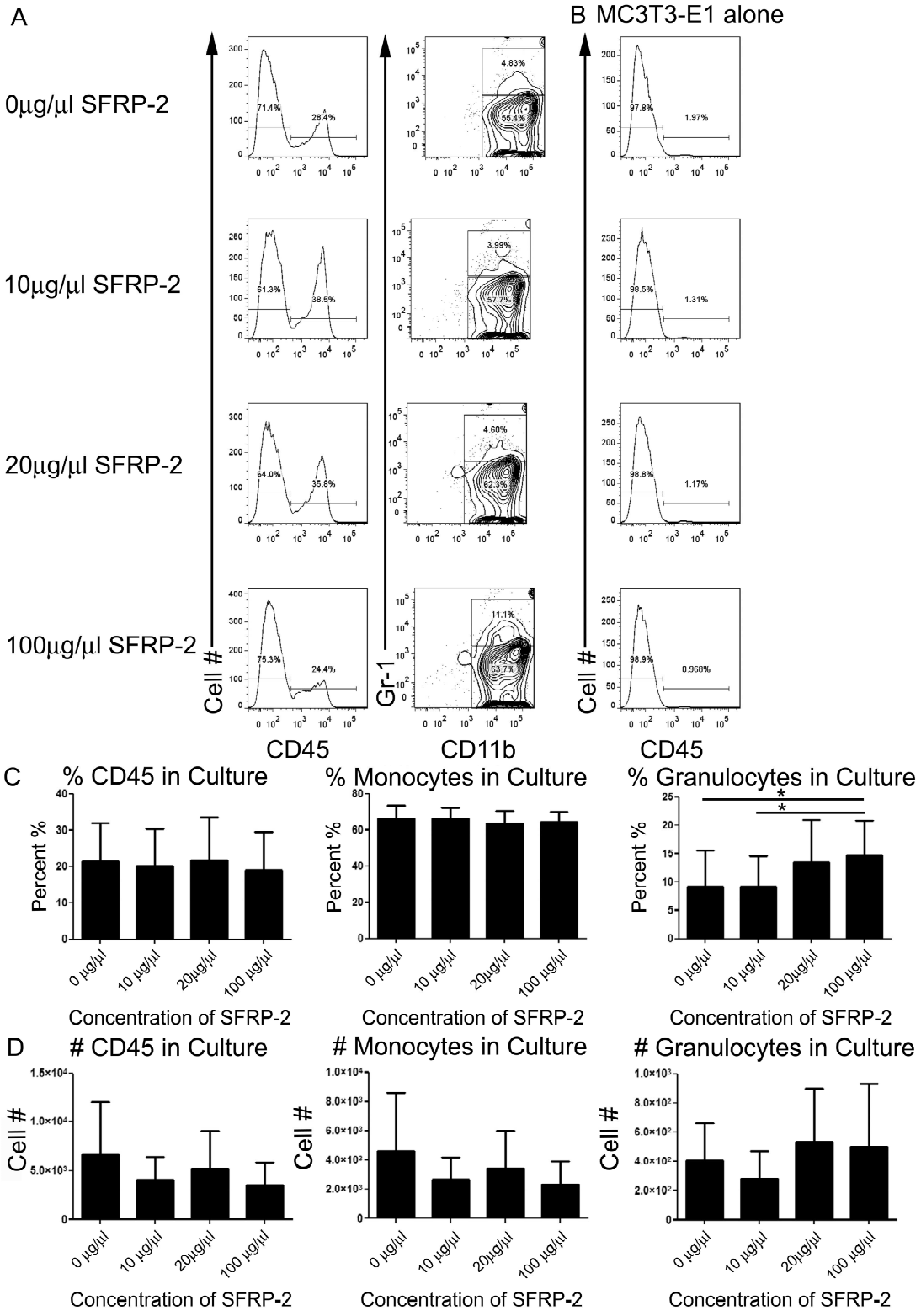
A
B MC3T3-E1 alone
0μg/μl SFRP-2
10μg/μl SFRP-2
20μg/μl SFRP-2
100μg/μl SFRP-2
Cell #
Gr-1
CD45
CD11b
CD45
C
% CD45 in Culture
% Monocytes in Culture
% Granulocytes in Culture
Percent %
0 μg/μl
10 μg/μl
20μg/μl
100 μg/μl
Concentration of SFRP-2
D
CD45 in Culture
Monocytes in Culture
Granulocytes in Culture
Cell #
Concentration of SFRP-2

Figure 2.6: Addition of Secreted Frizzled Protein 2 (SFRP-2) does not result in reduced hematopoiesis. (A) Representative flow cytometry plots of the addition of SFRP-2 at 0 ug/ml (top panel), 10 ug/ml (top middle panel), 20 ug/ml (bottom middle panel), and 100 ug/ml (bottom panel). (B) MC3T3-E1 cultures with no hematopoietic cells at 0 ug/ml (top panel), 10 ug/ml (top middle panel), 20 ug/ml (bottom middle panel), and 100 ug/ml (bottom panel). (C) Percentage of CD45 cells (left panel), $CD11b^+$ monocytes (middle panel) and $CD11b^+$ $Gr\text{-}1^+$ granulocytes (right panel). (D) Total cell number of CD45 cells (left panel), $CD11b^+$ monocytes (middle panel) and $CD11b^+$ $Gr\text{-}1^+$ granulocytes (right panel). Mean ± SD are shown and were considered to be statistically significant Student's T-test if $*p<0.05$, $**p<0.01$, $***p<0.001$.

2.4 Discussion

We have demonstrated that the MC3T3-E1 cell line expresses genes that are involved in both hematopoietic stem cell self renewal and differentiation and that MC3T3-E1 cell lines can support hematopoietic stem cell differentiation, but not HSC self renewal. Our study also revealed that as mineralization increases in MC3T3-E1 cell lines, the ability to support myeloid proliferation and differentiation is dramatically reduced. We observed differences in expression of Wnt signaling genes; in particular, a decrease in *Sfrp-2 and Wif-1*. Adding exogenous SFRP-2 did not rescue the myeloid reduction observed in MC3T3-E1 co-cultures.

Wnt antagonists are only beginning to be appreciated as having a role in hematopoiesis. DKK-1, SFRP-1, SFRP-2 and WIF-1 all have been shown to influence hematopoietic stem cell function [56,57,61,62]. In a study by Nakajima and colleagues, the addition of exogenous SFRP-2 *in vitro* resulted in increased hematopoietic colony formation that contained exogenous Stem Cell Factor (SCF) and Thrombopoietin (TPO), as well as increased engraftment efficiency in HSCs after secondary transplantation [57]. In the same study, SFRP-1 was also shown to increase hematopoietic colony formation *in vitro*. The colony forming assays performed in Nakajima and colleagues study differed significantly from our study, as we utilized a system akin to the OP9 co-culture system, which requires the addition of Interleukin 7 and FLT-3 ligand to enhance lymphoid generation[107]. Although our studies do not indicate a specific role of SFRP-2 in promoting hematopoiesis, we have yet to perform functional studies on how SFRP-2 specifically influences myelopoiesis.

Another interesting finding was the elevated expression of *Wif-1* in mineralized MC3T3-E1 subclone 4 at Day 10. Recently, it has been shown that Wif-1, under the control of the Col2.3 promoter in osteoblasts (*Wif-1-Tg*), exhausted LT HSCs and altered normal hematopoiesis[61]. In the same study with *Wif-1-Tg* mice, it was shown that the decreases in LT HSC populations were non cell autonomous. Since Wif-1 can result in decreased LT HSCs and altered hematopoiesis, it could potentially explain the reduction observed in our studies. The MC3T3-E1 co-culture "add-back" experiment could subsequently be used with the addition of WIF-1 to identify if there are any influences on hematopoiesis in our co-cultures.

There are currently five known secreted Frizzled proteins in mice (SFRP1-5)[54]. *In vivo* studies using *Sfrp-1*$^{-/-}$ mice demonstrated a marked reduction in hematopoietic stem cell function [56]. SFRP-1 has also been shown to negatively influence secondary transplantation, but the mechanism for how SFRP-1 and SFRP-2 differentially regulate hematopoiesis is still unclear [57]. SFRP-1 levels did were not significantly different in MC3T3-E1 bulk and subclone 4 cells (Table 2.1 and Table 2.2). SFRP-1 and SFRP-2 have been shown to be redundant in early development, however, in hematopoiesis, the two proteins seem to have vastly different functions [68]. Not all SFRPs block Wnt signaling, which may partly explain why SFRP-1 and SFRP-2 have vastly different effects observed in our culture [121]. Our results do not seem to conflict with the results from Nakajima and colleagues, which showed an increase in proliferation of HSCs with the addition of both SFRP-1 and SFRP-2 *in vitro*, although it is interesting that the addition of exogenous SFRP-2 did not increase hematopoiesis in our cultures. This

indicates that the utilization of different culture systems can influence the output of hematopoietic cells.

Mineralization occurs as osteoblasts mature into OCY, however, it seems that as osteoblasts mature, another consequence is the loss of the ability to support hematopoiesis. Recently, Cheng and colleagues showed that maturing calvarial osteoblasts displayed reduced ability to support hematopoiesis, while Chetti and colleagues showed that *Runx2* expression in osteoblasts correlated to an increase in hematopoiesis *in vitro* [70,122]. MC3T3-E1 express *Runx2* before and after mineralization, but we still need to quantify the levels of *Runx2* expression after mineralization. Many pathways other than Wnt, such as the Notch, BMP and Hedgehog pathways, are also important regulators of both osteoblast and hematopoietic development [118], and their role in mineralizing MC3T3 cultures has yet to be investigated. In addition, the effects of these pathways and mineralization on the direct production of hematopoietic growth factors, such as M-CSF and GM-CSF, require additional study.

In summary, we have shown that the MC3T3-E1 monolayer system can be utilized to test the effects of distinct stages of osteoblast maturation on hematopoiesis, and could be a simple method to further the understanding of the crosstalk between osteoblasts and myeloid cells during their reciprocal differentiation and development. This system could also be advantageous in deciphering the interactions of other hematopoietic cell types, such as embryonic stem cell-derived hematopoietic progenitors with mature OBs. Finally, this system could also potentially be used to test the reciprocal

effects of the HSC on OB differentiation, which could occur after bone injury or fracture, and metastasis[10].

Chapter 3: Absence of Sclerostin Adversely Affects B cell Survival

3.1. Introduction:

It is well appreciated that cellular crosstalk between OBs and osteoclasts in the adult bone is required for proper bone homeostasis [123] and that disruption of the balanced activity between bone-building OBs and bone-resorbing OCs can result in altered bone metabolism, leading to high or low bone mass, respectively. More recently, the relationship between abnormal bone phenotypes on the development and differentiation of BM stromal cells and hematopoietic cells has been an active area of investigation [10,117]. At embryonic day 12, some MSCs begin expressing *Runx2*, solidifying commitment to the osteoblastic lineage [84]. Activation of Wnt signaling and expression of *Osterix* foster further differentiation to the osteoprogenitor stage [97]. Commitment to the mature OB stage is confirmed by the upregulation of mineralization genes [85]. Finally, terminal differentiation to the osteocyte requires downregulation of Wnt signaling by Wnt antagonists [85,97].

As was shown in Chapter 2, Wnt antagonists play a role in regulating hematopoiesis. Canonical and non-canonical Wnt signaling has been implicated in various aspects of hematopoiesis, particularly in B cell survival [24,124]. B lymphocyte development in the bone marrow of β-*catenin* deficient mice is normal [125], whereas B cell development is increased by non-canonical Wnt5a mediated signaling [19]. Wnt signaling is also important for osteoblast development, as canonical Wnt3a-signaling inhibited or promoted osteogenesis depending on the Wnt3a concentration and age of the mice examined [126]. Haploinsufficiency of the non-canonical *Wnt5a* gene in mice resulted in loss of bone mass and increased adipogenesis in the bone marrow *in vivo*

[127], but promoted osteogenesis from human mesenchymal stem cells *in vitro* [128]. Taken together, the role of Wnt signaling in hematopoiesis and osteogenesis is clearly influential in preserving bone homeostasis.

Sclerostin (*Sost*, Entrez GeneID: 50964) antagonizes canonical Wnt signaling by its binding to the Wnt co-receptors LRP4, LRP5, and/or LRP6 [55,73], blocking signaling via Frizzled receptors. SOST is a secreted protein that is primarily expressed by fully mature osteocytes and acts on OBs as a negative regulator of bone growth by inducing OB apoptosis in culture and effectively preventing osteoblast maturation into osteocytes [73]. Mice with deletions of the *Sost* coding region display highly mineralized bones with reduced BM cavity size, due to increased activity of OBs without affecting osteoclast development and activity [78]. Van Buchem's disease in humans has been traced to a 52 Kb deletion in the *Sost* regulatory region, which results in deforming increases in bone mass [129]. Despite the clear role of SOST in the regulation of Wnt signaling, osteoblast activity and the size of the BM cavity, the function of SOST in the regulation of bone marrow hematopoiesis has not been investigated. Here, we analyzed hematopoietic differentiation and the bone marrow environment in *Sost*$^{-/-}$ mice to examine whether the lack of *Sost* in the bone affects hematopoiesis, particularly B cell development.

3.2 Materials and Methods:

Mice. C57BL/6J and B6.SJL-Ptprc^{a} Pepc^{b}/BoyJ mice were obtained from The Jackson Laboratory (Bar Harbor, ME). *Sost*$^{-/-}$ mice on the B6 background were generated by Regeneron Pharmaceuticals, Inc. as a Sost-LacZ knock-in as part of the Knockout Mouse Project (KOMP) (http://www.velocigene.com/komp/detail/10069 [79]). Mice of both sexes were analyzed between 3 - 4 months of age. Data were combined from both male and female mice, as no sex-specific differences were observed [78,79], and data not shown). All mice were euthanized by CO_2 asphyxiation followed by cervical dislocation. All animal procedures were approved by the LLNL and UC Merced Institutional Animal Care and Usage Committees.

Antibodies. Monoclonal antibodies (mAb) were purchased either from eBioscience, Biolegend or BD Biosciences (San Diego, CA). The mAb clone name is listed in parentheses. Purified anti-CD16/32 (93) was used to block Fc receptors γII/III. Biotinylated-anti-CD3 (145-2C11), CD4 (GK1.5), CD8 (53-6.7), CD19 (6D5), CD11b (M1/70), NK1.1 (PK136), Gr-1 (RB6-8C5), and TER-119 (Ter119) were used for lineage depletions. Other antibodies and stains used are listed as follows: anti-c-Kit-eFluor-780 (ACK2), CD34-FITC (RAM34), CD135-PE (A2F10.1), CD16/32-PerCp-Cy5.5 (93), CD25-PerCp-Cy5.5 (PC61), Sca-1-APC (D7), IL7Rα-PECy7 (A7R34), AA4.1-APC (AA4.1), B220-FITC (RA3-6B2), IgD-PerCp-Cy5.5 (11-26c.2a), CD19-APCCy7, -APC, or -PE (6D5), IgM-PE (RMM-1), CD21-FITC (7G6), and CD23-Biotin (B3B4), CD45-FITC (30-F11), NK1.1-PeCy5 (PK136), CD3ε-APC (145-2C11), TER-119-PeCy7 (Ter119,) Gr-1-PECy5 (RB6-85C), CD11b-PE (M1/70), CD45.1-FITC (A20), CD45.1-APC (A20), CD45.2-PE (104), CD45.2-APC-Cy7 (104).

Sorting and analysis of hematopoietic progenitor and stromal populations by flow cytometry (FCM). Bone marrow cells were obtained and counted as described [108]. For stromal cells, flushed tibiae and femora were digested in M199+ containing 0.125% (w/v) collagenase D (Roche) and 0.1% DNase (Roche) on an agitator at 37^{o}C, in which fresh media was added every 15 minutes, for a total of 75 minutes. Following digestion, 0.125% Neutral Protease (Worthington) was added for 15 minutes and then stromal cells were incubated in a mixture of PBS, 5 mM EDTA, 1% FCS, 0.02% NaN_3 for 10 minutes to help disrupt cellular fragments.

All cells were incubated with purified anti-CD16/32 to block Fc receptors and lineage^{+} were MACS depleted as described [108]. Live, Lineage^{-} cells were then counted by hemocytometer using Trypan Blue exclusion. All Lineage^{-} cells were stained with antibodies specific for c-Kit, Sca-1 and IL7Rα for 20 min. at 4^{o}C, washed and resuspended in M199+ media with 0.1 μg/ml of DAPI (Fisher). LSK HSC, MPP, CLP, CMP, MEP/GMP populations were then sorted using a FACS Aria II (BD Biosciences, San Jose, CA). All populations were sorted to 80-90% purity, as verified by post-sort analysis. Analysis of flow cytometric data was performed with FlowJo software (Treestar, Ashland, OR).

Flow cytometric sorting and analysis of committed cell lineage population in the bone marrow and spleen. Bone marrow cells were isolated as described [108], counted, and cells were stained with anti-CD16/32 and then stained with fluorochrome-conjugated Abs specific for CD3, CD19, NK1.1, Ter119, CD11b, and Gr-1. Splenocytes were obtained by gentle physical disruption of spleens with the base of a 5 ml syringe and

resuspended in M199+. Splenocytes were filtered, treated with ACK lysis buffer, incubated with anti-CD16/32, and then either stained with fluorochrome-conjugated Abs specific for CD3, CD19, NK1.1, Ter119, CD11b, and Gr-1, or fluorochrome-conjugated Abs specific for AA1.1, CD19, IgM, CD21, and CD23. Analysis was performed as described above.

RNA Isolation, cDNA synthesis, and PCR. RNA from cells was collected from collagenase-digested bones, FACS-sorted cells and whole bone, as described [108]. Briefly, cells were placed in Trizol (Invitrogen, Grand Island, NY) and RNA was purified using phenol-chloroform extraction. Purified mRNA was then used as a template to synthesize cDNA using oligo-dT primers with the Superscript III kit (Invitrogen). Conventional reverse-transcriptase PCR (RT-PCR) of cDNA was performed using the following thermocycler conditions: 90°C for 5 min, then 35-40 cycles of 95°C for 1min, 55-60°C for 30 sec. and 72°C for 1 min, followed by a 5 min 72°C extension. PCR products were visualized by electrophoresis on a 1.5% agarose gel.

Quantitative real-time PCR (qPCR) was performed as described [108]. All primers used were validated for efficiency using standard curves on control tissues and were used only if the primer efficiencies exceeded 90% and only one PCR product was visualized after gel electrophoresis.

Analysis of apoptosis and cell death in B cells. Bone marrow B cells were enriched as described above and stained with fluorochrome-conjugated antibodies specific for B220, IgM, c-Kit, and CD19. Cells were washed in M199+ one time, and then subsequently washed twice in 100 µl of Annexin V Binding Buffer (Biolegend) and then resuspended at a concentration of 10^6 cells/ml in Annexin Binding Buffer. 5 µl of

Annexin V-FITC (Biolegend) and 10 μl of 7-AAD (eBioscience) were then added for 15 minutes and washed with Annexin-V binding buffer and analyzed by FCM.

LacZ staining of bone marrow sections. Tibiae and calvariae from 6-month old and *Sost*$^{-/-}$ and wild-type littermate control mice were prepared and sectioned as previously described [130]. Samples were decalcified, stained with 5-bromo-4chloro-indolyl-β-D-glacotpyranoside (X-gal), paraffin processed, sectioned and counterstained with Nuclear Fast Red. All images were taken near growth plates and trabecular bone regions at 1000X magnification under oil immersion.

Bone marrow transplantation assay. *Sost*$^{-/-}$→WT and WT→*Sost*$^{-/-}$ bone marrow chimeras were generated. All recipient mice were lethally irradiated with 1000 rads using a Cesium-137 source (J.L. Shepherd and Associates, San Fernando, CA), and a minimum of 4 hours were allowed to pass before bone marrow reconstitution. For the *Sost*$^{-/-}$→WT chimeras, B6.SJL-*Ptprc*^{a} *Pepc*^{b}/BoyJ (CD45.1^{+}) recipients were transplanted with 5 x 10^{6} *Sost*$^{-/-}$ CD45.2^{+} bone marrow cells (BMC) via retro-orbital intravenous injection. Control WT (CD45.2)→WT (CD45.1) chimeras were prepared by transplantation of wildtype C57BL/6J BMC into wildtype or B6.SJL-*Ptprc*^{a} *Pepc*^{b}/BoyJ (CD45.1^{+}) recipients. For the reciprocal WT→*Sost*$^{-/-}$ chimeras, C57BL/6J or *Sost*$^{-/-}$ recipients (both CD45.2^{+}) were transplanted with B6.SJL-*Ptprc*^{a} *Pepc*^{b}/BoyJ (CD45.1) BMC, and control WT (CD45.1) →WT (CD45.2) chimeras were prepared as described above. Peripheral blood samples were stained with CD45.1, CD45.2, Gr-1, CD11b, CD3ε, and CD19 and analyzed for the presence of donor chimerism at 3 weeks by FACS. Chimeras were euthanized at 5 weeks post-transplantation for analysis of donor hematopoietic lineages in the bone marrow and spleen.

B cell proliferation assay. Splenocytes from *Sost*$^{+/+}$ and *Sost*$^{-/-}$ mice were sterilely isolated and B cells were enriched by MACS depletion of CD3ε, CD4, CD8α, NK1.1, Ter119, NK 1.1, CD11b and Gr-1-positive cells. B cell purity was found to be >95% B220^{+} CD19^{+} (data not shown). MACS-purified B cells were washed four times with 1x PBS. Cells were then washed two more times with culture media containing DMEM (Invitrogen) with 10% FCS (Atlanta Biologicals), 1x penicillin/streptomycin (Invitrogen), and 5 x10^{-5} M 2-mercaptoethanol. Cells were then plated at a concentration of 2.0- 5.0 x 10^{5} cells per well, in triplicate, in a 96-well flat bottom plate (Fisher Scientific), in the presence of 0, 10, or 100 μg/ml LPS (Sigma-Aldrich). Cells were then kept in a humidified cell incubator with 5% CO_2 at 37^{o}C for 48 or 72 hours. After incubation, cultures were harvested, counted and analyzed by FCM.

Statistical analysis. Differences between the means of biological replicates for all samples were calculated using two tailed Student's T-test (GraphPad Prism, La Jolla, CA, USA). The two tailed Student's T-test was justified by the assumption that all samples follow a Gaussian distribution even though sample sizes are small, and are not paired samples. All samples were considered statistically significant if $p < 0.05$.

3.3 Results:

Reduction of B cells in the bone marrow of Sost$^{-/-}$ mice

Sost$^{-/-}$ mice were generated using conventional gene targeting methods, in which the Sost open reading frame was replaced with *LacZ* to generate the null allele [79]. *Sost*$^{-/-}$ mice display a high bone mass phenotype and reduced BM cavity volume in both male and female mice, very similar to the phenotype of the *Sost* knockout mice generated by Li et al. [78,79]. Consistent with this, the total numbers of BM cells and CD45^{+} (hematopoietic) cells were significantly decreased in *Sost*$^{-/-}$ mice (Figure 3.1A). However, no difference in the percentage of CD45^{+} cells was observed between *Sost*$^{-/-}$ and wild-type (*Sost*$^{+/+}$) controls (Figure 3.1A).

We also examined the frequencies of committed lymphoid and myeloid lineages in *Sost*$^{-/-}$ mice. Consistent with the clear reduction in overall BM cellularity, the numbers of cells amongst all lymphoid and myeloid lineages were severely reduced in *Sost*$^{-/-}$ mice. No differences in the frequencies of T lymphocytes (CD3ε^{+}), natural killer cells (NK1.1^{+}), monocytes (CD11b^{+} Gr-1^{-}), granulocytes (CD11b^{+} Gr-1^{+}) and erythroid cells (TER-119^{+}) were observed in the BM (Figures 3.1B – 1D). However, CD19^{+} B cells were significantly reduced in both their frequency and cell number in the BM (Figures 3.1C, 1D), indicating a B cell-specific defect due to the absence of *Sost.*

Elevated apoptosis in B cells in the bone marrow of Sost$^{-/-}$ mice

B cell maturation in the BM proceeds through a series of steps that have been defined by cell surface marker expression. HSCs differentiate into CLP, which then give rise to the early pre/pro-B cell progenitor (also known as Fraction A) identified as negative for

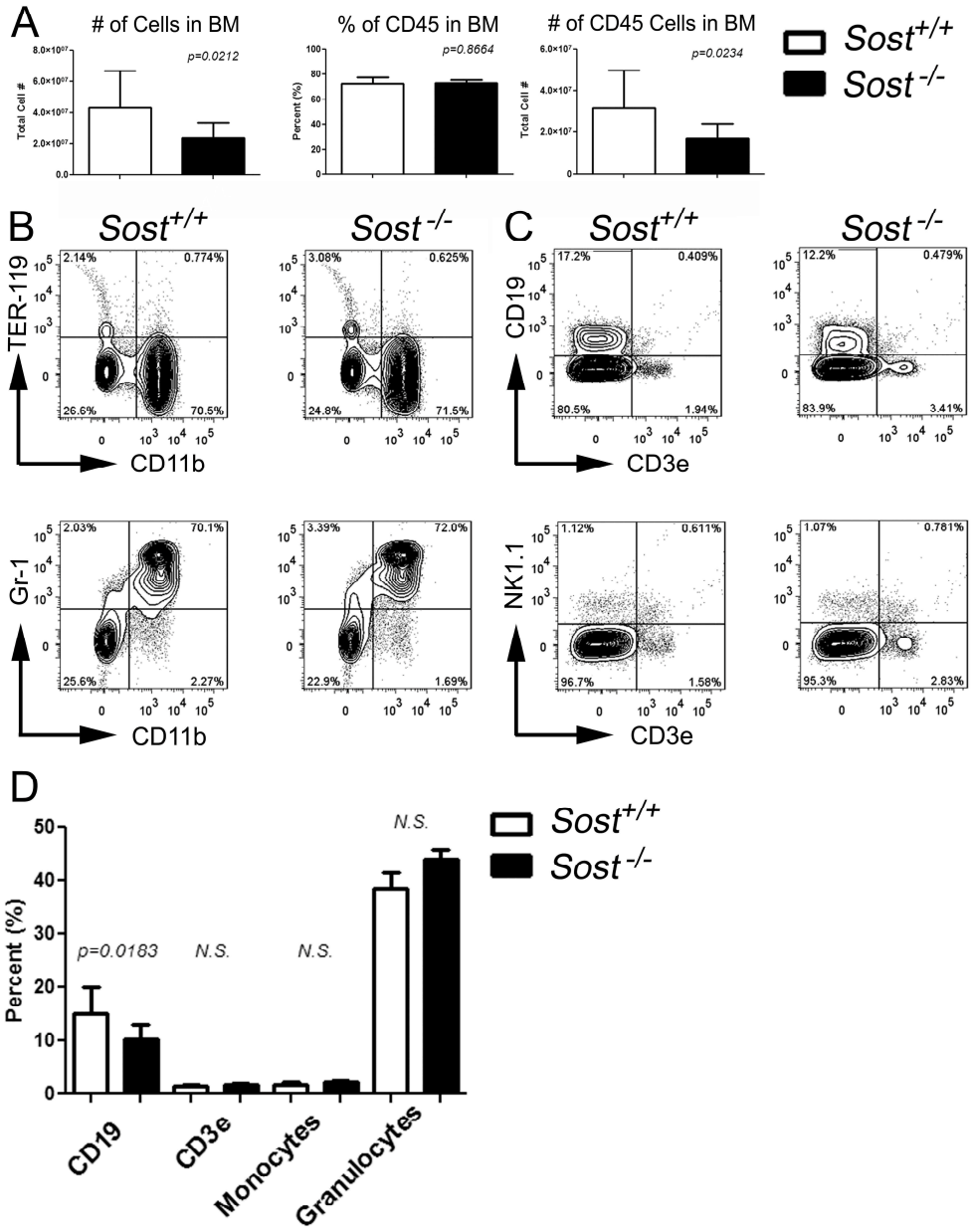

Figure 3.1: CD19^{pos} B cell populations in the bone marrow are reduced in Sost$^{-/-}$ mice. **(A)** Total number of bone marrow cells (left panel), total percentage (middle panel) and total number of CD45^{+} (right panel) in the bone marrow. **(B)** FCM plots of myeloid lineages in wildtype (*Sost*$^{+/+}$) and *Sost*$^{-/-}$ mice. **(C)** FCM plots of lymphoid lineages in wild type and *Sost*$^{-/-}$ mice. **(D)** Total percentages of B cells (CD19^{+}), T cells (CD3ε^{+}), monocytes (CD11b^{+} Gr-1^{-}) and granulocytes (CD11b^{+} Gr-1^{+}). Data are representative of *Sost*$^{+/+}$ (n=6) and *Sost*$^{-/-}$ (n=12) of pooled sexes at 8 to 13 weeks of age. Mean ± SD are shown, and were considered to be statistically significant if $p < 0.05$, two-tailed Student's T-test.

CD3ε, CD4, CD8, CD11b, Gr-1, NK1.1, Ter119, CD19, IgM, and c-Kit and positive for B220 [91]. Subsequent immunoglobulin heavy chain gene rearrangements ensure commitment and differentiation into pro-B cells (also known as Fraction B/C) that are $CD19^{+}$ $B220^{lo}$ c-Kit^{+} IgM^{-} [131,132], but negative for other lineage-specific markers. Further rearrangement of light chain genes confers differentiation into the pre-B cell (also known as Fraction D) with subsequent c-Kit downregulation. Functionally immature B cells ($CD19^{lo}$ $B220^{lo}$ c-Kit^{-} IgM^{+}) that survive negative selection become mature IgD-expressing B cells, which then migrate out of the BM into the periphery. These mature, recirculating B cells can then be identified by their surface phenotype ($CD19^{high}$ $B220^{high}$ c-Kit^{-} IgM^{+}) when they return to the BM [91,132].

To identify if and where a block in B cell development occurred in *Sost*$^{-/-}$ mice, we examined the frequencies of the stages of B cell differentiation in the BM in *Sost*$^{+/+}$ and *Sost*$^{-/-}$ mice. In our analysis, we used a staining strategy in which pre/pro-, pro- and pre-B cells are observed as one group (designated "B cell precursors" for simplicity), but immature and recirculating B cells in the BM can be distinguished [131,132,133]. We observed significant decreases in the frequencies of all committed B cell developmental stages (Figures 3.2A, 2C). Additional flow cytometric analysis using the Hardy nomenclature confirmed that block in B cell development occurred very early at the Fraction B (pro-B/pre-B-1) stage, and this block is maintained until the Fraction D (late pre-B) stage in *Sost*$^{-/-}$ mice (Figure 3.3A-D). In addition, the number of mature B cells in Fraction F was notably decreased (Figure 3.3E). The decline in B cells directly correlated with increased levels of apoptotic cells at the "precursor", immature and recirculating stages of B cell development in *Sost*$^{-/-}$ mice, as measured by co-staining

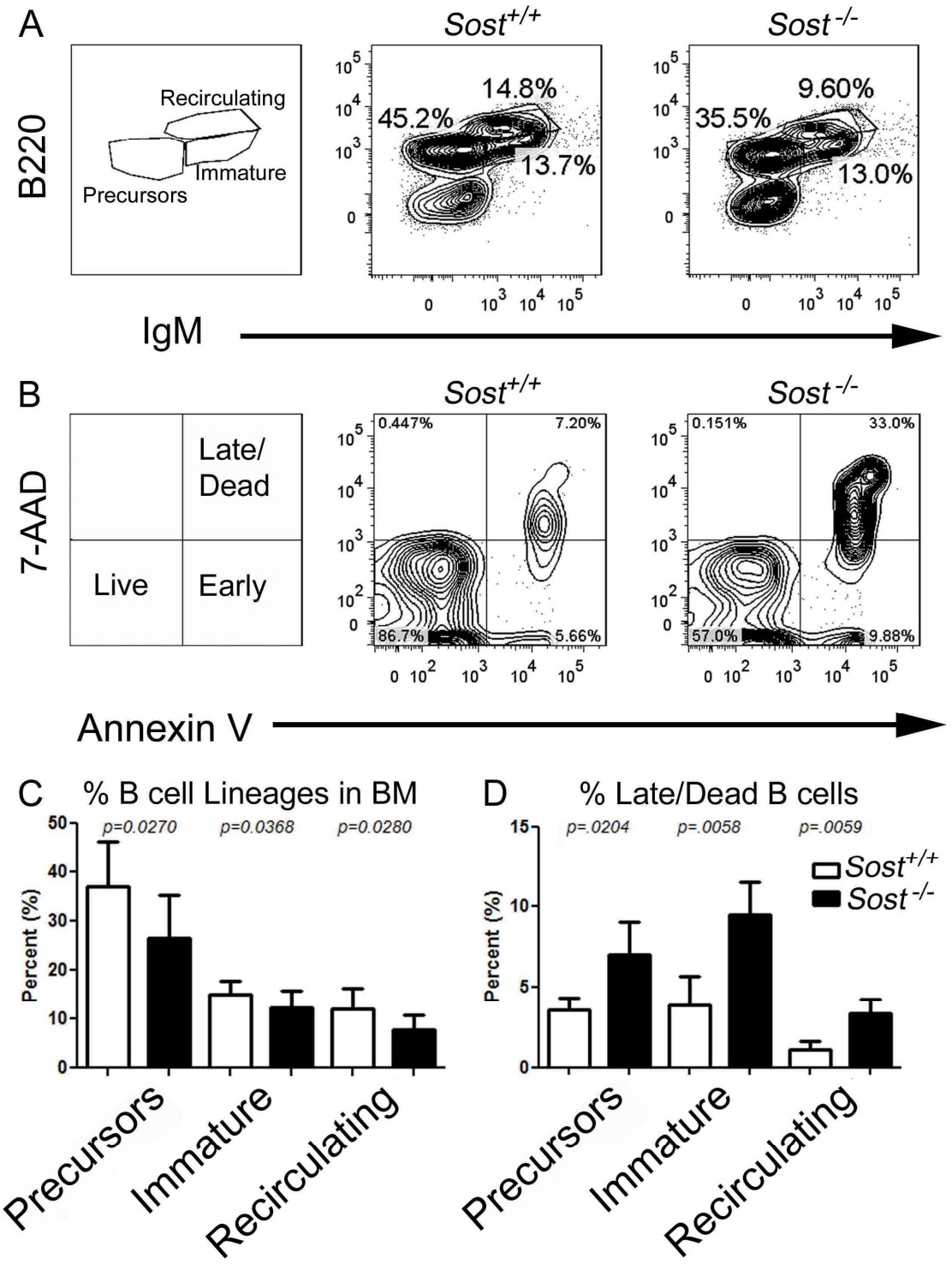
A
B220
Recirculating
Immature
Precursors
Sost+/+
Sost -/-
14.8%
45.2%
13.7%
9.60%
35.5%
13.0%
IgM
B
7-AAD
Late/
Dead
Live
Early
0.447%
7.20%
86.7%
5.66%
0.151%
33.0%
57.0%
9.88%
Annexin V
C
% B cell Lineages in BM
p=0.0270
p=0.0368
p=0.0280
Percent (%)
Precursors
Immature
Recirculating
D
% Late/Dead B cells
p=.0204
p=.0058
p=.0059
Sost+/+
Sost -/-
Percent (%)
Precursors
Immature
Recirculating

Figure 3.2: Elevated B cell apoptosis in Sost$^{-/-}$ mice. **(A)** FCM plots showing B cell developmental stages from bone marrow. The left panel shows the gating strategy for "precursors", immature and recirculating B cell populations. The middle and the right panels represent staining from the *Sost*$^{+/+}$ and *Sost*$^{-/-}$ mice, respectively. **(B)** Representative analysis of apoptosis by FCM in "precursor" B cells, as measured by staining with Annexin-V and 7-AAD. Live (Annexin-V^{-} 7-AAD^{-}), early apoptotic (Annexin-V^{+} 7-AAD^{-}) and combined late apoptotic and dead (Annexin-V^{+} 7-AAD^{+}) B cells are discriminated. **(C)** Total percentages of pre/pro-, pro- and pre-B cells combined ("precursors": B220^{+} IgM^{-}) (left panel), immature (B220^{+} IgM^{+}) (middle panel) and recirculating (B220^{high} IgM^{+}) (right panel) B cells in *Sost*$^{+/+}$ (n=8) and *Sost*$^{-/-}$ (n=10) mice. **(D)** Total percentages of Annexin-V^{+}, 7-AAD^{+} "precursors" (left panel), immature (middle panel) and recirculating (right panel) B cells in *Sost*$^{+/+}$ and *Sost*$^{-/-}$ bone marrow. Data are representative of *Sost*$^{+/+}$ (n=4) and *Sost*$^{-/-}$ (n=3) that are of pooled sexes and 12 to 15 weeks of age. Mean ± SD are shown, and all data were considered to be statistically significant if $p < 0.05$, two-tailed Student's T-test.

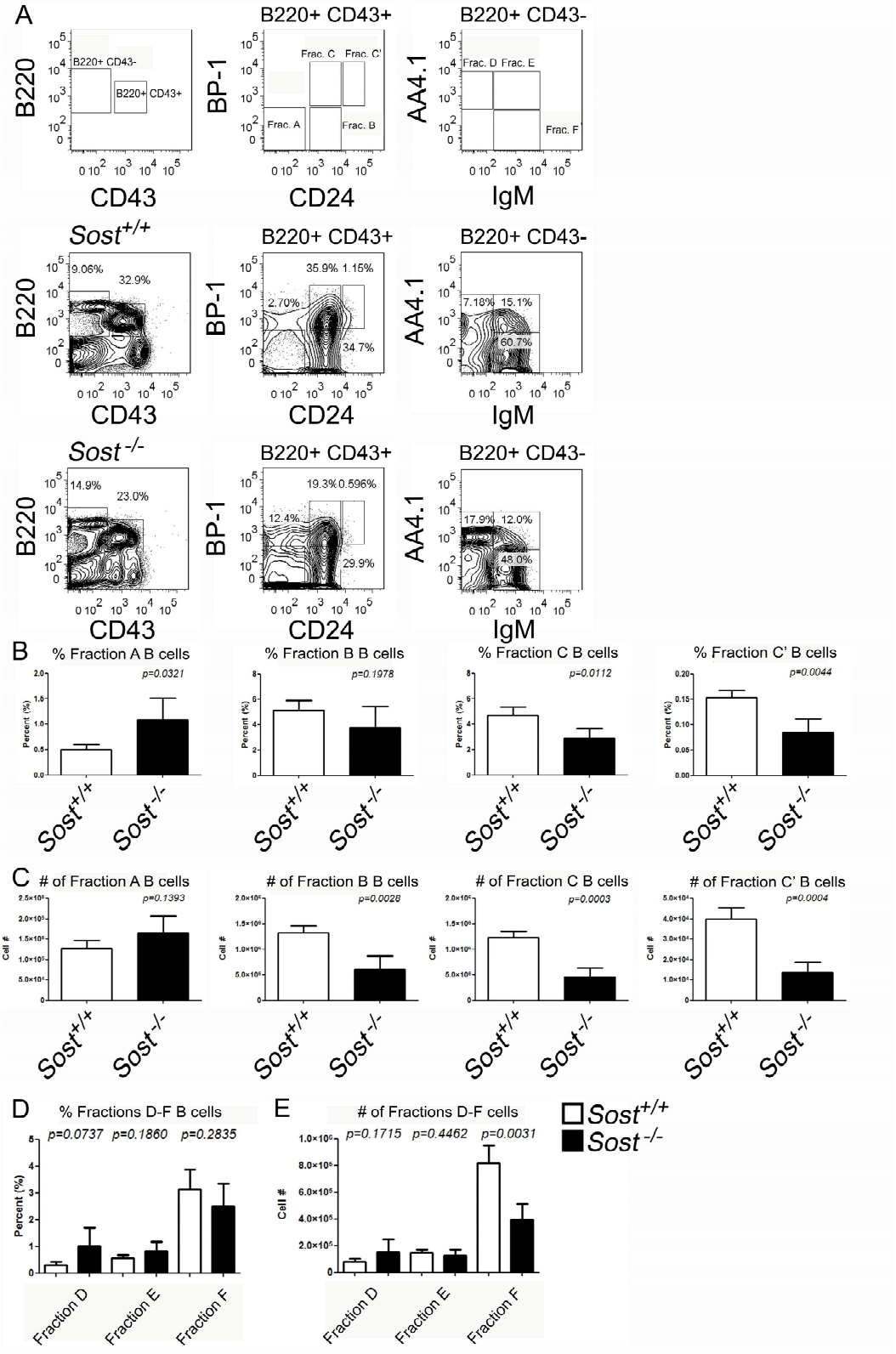
A
B220+ CD43+
B220+ CD43-
B220
BP-1
AA4.1
CD43
CD24
IgM
B220+ CD43-
Frac. A
Frac. B
Frac. C
Frac. C'
Frac. D
Frac. E
Frac. F
Sost+/+
Sost -/-
9.06%
32.9%
35.9%
1.15%
2.70%
34.7%
7.18%
15.1%
60.7%
14.9%
23.0%
19.3%
0.596%
12.4%
29.9%
17.9%
12.0%
48.0%
B
% Fraction A B cells
% Fraction B B cells
% Fraction C B cells
% Fraction C' B cells
p=0.0321
p=0.1978
p=0.0112
p=0.0044
Percent (%)
C
# of Fraction A B cells
# of Fraction B B cells
# of Fraction C B cells
# of Fraction C' B cells
p=0.1393
p=0.0028
p=0.0003
p=0.0004
Cell #
D
% Fractions D-F B cells
p=0.0737
p=0.1860
p=0.2835
Fraction D
Fraction E
Fraction F
E
# of Fractions D-F cells
p=0.1715
p=0.4462
p=0.0031
Sost+/+
Sost -/-

Figure 3.3: Early B cell progenitors are reduced in Sost$^{-/-}$ mice. (A) Representative FCM plots of bone marrow B cell fractions A through F. The top panels show the gating strategy for B cell Fractions A-F using B220, CD43, BP-1, CD24, and IgM and the bottom histograms show AA4.1 staining in those Fractions. Data from representative *Sost*$^{+/+}$ and *Sost*$^{-/-}$ mice are shown. B cell fractions were phenotypically defined as follows: *Fraction A:* Lineage^{-} B220^{+} CD43^{+} BP-1^{-} CD24^{-} AA4.1^{+}; *Fraction B:* Lineage^{-} B220^{+} CD43^{+} BP-1^{-} CD24^{+} AA4.1^{+}; *Fraction C:* Lineage^{-} , B220^{+} CD43^{+} BP-1^{+} CD24^{+} AA4.1^{+}; *Fraction C'*: Lineage^{-} B220^{+} CD43^{+} BP-1^{+} CD24^{high} AA4.1^{+}; *Fraction D*: Lineage^{-} B220^{+} CD43^{-} AA4.1^{+} IgM^{-}; *Fraction E*: Lineage^{-} B220^{+} CD43^{-} AA4.1^{+} IgM^{+}. *Fraction F*: Lineage^{-} B220^{+} CD43^{-} AA4.1^{-} IgM^{+} (**B)** Frequencies of cells within the Fractions A through C'. **(C)** Total cell numbers in Fractions A through C'. **(D)** Frequencies of B cell Fractions D through F. **(E)** Total cell numbers of B cell Fractions D through F. **(B-E)** Data shown are representative of 4 *Sost*$^{+/+}$ and 4 *Sost*$^{-/-}$ age and sex matched mice. Mean ± SD are shown, and all differences were considered statistically significant if $p<0.05$ by Student's two-tailed T-test.

with Annexin V and 7-AAD (Figures 3.2B and 3.2D). However, no difference in apoptosis was evident in the Lineage$^-$ CD19$^-$ B220$^-$ IgM$^-$ populations, which contain the HSC, CLP, and stromal populations in the bone marrow (data not shown). Interestingly, the observed decrease in B cell populations in the bone marrow did not extend to the spleen, and but we did note an increase in splenic granulocytes in *Sost*$^{-/-}$ mice (Figures 3.4 and 3.5). Splenic B cells in *Sost*$^{-/-}$ mice were comparable to B cells in wildtype mice, both in frequency and in function when stimulated by lipopolysaccharide (Figures 3.6 and 3.7). These data indicate that the reduction of B cells observed in the BM of *Sost*$^{-/-}$ mice is due to increased apoptosis at all committed B cell developmental stages in the bone marrow, but does not affect survival and antigen response in peripheral lymphoid organs.

Expression of Wnt signaling pathway and target genes in B cells

High expression of *Sost* mRNA has been reported in osteocytes, with associated diffuse SOST protein staining in osteocytic dendrites and canaliculi [134]. To assess whether the B cell phenotype observed in *Sost*$^{-/-}$ mice is due to a cell-autonomous versus non-cell-autonomous defect in the BM niche, we examined purified "precursor", immature, and recirculating B cell populations from the bone marrow for expression of *Sost* by RT-PCR. *Sost* expression was not observed in any B cell population (Figures 3.8A and 3.8B), supporting that the effect of the absence of *Sost* on B cells is non-cell-autonomous.

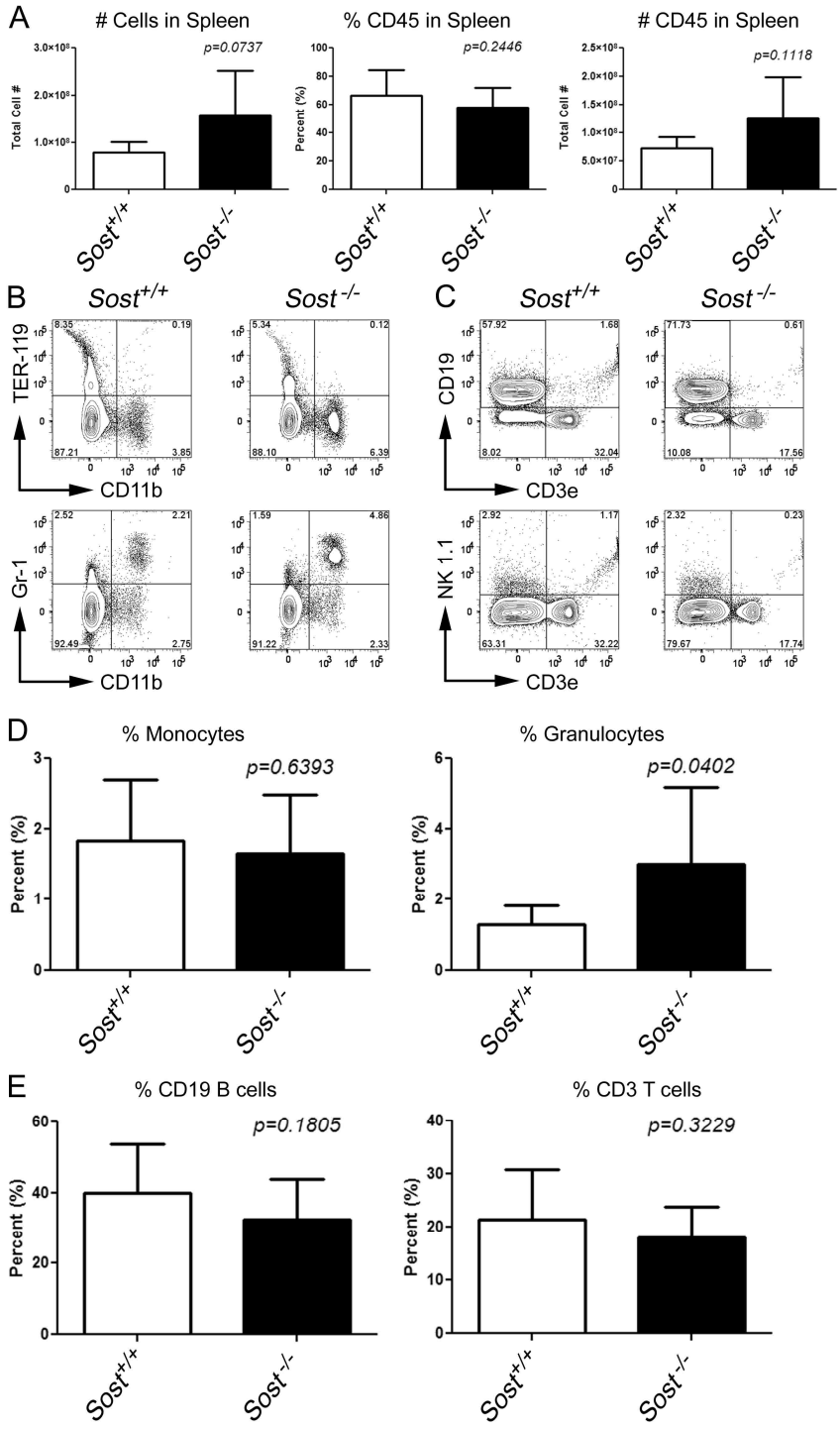
A
# Cells in Spleen
p=0.0737
Total Cell #
% CD45 in Spleen
p=0.2446
Percent (%)
# CD45 in Spleen
p=0.1118
Total Cell #
Sost+/+
Sost-/-
B
Sost+/+
Sost -/-
TER-119
CD11b
Gr-1
CD11b
C
Sost+/+
Sost -/-
CD19
CD3e
NK 1.1
CD3e
D
% Monocytes
p=0.6393
Percent (%)
% Granulocytes
p=0.0402
Percent (%)
E
% CD19 B cells
p=0.1805
Percent (%)
% CD3 T cells
p=0.3229
Percent (%)

Figure 3.4: Splenic myeloid lineages are altered in Sost$^{-/-}$ mice. **(A)** Total number (left panel, 6 *Sost*$^{+/+}$ and 12 *Sost*$^{-/-}$ mice), total percentage (middle panel, left panel, 8 *Sost*$^{+/+}$ and 14 *Sost*$^{-/-}$ mice) and total number of CD45^{+} (right panel, left panel, 8 *Sost*$^{+/+}$ and 14 *Sost*$^{-/-}$ mice) in the spleen. **(B)** Representative FCM plots of splenic myeloid lineages in wildtype and *Sost*$^{-/-}$ mice. **(C)** Representative FCM plots of splenic lymphoid lineages in wildtype and *Sost*$^{-/-}$ mice. **(D)** Frequencies of CD11b^{+}, Gr-1^{+} granulocytes (left panel), and CD11b^{+} monocytes (right panel) in the bone marrow. **(E)** Frequencies of CD19^{+} B cells (left panel) and CD3ε $^{+}$ T cells (right panel) in the bone marrow. For **(B-E)**, data shown are representative of 8 *Sost*$^{+/+}$ and 14 *Sost*$^{-/-}$ mice. Data were collected from a pool of mixed sexes and 8 to 13 weeks of age. Mean ± SD are shown, and all differences were considered statistically significant if $p<0.05$ by two-tailed Student's T-test.

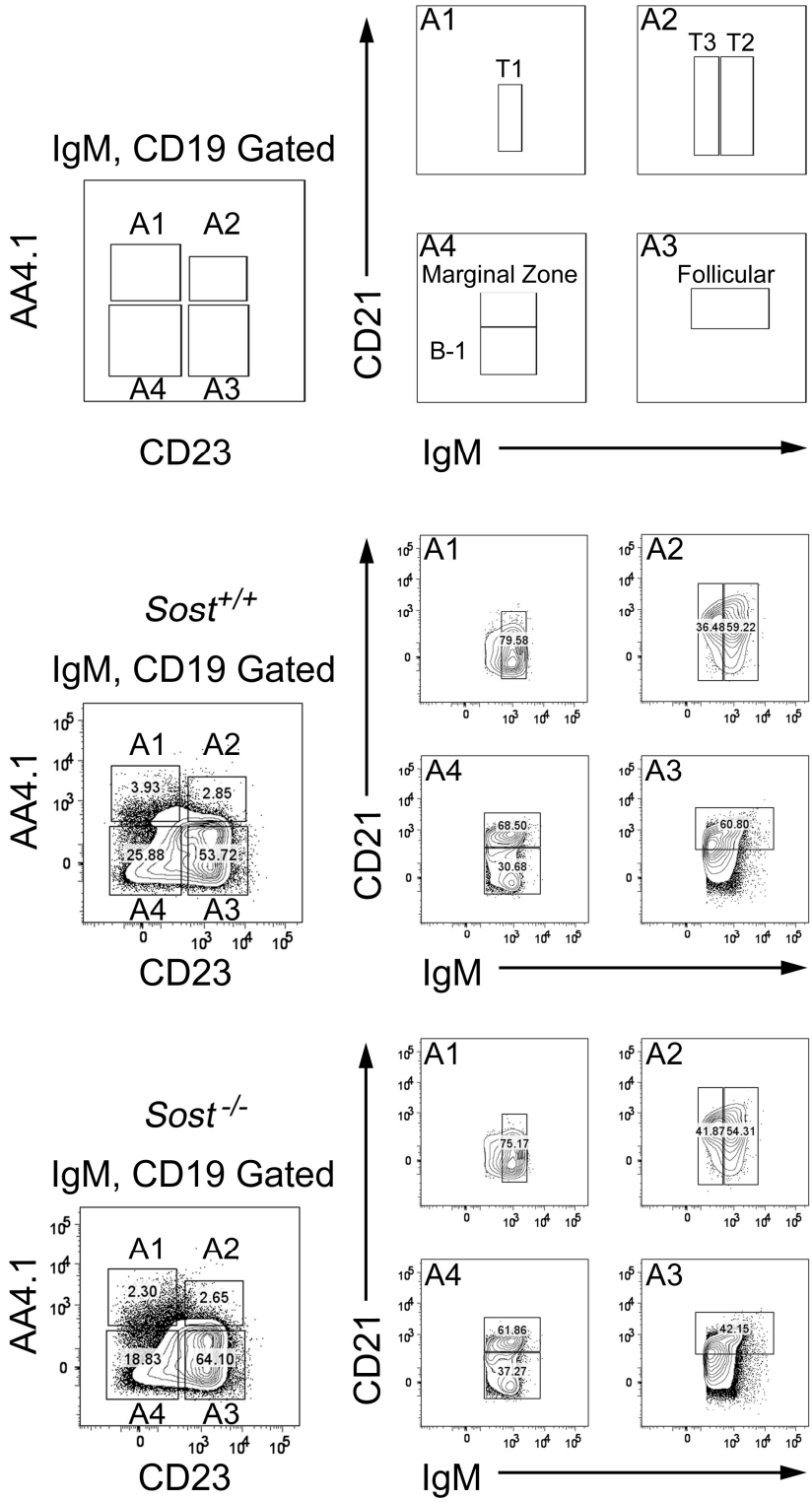
IgM, CD19 Gated
AA4.1
CD23
A1
A2
A4
A3
CD21
IgM
T1
T3 T2
Marginal Zone
B-1
Follicular
Sost+/+
3.93
2.85
25.88
53.72
79.58
36.48
59.22
68.50
30.68
60.80
Sost -/-
2.30
2.65
18.83
64.10
75.17
41.87
54.31
61.86
37.27
42.15

Figure 3.5: Splenic B cell populations appear to be unaffected by the absence of Sost. Representative FCM plots of splenic B cell populations in *Sost*$^{+/+}$ and *Sost*$^{-/-}$ mice. The top panel shows the gating strategy for splenic B cell populations from transitional 1-3, follicular, marginal zone and B-1 cells in the spleen. The middle and lower panel show representative FCM plots for wildtype and *Sost*$^{-/-}$ mice respectively. Data shown are representative of 4 *Sost*$^{+/+}$ and 3 *Sost*$^{-/-}$ pooled mice of mixed sexes and 8 to 13 weeks of age.

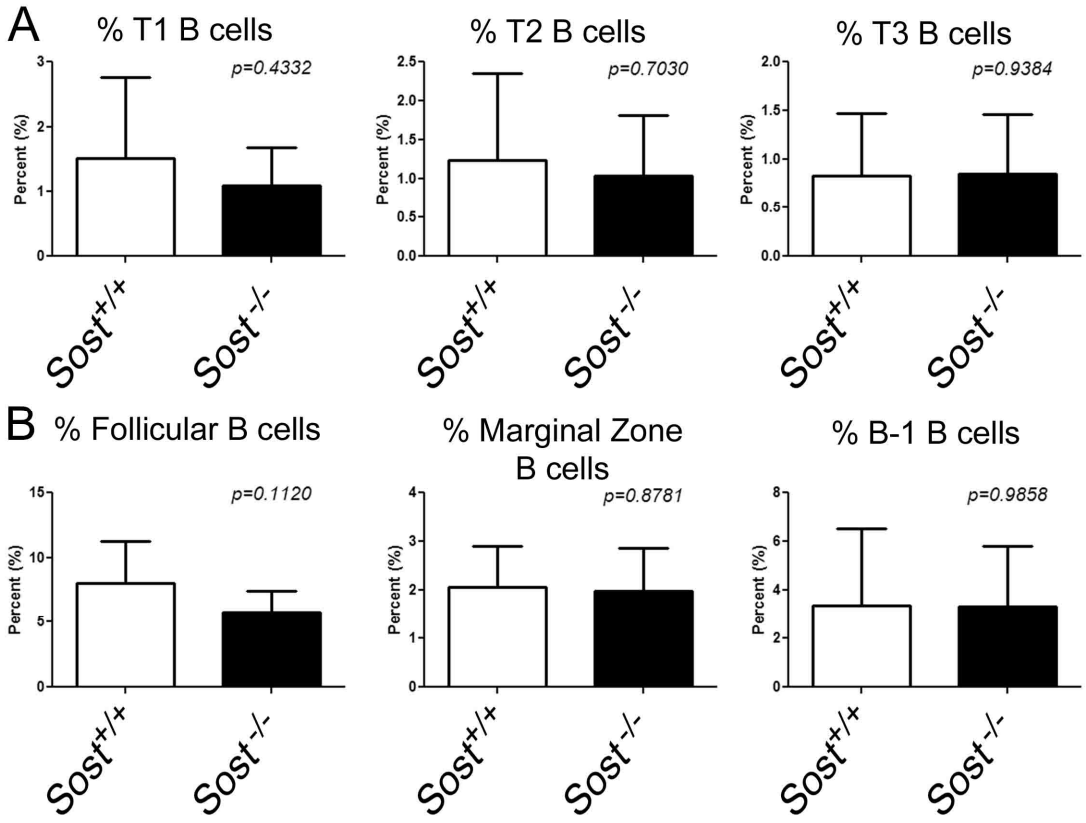

Figure 3.6: Quantification of splenic B cell frequencies in Sost$^{-/-}$ mice. **(A)** Total percentages for transitional 1 (left panel), transitional 2 (middle panel) and transitional 3 (right panel) B cells in *Sost*$^{+/+}$ and *Sost*$^{-/-}$ mice. **(B)** Total percentages for follicular (left panel), marginal zone (middle panel), and B-1 B cells (right panel) in *Sost*$^{+/+}$ and *Sost*$^{-/-}$ mice. Data shown are representative of 4 *Sost*$^{+/+}$ and 3 *Sost*$^{-/-}$ mice of mixed sexes and 8 to 13 weeks of age. Mean ± SD are shown, and differences were considered statistically significant if $p<0.05$ by two-tailed Student's T-test.

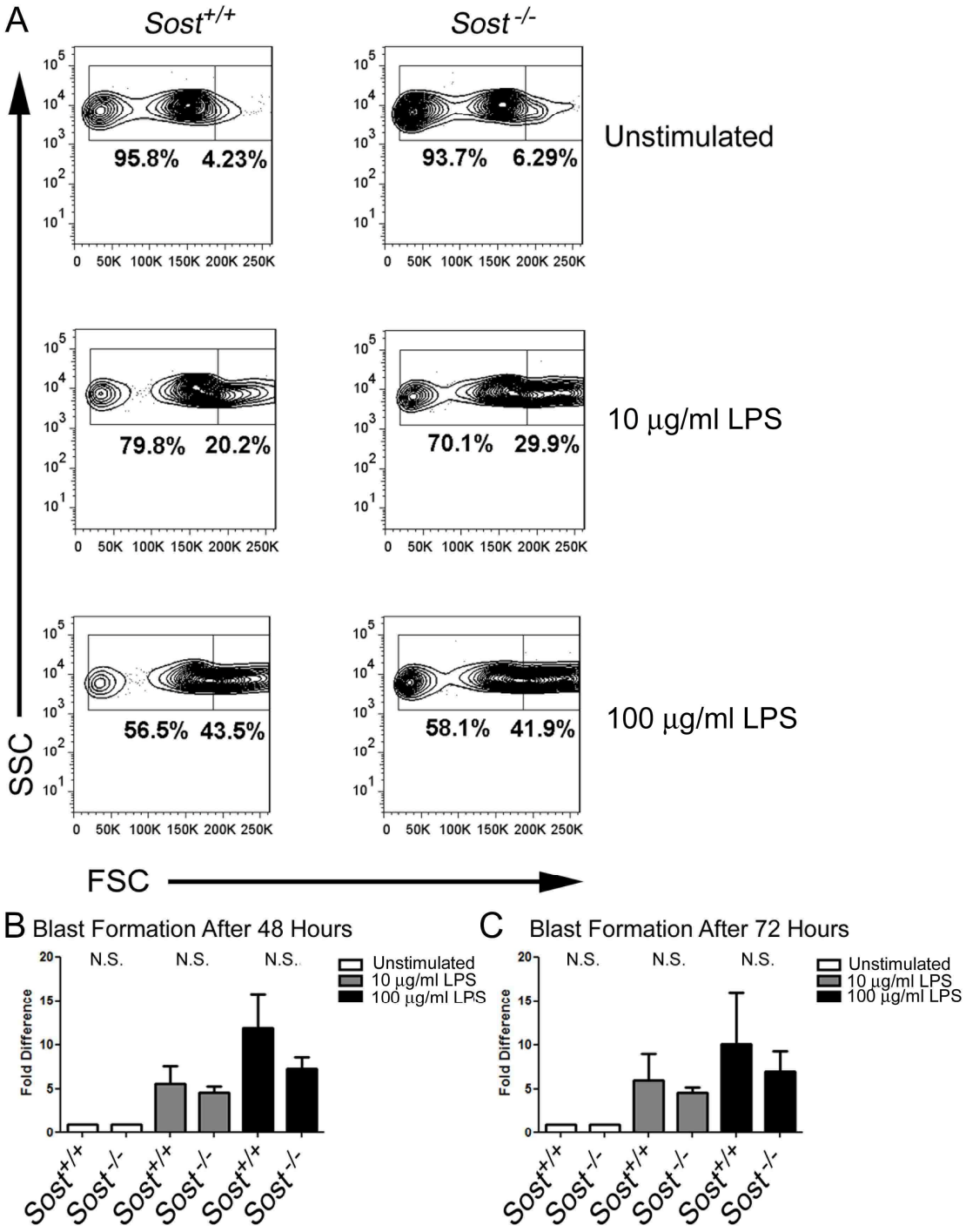
A
Sost+/+
Sost -/-
Unstimulated
10 μg/ml LPS
100 μg/ml LPS
95.8% 4.23%
93.7% 6.29%
79.8% 20.2%
70.1% 29.9%
56.5% 43.5%
58.1% 41.9%
SSC
FSC
0 50K 100K 150K 200K 250K
B Blast Formation After 48 Hours
C Blast Formation After 72 Hours
Fold Difference
N.S.
Unstimulated
10 μg/ml LPS
100 μg/ml LPS
Sost+/+
Sost-/-

Figure 3.7: SOST-deficient splenic B cells display normal proliferative responses to LPS. **(A)** FCM plots showing blast formation as measured by forward scatter (FSC) and side scatter (SSC) measures of cell size. Lineage-depleted (negative for CD3ε, CD4, CD8, NK 1.1, CD11b, Gr-1 and TER-119) splenic B cells were stimulated with 0, 10 or 100 μg/ml of LPS. A representative FCM plot from B cells stimulated for 48 hours is shown. **(B)** Changes in the mean percentages of blasts formed after 48 hours in culture. **(C)** Changes in the mean percentages of blasts formed after 72 hours in culture. Fold differences in **(B)** and **(C)** are normalized to the mean percentage of blasts present in 0 μg/ml cultures for each genotype. Data are representative of *Sost*$^{+/+}$, n=4 and *Sost*$^{-/-}$, n=3 mice of mixed sexes and 8 to 13 weeks of age. Mean ± SD are shown, and were considered to be statistically significant if $p < 0.05$, two-tailed Student's T-test.

All purified B cell populations expressed *Lrp5* and *Lrp6* but lacked expression of *Lrp4* (Figure 3.8A). We hypothesized that the lack of SOST binding to LRP5 and/or LRP6 on developing B cells could result in hyperactive Wnt signaling. This could then be measured in *Sost*$^{-/-}$ B cells by the expression of known Wnt target genes, such as *Ccnd1* (also known as cyclin-D1), *Lef-1*, and *c-Myc* to see if these genes were increased in the absence of *Sost* [43,45]. Amongst "precursor" and immature B cells, no differences in *Lef-1*, *c-Myc* or *Ccnd1* expression was observed. Expression of *c-Myc* increased up to two-fold in the recirculating B cells in *Sost*$^{-/-}$ mice (Figure 3.8C). These data showed that in the absence of *Sost*, expression of these Wnt target genes was unchanged in the early stage B cells, but differentially affected in recirculating B cells.

Sost is not expressed in any hematopoietic lineages in the bone marrow

We also examined all hematopoietic progenitors and committed lineages in the BM of *Sost*$^{+/+}$ mice for *Sost* expression by RT-PCR, and did not observe *Sost* expression in any of these cells (Figure 3.9A and data not shown). In contrast, *Sost* was clearly expressed in cells obtained from collagenase-digested bone (Figure 3.9A). These results were confirmed by RT-PCR for *LacZ*, which is a knocked-in reporter for endogenous *Sost* expression in *Sost*$^{-/-}$ mice (Figure 3.9B). The RT-PCR results were further validated by histology of whole bone sections (in which osteocytes as well as the BM cavity cells can be observed). *Sost* expression, as reported by *LacZ* activity, was clearly observed in the osteocytes in the tibias and calvaria of *Sost*$^{-/-}$ mice, but not in wildtype mice. In contrast, very low levels of *LacZ* activity were observed in the BM cavity (Figure 3.9C).

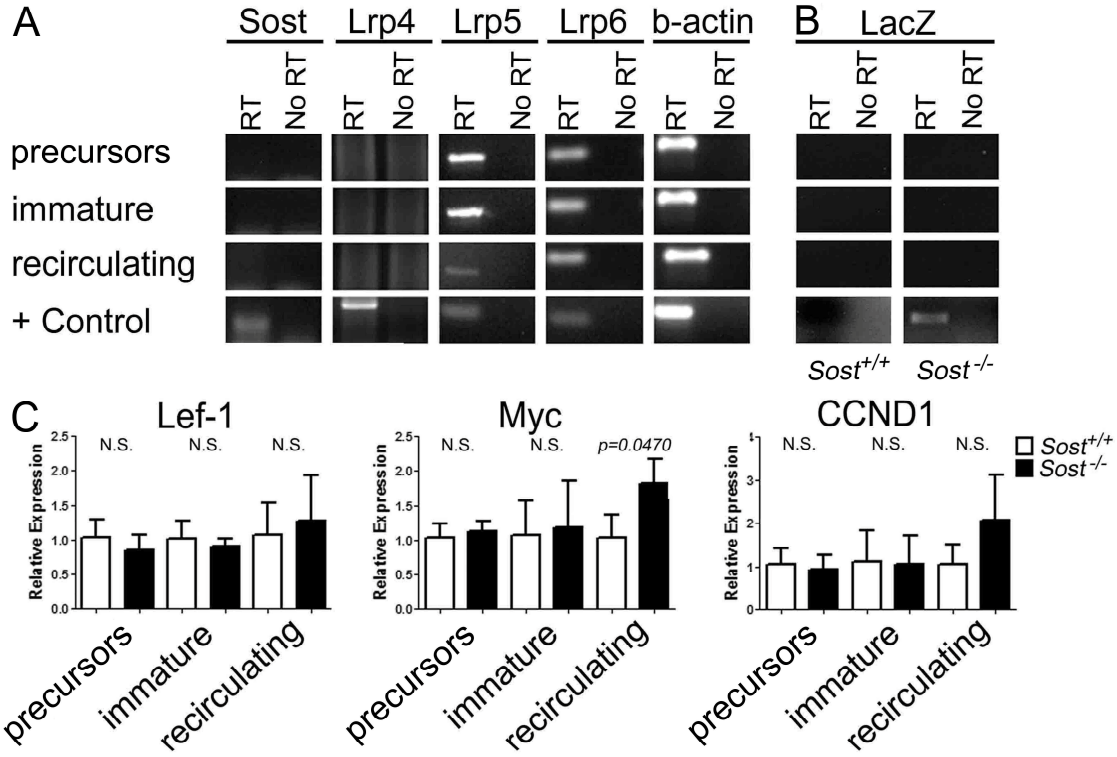

Figure 3.8: Wnt target genes in Sost$^{-/-}$ B cell populations. **(A)** Pre/pro, Pre- and Pro- ("Precursors"), immature and recirculating B cells were examined for the expression of *Sost*, *Lrp4*, *Lrp5*, and *Lrp6*, and β-actin. *Sost*$^{+/+}$ bone was used as the positive control ("+ control") tissue. **(B)** LacZ RT-PCR analysis to determine *Sost* expression in *Sost*$^{+/+}$ (left) and *Sost*$^{-/-}$ (right) B cell subsets. *Sost*$^{-/-}$ collagenase-digested bone was used as the positive control tissue for LacZ. **(C)** qRT-PCR for Wnt target genes *Lef-1*, c-*Myc and Ccnd1* in sorted B cell subsets. *Rpl-7* was used as the housekeeping gene. Relative gene expression in *Sost*$^{-/-}$ mice was calculated by normalizing to expression in the *Sost*$^{+/+}$ controls. Mean ± SD are shown from three mice of each genotype, and were considered to be statistically significant if $p < 0.05$, two-tailed Student's T-test.

Cxcl12 expression is significantly reduced in bone marrow stromal cells in Sost$^{-/-}$ mice

The lack of *Sost* expression in hematopoietic cells and its clear expression in the non-hematopoietic cell compartments supported the idea that the B cell defect observed in *Sost*$^{-/-}$ mice is non-cell autonomous, and implicated the osteoblast, osteocyte or other stromal cell populations in the bone as the source of SOST. B cell development, proliferation and survival in the BM rely on the production of interleukin-7 (IL-7), stem cell factor (SCF), and CXCL12 (also known as SDF-1), which are produced by BM stromal cells [91]. Examination of *Il7* and *Scf* levels by quantitative PCR of collagenase digested bones showed no statistical difference between *Sost*$^{-/-}$ and wildtype controls, although *Sost*$^{-/-}$ *Scf* levels were reduced, but did not reach statistical significance (Figures 3.10A and 3.10B). *Cxcl12* is highly expressed in bone marrow stromal cells including osteoblasts, endothelial cells and reticular cells, but is not expressed in hematopoietic cells [91,135]. *Cxcl12* was significantly reduced in *Sost*$^{-/-}$ mice, providing a possible explanation for their altered B cell development (Figure 3.10C).

Bone marrow transplantation assays confirm a non-cell autonomous role of Sost on B cell development

The reduction of *Cxcl12* and the lack of *Sost* expression in hematopoietic cell populations indicated that the reduction of B cells in *Sost*$^{-/-}$ mice was indeed due to a non-cell autonomous effect. To further test this hypothesis, we performed reciprocal bone marrow transplantation experiments, in which WT →*Sost*$^{-/-}$ and *Sost*$^{-/-}$→WT bone marrow chimeras were prepared. We hypothesized that if the effect of the absence of *Sost* on bone marrow B cells was cell extrinsic, then transplantation of WT bone marrow

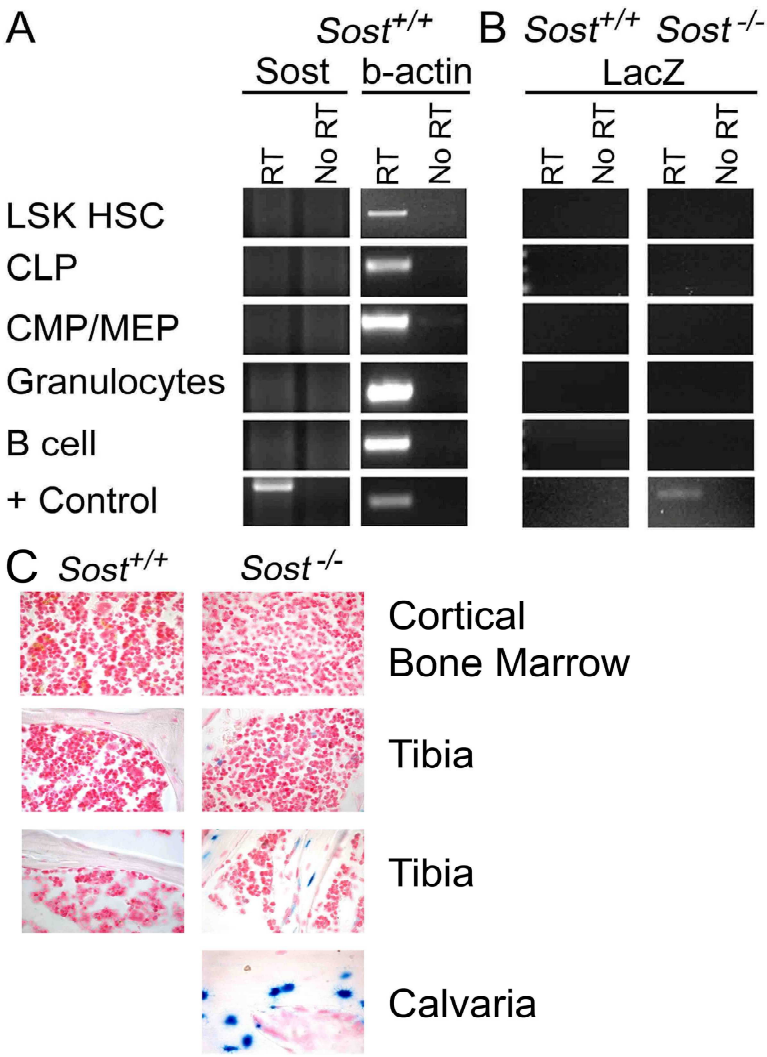

Figure 3.9: Sost is restricted to non-hematopoietic lineages. **(A)** *Sost* expression was determined using RT-PCR of mRNA isolated from FCM-sorted LSK HSC, CLP, CMP, granulocytes and B cells from *Sost*$^{+/+}$ mice. β-actin was used as a housekeeping gene and internal control. The positive control tissue for *Sost* expression was collagenase-digested bone. **(B)** RT-PCR for *LacZ* in sorted hematopoietic cell lineages in *Sost*$^{-/-}$ mice. mRNA from collagenase-digested bones from *Sost*$^{-/-}$ mice was used as the positive control for *LacZ*. RT-PCR for *Sost* in the *Sost*$^{-/-}$ mice was negative in all tissues examined (data not shown). **(C)** *Sost*$^{+/+}$ and *Sost*$^{-/-}$ cortical bone marrow (top), trabecular (two middle) and calvarial (bottom) 6 μm whole bone sections were stained for LacZ activity using X-gal (blue) and counterstained with Nuclear Fast Red. *Sost*$^{-/-}$ calvaria sections were used as a positive control for *LacZ* activity. Representative images from 20 slides prepared from 2 *Sost*$^{+/+}$ and 2 *Sost*$^{-/-}$ mice are shown.

into *Sost*$^{-/-}$ mice would result in a block in B cell development beginning at the "precursor" stage, but *Sost*$^{-/-}$ bone marrow transplanted into WT recipients would be result in normal B cell development. *Sost*$^{-/-}$ bone marrow transplanted into WT hosts engrafted and differentiated similarly to WT → WT control chimeras (Figure 3.10D). In contrast, transplantation of WT bone marrow into *Sost*$^{-/-}$ recipients resulted in a decrease in CD19^{+} B cells as well as a significant decrease in immature and recirculating B cell populations (Figure 3.10E) in the chimeras, similar to that observed in the *Sost*$^{-/-}$ mice (Figure 3.2). These results confirm that the bone microenvironment of the *Sost*$^{-/-}$ mice is unable to sufficiently support B cell development in the bone marrow, and the effect of *Sost* on B cell development is non-cell autonomous.

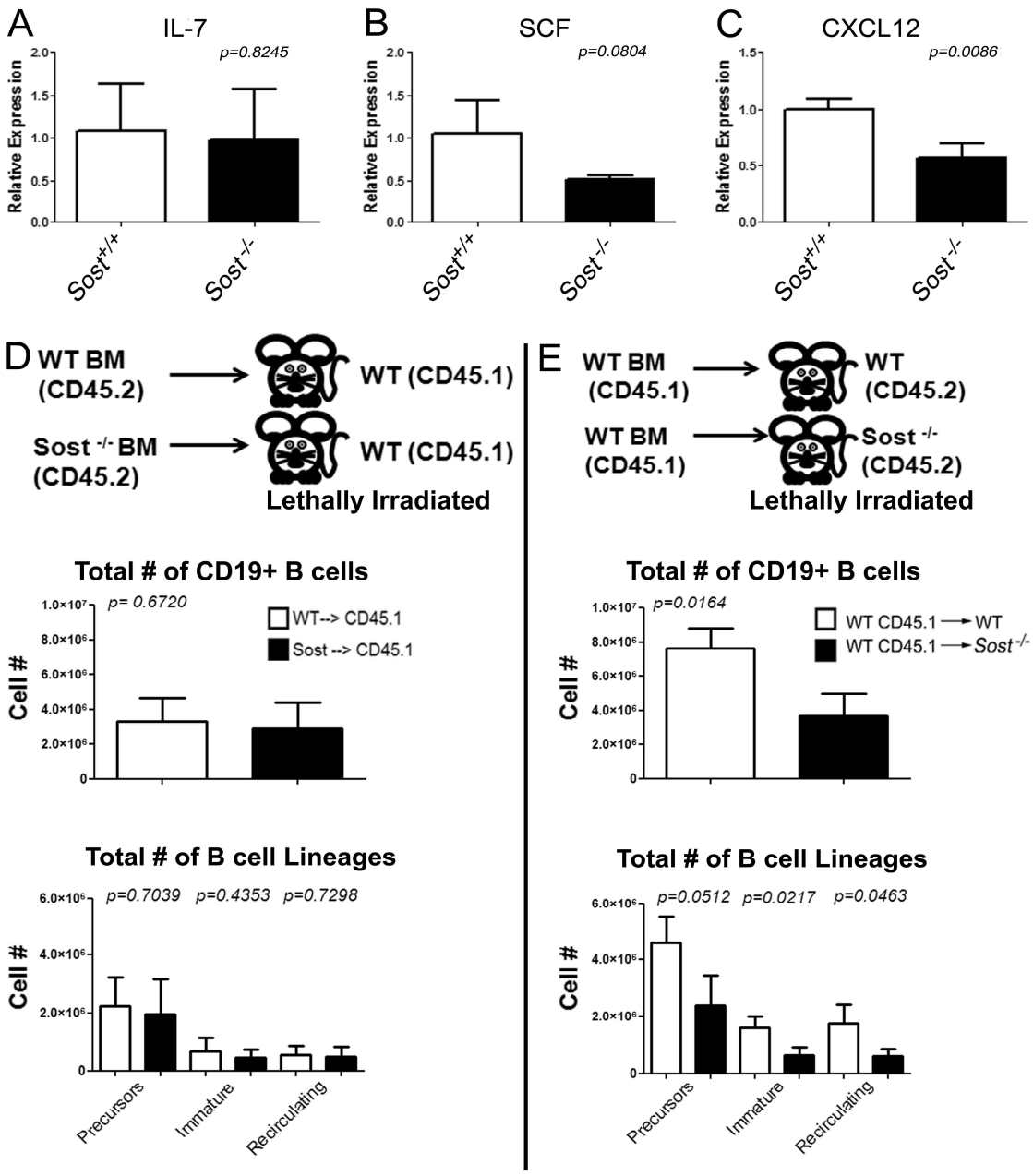
A
IL-7
p=0.8245
Relative Expression
Sost+/+
Sost-/-
B
SCF
p=0.0804
C
CXCL12
p=0.0086
D
WT BM (CD45.2)
WT (CD45.1)
Sost -/- BM (CD45.2)
Lethally Irradiated
E
WT BM (CD45.1)
WT (CD45.2)
Sost -/- (CD45.2)
Total # of CD19+ B cells
p= 0.6720
WT--> CD45.1
Sost --> CD45.1
Cell #
p=0.0164
WT CD45.1 → WT
WT CD45.1 → Sost -/-
Total # of B cell Lineages
p=0.7039 p=0.4353 p=0.7298
Precursors
Immature
Recirculating
p=0.0512 p=0.0217 p=0.0463

Figure 3.10: Evidence that the B cell defect in Sost$^{-/-}$ mice is cell-extrinsic. Expression analysis of *Il7* **(A)**, *Scf* **(B)** and *Cxc12* **(C)** by qRT-PCR. mRNA was extracted from digested, bone-marrow flushed bones. *Rpl-7* was used as the housekeeping gene. Relative gene expression in *Sost*$^{-/-}$ mice was calculated by normalizing to expression in the *Sost*$^{+/+}$ control. (**D**) Experimental scheme of bone marrow transplantation of CD45.2^{+} WT (n=5) or *Sost*$^{-/-}$ (n=5) bone marrow into CD45.1^{+} WT recipients (top panel). CD45.2^{+} (donor) cells were gated for analysis post-transplantation. The total number of donor-derived CD19^{+} cells in the bone marrow (middle panel), and the total number of "Precursors", immature and recirculating B cells (bottom panel) in WT(CD45.2)→WT(CD45.1) and *Sost*$^{-/-}$→WT chimeras are shown. (**E**) Scheme of reciprocal bone marrow transplantation of CD45.1^{+} WT bone marrow into CD45.2^{+} WT (n=3) or *Sost*$^{-/-}$ (n=3) mice (top panel). Donor CD45.1+ cells were gated for analysis post-transplantation, and the total number of donor-derived CD19^{+} cells in the bone marrow (middle panel), and the total number of donor-derived "Precursors", immature and recirculating B cells (bottom panel) in WT(CD45.1)→WT(CD45.2) and WT→*Sost*$^{-/-}$ chimeras are shown. Mean ± SD are shown from age and sex matched mice , and were considered to be statistically significant if $p < 0.05$, two-tailed Student's T-test.

3.4 Discussion:

Here, we demonstrate that the Wnt antagonist SOST plays an important role in bone marrow B cell development in the BM through a non-cell autonomous mechanism. Substantial reductions in CXCL12 in the stromal cells of *Sost*$^{-/-}$ mice are likely to be the causative mechanism for reduced B cell numbers in these mice [136]. Very recently, it has been shown that activation of Wnt signaling decreases CXCL12 expression in BM stromal cells *in vitro* [102], which supports our conclusions and provides a feasible link between *Sost*, Wnt signaling, and B cell development. Conditional ablation of osteoblasts resulted in blocks at the early pre/pro-B, pre-B and/or pro-B cell developmental stages or total loss of B cell development in the BM [90,93,137]. We propose a model in which osteocyte-secreted SOST regulates Wnt signaling in BM stromal cells and their production of *Cxcl12* at levels that are permissive for the support of B cell differentiation (Figure 3.11A). According to this model, overactive Wnt signaling in the stromal cells in the absence of *Sost* results in a reduction of *Cxcl12* to levels that are not conducive for B cell survival (Figure 3.11B). We speculate that this occurs via a set of events in which *Sost* normally promotes bone homeostasis by blocking osteoblast differentiation directly [134], which in turn, perhaps affects the differentiation or function of early mesenchymal stem cells (MSC) or osteoprogenitor populations. MSC and other BM stromal cells (namely, CAR cells [6] are located in the BM cavity and have been shown to express CXCL12 and produce appropriate B cell microenvironments. However, the causative link between *Sost*, changes in osteolineage cells, the reduction in *Cxcl12* expression and altered B cell development must still be experimentally verified. Clearly, the elucidation of the exact mechanisms by which

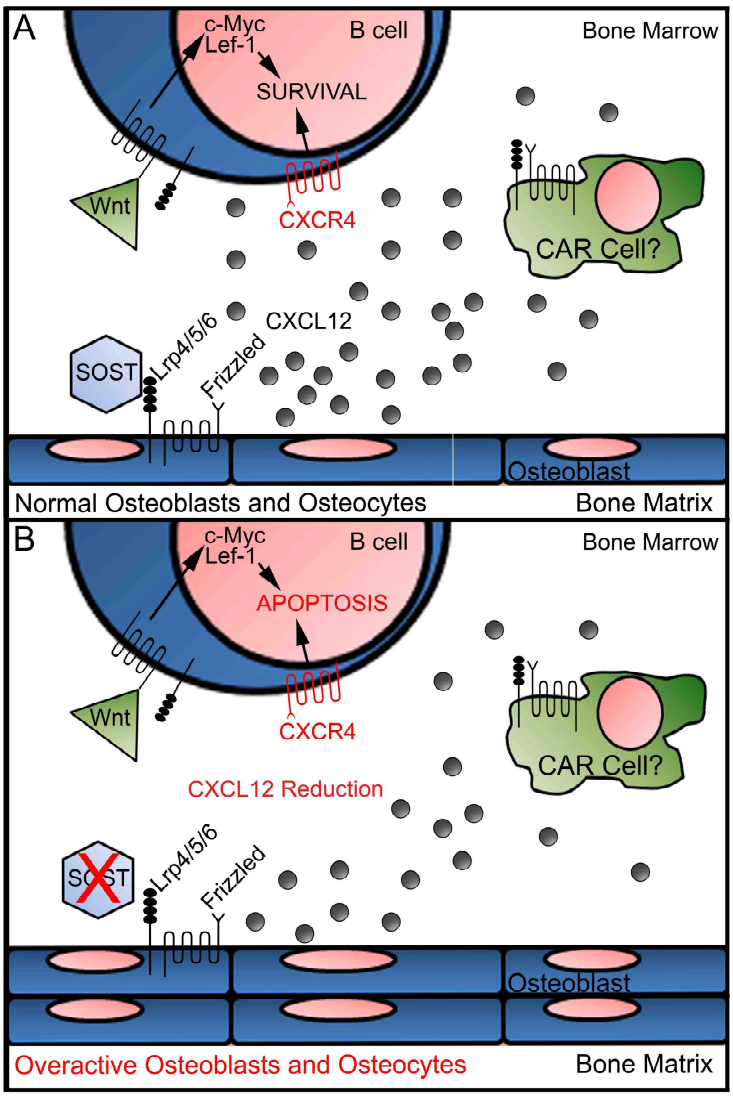

Figure 3.11: Proposed model for the effect of Sost on B lymphopoiesis. **(A)** Under normal circumstances, osteocytes secrete SOST, which binds to LRP5 or LRP6 (which are associated with Frizzled receptors) to regulate maturation of osteoblasts into osteocytes. It is unclear whether SOST can directly bind to LRP5/6 receptors on B cells or if SOST can regulate Wnt signaling in other cell types (i.e. CXCL12 abundant reticular (CAR) cells or osteoclasts (not shown in figure)). In this model, CXCL12 expression by endosteal OBs and CAR cells is activated by downregulation of Wnt signaling via SOST, to promote B cell survival via CXCL12/CXCR4 signaling. **(B)** *Sost* deletion results in excessive osteoblast differentiation into osteocytes, resulting in high bone mass. In addition, CXCL12 expression by *Sost*$^{-/-}$ osteoblasts and/or other stromal cell populations is reduced due to lack of SOST-mediated inhibition of Wnt signaling. In turn, this reduction of CXCL12 results in the induction of apoptosis at all B cell stages in the bone marrow.

SOST indirectly promotes B cell development will benefit from the creation of new osteoprogenitor-specific and BM stromal-cell specific transgenic and knockout mouse strains, and identification of biomarkers that can distinguish between cells at distinct stages of osteogenesis as well as different stromal cell types [103].

The possibility that SOST could directly bind to LRP5 or LRP6 on developing B cells to antagonize Wnt activation is not formally excluded by our results. *Lrp5*$^{-/-}$ mice display an osteoporotic bone phenotype, but have normal B cell development (C.J.C., unpublished results). *Lrp6*$^{-/-}$ mice are embryonically lethal [73], hence precluding the study of B cell development in these mice. Our results, which show no difference in the expression of Wnt target genes in "precursor" and immature stages of B cell development, suggest that direct regulation of Wnt signaling by SOST at these stages is irrelevant for their development and support the idea that the effect of SOST on B cell development is non-cell autonomous. Our bone marrow transplantation studies confirm the hypothesis that the reduction in B cells is due to alterations in the bone microenvironment in *Sost*$^{-/-}$ mice. The increase in *c-Myc* expression in mature, recirculating B cells and its relationship to apoptosis is unclear, as recirculating B cells in *c-Myc*-deficient mice do not undergo apoptosis, and no studies have explicitly examined *c-Myc* overexpression and mature B cell survival together [138,139].

We cannot completely rule out that hematopoiesis and B cell development are simply negatively regulated by a hypermineralized environment or by the size of the BM cavity, independent of SOST. HSC self-renewal, colony-forming ability, and hematopoietic differentiation appears to be negatively affected by osteoblast mineralization *in vitro* [[70] and Chapter 2)]. Several knockout mouse models which

display reduced BM cavity size and similar defects in hematopoiesis to that observed in *Sost*$^{-/-}$ mice exist. For example, the *op/op, oc/oc, mi/mi,* and *Fos*$^{-/-}$ mice are models of osteopetrotic disease that present with small BM cavities and defective B lymphopoiesis in the BM. In contrast to the *Sost*$^{-/-}$ mice, whose high bone mass is caused by overactive osteoblasts that produce high quality bone, the high bone mass in the aforementioned mice are caused by defective or absent osteoclasts, which results in poor quality, fragile bone [80,140]. Pharmacological inhibition of osteoclasts by zoledronic acid also adversely affects B cell differentiation by reducing the levels of CXCL12 and IL-7 produced by BM stromal cells [140]. In *Sost*$^{-/-}$ mice, we observed reduction of *Cxcl12* in digested bone, but no changes in *Il-7* or *Scf* expression. Interestingly, evidence that B cells are needed for proper bone homeostasis also exists. For example, IL-7R knockout mice lack B cell development past the pre-B cell stage, and present with increased bone mineral density [141]. Paradoxically, μMT-knockout mice with a genetic mutation of the mu immunoglobulin heavy-chain constant region, also display a block at the pre-B cell stage but have the opposite bone phenotype [142]. In addition, B cells are an important source of RANK ligand that induces osteoclast maturation, promoting bone homeostasis [117]. Taken together, our results and these data reinforce the idea that reciprocally beneficial crosstalk exists between cells involved in bone homeostasis and hematopoiesis. Further experimentation is required to investigate the mechanisms by which physical space is detected and interpreted by developing B cells in the BM.

Other Wnt antagonists, such as Dickkopf-1 (DKK1) and SFRP-1, are robustly expressed in osteoblasts and possibly other cell types in the BM, and it is possible that DKK1 could compensate for the loss of SOST [57,62]. *Dkk1* deficiency results in high

bone mass phenotypes, while the overexpression of *Dkk1* in osteoblasts of *Dkk1*-transgenic (Tg) mice resulted in reduction of trabecular bone [62]. *Dkk-1*-Tg mice did not display any overt phenotype in the frequencies or absolute numbers of any hematopoietic cell lineages, similar to our observations in the *Sost*$^{-/-}$ mice. We have observed an increase in *Dkk1* mRNA expression in *Sost*$^{-/-}$ mice (data not shown). The effect of *Dkk1* loss-of-function on hematopoiesis is unknown, and it would be interesting to investigate whether different Wnt antagonists render distinct effects on HSC maintenance and differentiation.

The spleen is an alternative site of hematopoiesis that can sometimes compensate for non-ideal BM environments. Spleens of *Sost*$^{-/-}$ mice are increased in mass, but show no evidence of extramedullary hematopoiesis or an increase in HSCs (data not shown), which supports that the role of *Sost* in hematopoiesis is limited to B cell development in the bone marrow [136,143]. Recirculating B cells in the bone marrow include plasma cells which produce high levels of antigen-specific antibodies after stimulation in secondary lymphoid organs. Plasma cell migration back to the BM is believed to act as an efficient way to release these antibodies into the circulation during infection. The reduction of recirculating B cells in the BM suggests that the BM environment of *Sost*$^{-/-}$ mice is not conducive for B cell survival or plasma cell maintenance even after they mature in the periphery, and/or that the low levels of CXCL12 in the *Sost*$^{-/-}$ BM is not sufficient for retention of mature B cells homing from the periphery.

Since inhibition of SOST has been proposed as a pharmacologic target for the anabolic stimulation of bone formation in the treatment for osteoporosis and other bone thinning disorders [144], our findings that B cell survival is impaired in the *Sost*$^{-/-}$ mice

suggest that patients receiving these treatments be closely monitored for alterations in B cell development and their ability to combat infection. Common variable immunodeficiency disease can be diagnosed by antibody deficiency and impaired immune responses to bacterial infections or vaccinations [145]. Although LPS-induced proliferation of *Sost*$^{-/-}$ splenic B cells was normal, it is possible that B cell-mediated immune responses to diverse antigenic challenges may be affected in the absence of SOST. Further detailed analyses of B cell proliferation to T-dependent antigens, cytokine production, isotype class switching and the development and survival of plasma cells and memory B cells are required to identify any contribution of SOST in acquired immunity and susceptibility to infection.

Chapter 4: Subtle Alterations to Hematopoietic Stem Cell Populations in the absence of Sclerostin

4.1. Introduction:

In Chapter 3, we described the importance of the Wnt antagonist SOST in B cell survival. Hematopoietic stem cells also rely on Wnt signaling and it has been established that canonical and non-canonical Wnt signaling is important for hematopoiesis [24,124]. For example, activation of canonical Wnt signaling via exogenous Wnt3a ligand has been shown to preserve HSC populations *in vitro*, while *Wnt3a* deficiency resulted in a decrease in the number of HSCs and progenitor cells in the fetal liver (FL), as well as a reduced capacity to reconstitute as measured by secondary transplantation [41]. Wnt antagonists can also play in role in hematopoietic stem cell self renewal. *Sfrp-1*$^{-/-}$ mice and *Wif-1* over expressing mice under the control of the Col2.3 promoter (*Wif-1-Tg)* mice both showed alterations in quiescent HSC populations [56,61] while Col2.3-DKK-1 (*Dkk-1-Tg)* mice also had observable defects in quiescent hematopoiesis after serial transplantation [62]. More recently Sclerostin (SOST) has been shown to be important for B cell development, although the contributions to hematopoietic stem cell self renewal and function is not known [58].

As stated in Chapter 3, the Wnt antagonist SOST blocks canonical Wnt signaling by its binding to the Wnt co-receptors LRP4, LRP5, and/or LRP6 blocking signaling via Frizzled receptors [55,73]. Fully mature osteocytes secrete SOST, which acts on OBs as a negative regulator of bone growth, effectively preventing osteoblast maturation into osteocytes [73]. Despite the clear role of SOST in the regulation of Wnt signaling, osteoblast activity and the size of the BM cavity, the function of SOST in the regulation

of hematopoietic stem cell quiescence and function has not been investigated. Given the increase in osteoblast populations observed in *Sost*$^{-/-}$ mice [58], we hypothesized that HSC numbers and HSC quiescence and function would be altered in the *Sost*$^{-/-}$ bone marrow microenvironment.

4.2. Materials and methods:

Mice. C57BL/6J and B6.SJL-Ptprc^{a} Pepc^{b}/BoyJ were used as described in Chapter 3.2. Mice that expressed both CD45.1 and CD45.2 were a cross of C57BL/6J and B6.SJL-Ptprc^{a}Pepc^{b}/BoyJ mice. The generation of *Sost*$^{-/-}$ mice is described in Chapter 3.2. *Lrp5*$^{-/-}$ mice were obtained from Dr. Gabriela Loots at Lawerence Livermore National Laboratory (LLNL). Mice of both sexes were analyzed between 3 - 4 months of age. Data were combined from both male and female mice, as no sex-specific differences were observed [78,79], and data not shown. Euthanization of mice is described in Chapter 3.2.

Antibodies. Monoclonal antibodies (mAb) were purchased either from eBioscience, Biolegend or BD Biosciences (San Diego, CA). The mAb clone name is listed in parentheses. The majority of antibodies used in Chapter 4 are described in detail in Chapter 3.2 with the exception of Sca-1-APC (D7), Sca-1-PE (E13 161.7), CD150-PECy5 (TC15 12F12.2).

Sorting and analysis of hematopoietic progenitor and stromal populations by flow cytometry (FCM). Bone marrow cells were obtained, counted and were incubated with purified anti-CD16/32 to block Fc receptors γII/III and MACS depleted as described [108]. Live Lineage^{-} cells were then counted by hemocytometer using Trypan Blue exclusion. All Lineage^{-} cells were stained with antibodies specific for c-Kit, Sca-1 and IL7Rα for 20 min. at 4°C, washed and resuspended in M199+ media with 0.1μg/ml of DAPI (Fisher). LSK HSC, MPP, CLP, CMP, MEP/GMP populations were then sorted using a FACS Aria II (BD Biosciences, San Jose, CA). All populations were sorted to

80-90% purity, as verified by post-sort analysis. Analysis of flow cytometric data was performed with FlowJo software (Treestar, Ashland, OR).

RNA Isolation, cDNA synthesis, and PCR. mRNA isolation, cDNA synthesis and PCR are all described in Chapter 3.2.

Primary bone marrow transplantation assay. *Sost*$^{-/-}$→WT and WT→*Sost*$^{-/-}$ bone marrow chimeras were generated. All recipient mice were lethally irradiated with 1000 rads using a Cesium-137 source (J.L. Shepherd and Associates, San Fernando, CA), and a minimum of 4 hours were allowed to pass before bone marrow reconstitution. For the *Sost*$^{-/-}$→WT chimeras, B6.SJL-*Ptprc*^{a} *Pepc*^{b}/BoyJ (CD45.1^{+}) recipients were transplanted with 5 x 10^{6} *Sost*$^{-/-}$ CD45.2^{+} bone marrow cells (BMC) via retro-orbital intravenous injection. Control WT (CD45.2)→WT (CD45.1) chimeras were prepared by transplantation of wildtype C57BL/6J BMC into wildtype or B6.SJL-*Ptprc*^{a}*Pepc*^{b}/BoyJ (CD45.1^{+}) recipients. For the reciprocal WT→ *Sost*$^{-/-}$ chimeras, C57BL/6J or *Sost*$^{-/-}$ recipients (both CD45.2^{+}) were transplanted with B6.SJL-*Ptprc*^{a} *Pepc*^{b}/BoyJ (CD45.1) BMC, and control WT (CD45.1)→WT (CD45.2) chimeras were prepared as described above. Peripheral blood samples were stained for CD45.1, CD45.2, Gr-1, CD11b, CD3ε, and CD19 and analyzed for the presence of donor chimerism at 3 weeks by FACS and % chimerism was calculated by the formula: % donor chimerism = (% CD45.1^{+} (donor) / [%CD45.1^{+} (donor) + %CD45.2^{+} (host)]). Chimeras were euthanized at 5 weeks post-transplantation for analysis of donor hematopoietic lineages in the bone marrow and spleen.

Serial bone marrow transplantation assay. WT (CD45.1)→*Sost*$^{-/-}$ (CD45.2) bone marrow chimeras were generated as described above. At 5 weeks after primary

transplantation, recipients were euthanized and bone marrow was sterilely harvested. Nine-hundred thousand "primary transplant" $CD45.1^+$ BM cells were transplanted with $3.0x10^5$ WT $CD45.2^+$ (facilitator) BM cells into lethally irradiated, $CD45.2^+$ C57BL/6J hosts. Peripheral blood samples were stained for CD45.1, CD45.2, Gr-1, CD11b, CD3ε, and CD19 and analyzed for the presence of donor chimerism at 3 weeks after serial transplantation by FACS and % chimerism was calculated by the formula: % donor chimerism = (% $CD45.1^+$ (donor) / [(% $CD45.1^+$ (donor) + % $CD45.1^-$ (Facilitator + host)]). After an additional 5 weeks, secondary transplant recipients were euthanized and bone marrow and spleens were isolated for analysis of $CD45.1^+$ bone marrow and spleen cells as described above. Ratios of LSK HSCs, LT HSCs, ST HSCs, and CLPs were calculated as follows: Ratio of WT or *Sost*$^{-/-}$ $CD45.1^+$ cells = (% $CD45.1^+$ (Donor) / [(% $CD45.1^+$ (Donor) + % $CD45.1^-$(Facilitator + Host)]).

Competitive bone marrow transplantation assay. Five-million WT or *Sost*$^{-/-}$ cells (CD45.2) were co-transplanted with $5.0x10^6$ WT ($CD45.1^+$ $CD45.2^+$) cells and transplanted into lethally irradiated B6.SJL-*Ptprc*^{a}*Pepc*^{b}/BoyJ (CD45.1) mice. Peripheral blood samples were stained for CD45.1, CD45.2, Gr-1, CD11b, CD3ε, and CD19 and analyzed for the presence of donor chimerism at 3 weeks after transplantation by FACS. At 5 weeks after transplantation, recipients were euthanized and bone marrow and spleen cells were harvested and analyzed as described above. Ratios of HSCs, CMP/MEPs, GMPs, and CLPs were calculated as follows: Ratio of CD45.2 WT cell = (% $CD45.2^+$ WT/ (% $CD45.2^+$ WT + % $CD45.1^+$ $CD45.2^+$ WT)); Ratio of CD45.2 KO cell = (% $CD45.2^+$ KO/ (% $CD45.2^+$ KO + % $CD45.1^+$ $CD45.2^+$ WT)); Ratio of $CD45.1^+$ $CD45.2^+$ WT cells = (% $CD45.1^+$ $CD45.2^+$ WT/ (% $CD45.2^+$ WT + % $CD45.1^+$ $CD45.2^+$ WT)).

Statistical analysis. All statistical analysis used for Chapter 4 is described in Chapter 3.2

4.3. Results

Hematopoietic stem and progenitor cell frequencies are normal in *Sost*$^{-/-}$ mice

Given their documented increase in osteoblast activity and Wnt signaling in *Sost*$^{-/-}$ mice, we hypothesized that *Sost*$^{-/-}$ mice would display an increase in HSCs [78]. On the contrary, we observed no differences in the frequency or absolute number of HSCs, common lymphoid progenitors (CLP), common myeloid/megakaryocyte erythroid progenitors (CMP/MEP), or granulocyte/monocyte progenitors (GMP) (Figure 4.1A and 4.1B). Therefore, the loss of *Sost* was not sufficient to influence changes in Lineage^{-} Sca-1^{high} c-kit^{high} (LSK) HSCs or other hematopoietic progenitor populations in *Sost*$^{-/-}$ mice. Mice that have altered hematopoietic stem cell microenvironments due to changes to the osteoblast populations often display extramedullary hematopoiesis in the spleen or liver [80,93]. We next examined *Sost*$^{-/-}$ mice to assess for any differences in hematopoietic stem cells and progenitor populations in the spleen.

Sost$^{-/-}$ mice do not show any evidence of extramedullary hematopoiesis.

OBs are required to support HSCs in bone marrow "niches" and also help to maintain normal hematopoiesis. When there are induced reductions to OB populations in the bone marrow, HSCs can migrate to other organs such as the spleen or liver to compensate for the diminished capacity to support HSC self renewal and differentiation [93]. Bone resorbing OCs are also important in maintaining HSC and when the development of OCs is altered, extramedullary hematopoiesis is often observed [80,146]. In addition to the observation that HSPC frequencies are normal in *Sost*$^{-/-}$ mice, we have reported previously that *Sost*$^{-/-}$ mouse spleens have increased granulocyte

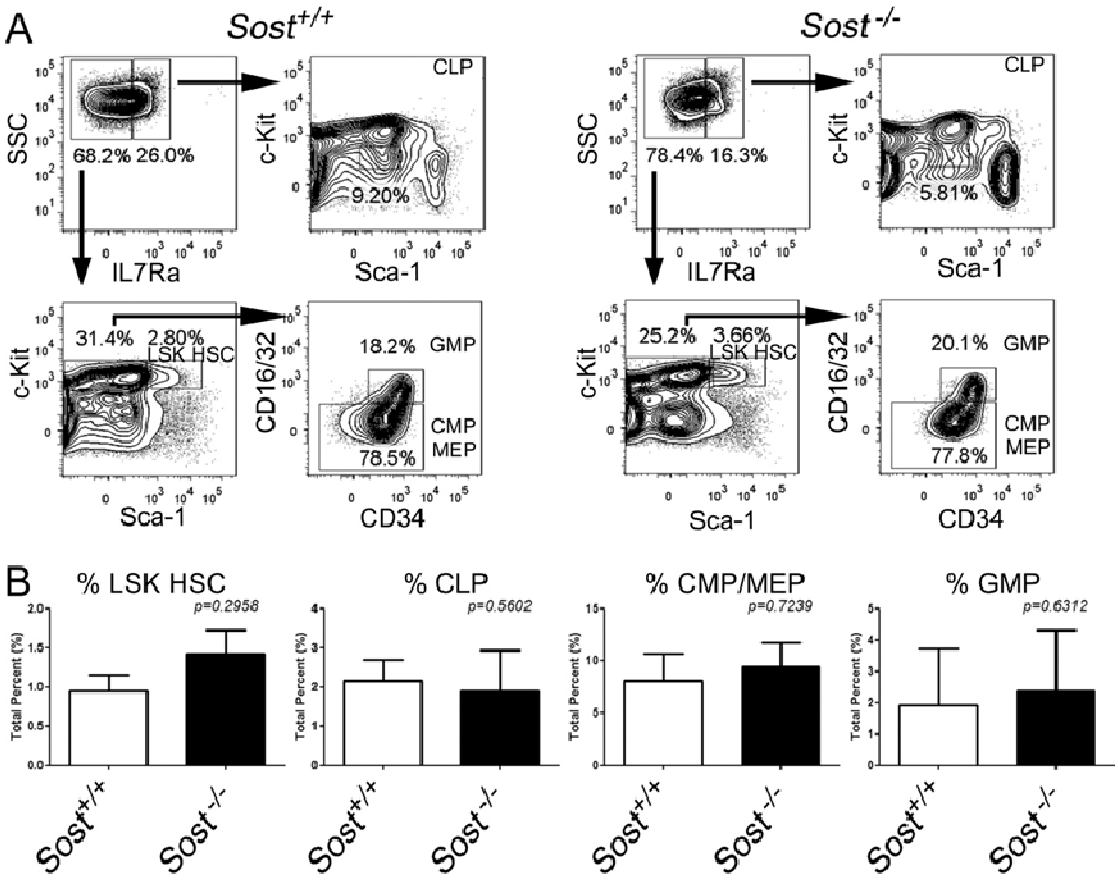

Figure 4.1: Sost ablation does not affect hematopoietic progenitors. **(A)** Representative FCM plots of hematopoietic progenitor frequencies. **(C)** Total percentage of LSK HSC (far left panel) CLP (middle left panel) CMP/MEP (middle right panel) and GMP (far right panel) from lineage-depleted bone marrow. Data are representative of *Sost*$^{+/+}$, n=7 (LSK HSC and CLP) and n=6 (CMP/MEP, GMP) and *Sost*$^{-/-}$, n=13 (LSK HSC and CLP) and n=11 (CMP/MEP, GMP). Data shown are representative mice of pooled sexes aged 8-13 weeks. Mean ± SD are shown, and were considered to be statistically significant if $p < 0.05$, two-tailed Student's T-test.

populations compared to WT, indicating that HSCs or other progenitor cells may be migrating to the spleen due to the reduced bone marrow cavity in *Sost*$^{-/-}$ mice [58]. To test the hypothesis that extramedullary hematopoiesis occurs in *Sost*$^{-/-}$ spleens, we quantified splenic HSPC populations in *Sost*$^{-/-}$ mice. Using FACS, we observed no differences in both LSK HSC frequency and cell numbers in *Sost*$^{-/-}$ mice (Figure 4.2A-C). Interestingly, we did observe a significant increase in both frequencies and cell numbers of CLP, CMP/MEP and GMP populations in the spleens of *Sost*$^{-/-}$ mice (Figure 4.2A-C). A corresponding increase in spleen mass was also observed, most likely due to the increase in granulocytes in *Sost*$^{-/-}$ spleens (Figure 4.2C). Although hematopoietic stem cell frequencies are unchanged, the increase in myeloid and lymphoid progenitors indicates their enhanced migration from to the spleen from the bone marrow.

The lack of *Lrp5*$^{-/-}$ does not alter hematopoietic stem cell frequencies

SOST binds to the Frizzled co-receptors LRP4, LRP5 and LRP6 to halt the transduction of Wnt signaling [144]. *Lrp6*$^{-/-}$ mice are embryonic lethal while *Lrp5*$^{-/-}$ are viable conventional knockouts, but are osteoporotic due to low osteoblast proliferation from a lack of Wnt signaling [124]. To our knowledge, hematopoietic stem cell and progenitor populations have not been analyzed in *Lrp5*$^{-/-}$ knockout mice. Since SOST binds to LRP5, and *Lrp5*$^{-/-}$ mice contain osteoporotic bones, we examined hematopoietic stem and progenitor populations in these mice, and we expected that the phenotype in *Lrp5*$^{-/-}$ mice would be the opposite of *Sost*$^{-/-}$ mice.

Surprisingly, *Lrp5*$^{-/-}$ mice showed normal hematopoiesis in the bone marrow and spleen (data not shown). Further investigation into the HSC and CLP populations of

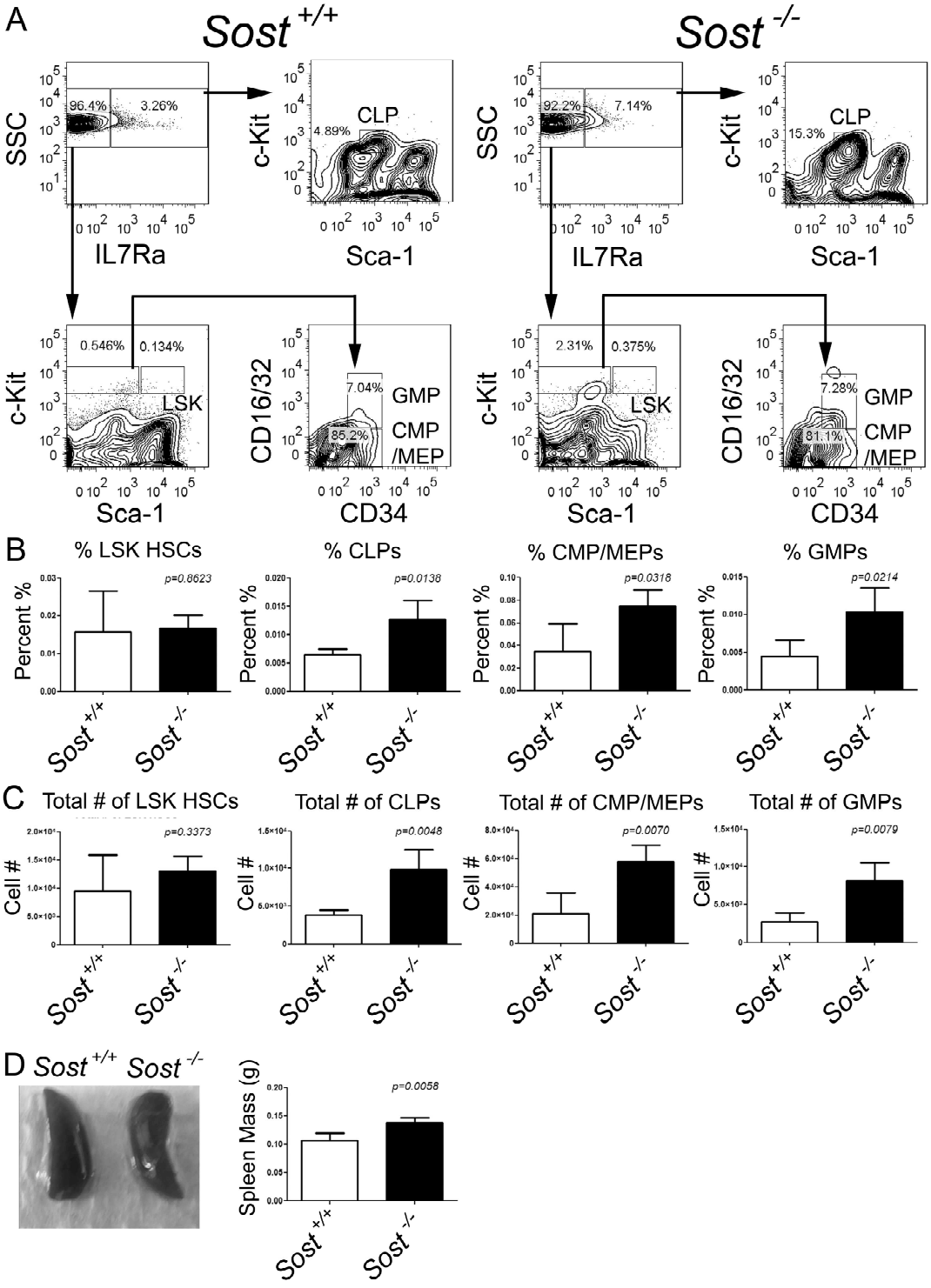
A
Sost +/+
Sost -/-
SSC
IL7Ra
c-Kit
Sca-1
CD16/32
CD34
96.4%
3.26%
4.89%
CLP
0.546%
0.134%
LSK
7.04%
GMP
85.2%
CMP
/MEP
92.2%
7.14%
15.3%
2.31%
0.375%
7.28%
81.1%
B
% LSK HSCs
% CLPs
% CMP/MEPs
% GMPs
Percent %
p=0.8623
p=0.0138
p=0.0318
p=0.0214
C
Total # of LSK HSCs
Total # of CLPs
Total # of CMP/MEPs
Total # of GMPs
Cell #
p=0.3373
p=0.0048
p=0.0070
p=0.0079
D
Spleen Mass (g)
p=0.0058

Figure 4.2: CLP, CMP/MEP and GMP are increased in Sost$^{-/-}$ Spleens. **(A)** Representative FCM plots of hematopoietic progenitor frequencies in *Sost*$^{-+/+}$ and *Sost*$^{-/-}$ spleens. **(B)** Total percentage of LSK HSC (far left panel) CLP (middle left panel) CMP/MEP (middle right panel) and GMP (far right panel) from lineage-depleted spleens. **(C)** Total cell numbers of LSK HSC (far left panel) CLP (middle left panel) CMP/MEP (middle right panel) and GMP (far right panel) from lineage-depleted spleens. **(D)** Representative Spleens (left) and Spleen mass from *Sost*$^{-+/+}$ and *Sost*$^{-/-}$ mice. Data are representative of *Sost*$^{+/+}$, n=4 and *Sost*$^{-/-}$, n=4. Mean ± SD are shown, and were considered to be statistically significant if $p < 0.05$, two-tailed Student's T-test.

Lrp5$^{-/-}$ revealed no significant differences in the frequencies of these cells, but a significant reduction in the absolute numbers of LSK HSCs and CLPs in the bone marrow (Figure 4.3A-C). Furthermore, when we measured the expression of *Lrp5* in wildtype mice, we observed expression of *Lrp5* in LSK HSCs as well as CMP/MEP populations, but not in CLPs or CD19^{+} B cells (Figure 4.4). *Lrp6* was expressed in LSK HSCs, CLPs, CMP/MEP, B cells and granulocytes, whereas *Lrp4* was not expressed on any hematopoietic cell type. The finding that *Lrp5* hematopoietic stem cell numbers are lower in the *Lrp5*$^{-/-}$ mice and that LSK HSCs express *Lrp5* indicates a potential mechanism for SOST to regulate HSCs function in the bone marrow.

Primary transplantation reveals no defect in HSC engraftment or function

We have previously shown in Chapter 3 that *Sost*$^{-/-}$ mice have altered B cell development, in response to changes in the *Sost*$^{-/-}$ mice bone marrow microenvironment [58]. To test if the *Sost*$^{-/-}$ microenvironment could alter wild type hematopoietic stem and progenitor cell frequencies and cell numbers, we transplanted wild type CD45.1 bone marrow into lethally irradiated CD45.2 wild type or *Sost*$^{-/-}$ mice (Figure 4.5A). CD45.1 gated LSK HSCs were not changed in both frequency and cell number in our CD45.1→ *Sost*$^{-/-}$ transplants (Figure 4.5B-D). Frequency and cell numbers of long term (LT, (LSK CD150^{+}) and short term HSCs (ST, LSK CD150^{-}) were increased in *Sost*$^{-/-}$ mice, but not significantly. Interestingly, CMP/MEP and GMP populations in the BM were also unaffected by transplantation into the *Sost*$^{-/-}$ microenvironment.

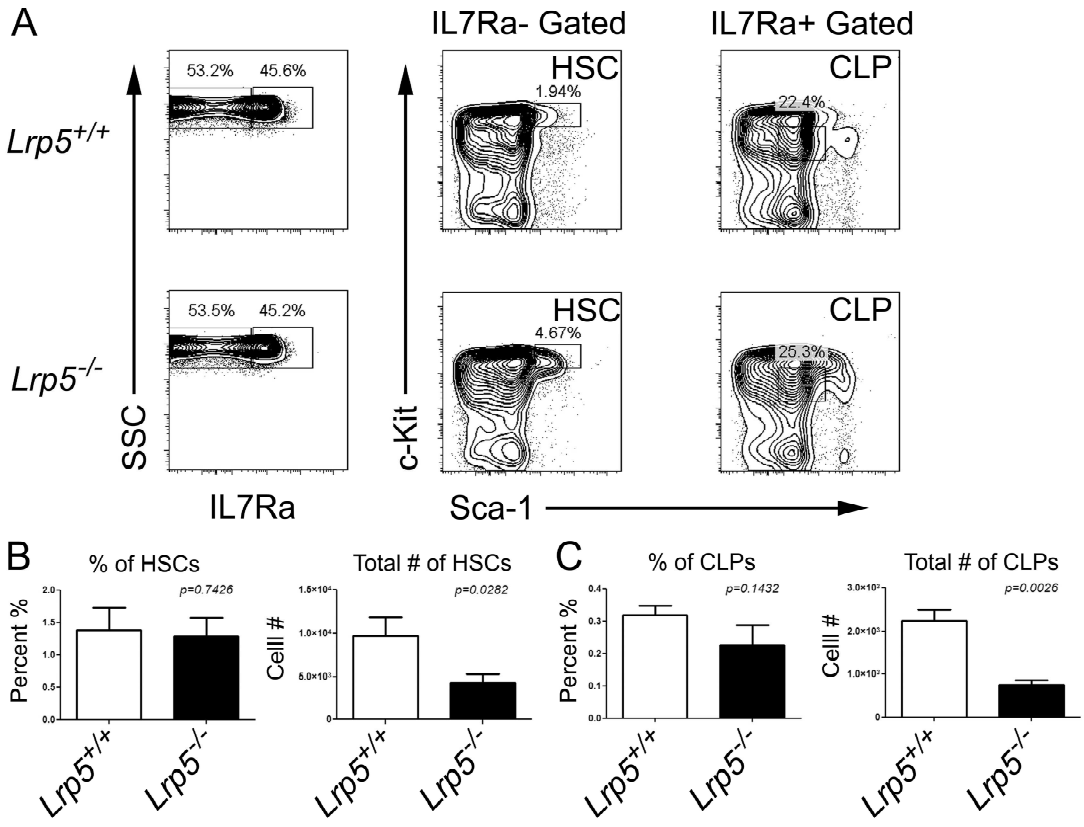

Figure 4.3: The deletion of Lrp5 does not affect hematopoietic stem and progenitors cells. **(A)** Representative FCM plots of hematopoietic stem and progenitor frequencies in *Lrp5*$^{+/+}$ and *Lrp5*$^{-/-}$ bone marrow **(B)** Total percentage of LSK HSCs (left panel) and CLPs (right panel) **(C)** Total cell numbers of LSK HSCs (left panel) and CLPs (right panel). Data are representative of *Lrp5*$^{+/+}$, n=2 and *Lrp5*$^{-/-}$, n=3. Mean ± SD are shown, and were considered to be statistically significant if $p < 0.05$, two-tailed Student's T-test.

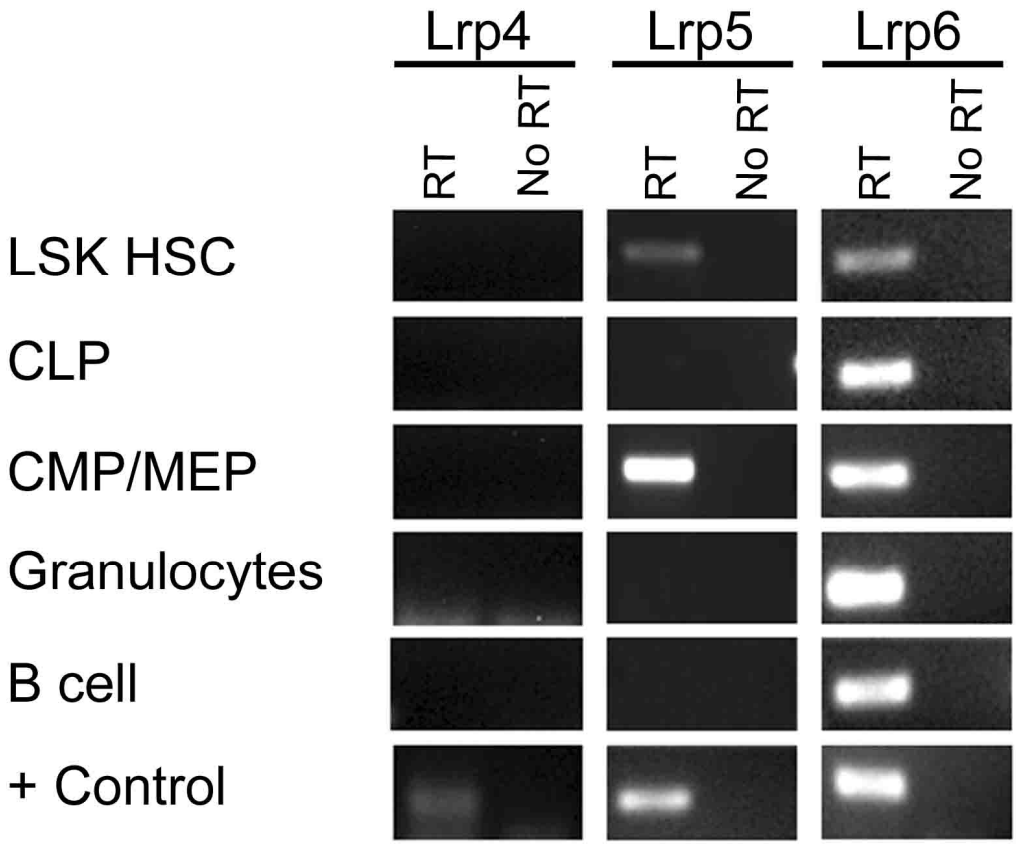

Figure 4.4: Differential expression of Lrp4, 5, and 6 on selected hematopoietic subsets. *Lrp4, Lrp5 and Lrp6* expression was determined using RT-PCR from mRNA isolated from FCM-sorted LSK HSC, CLP, CMP, granulocytes and B cells from wild-type mice. β-actin was used as a housekeeping gene control. The positive control tissue is bone that was flushed of bone marrow.

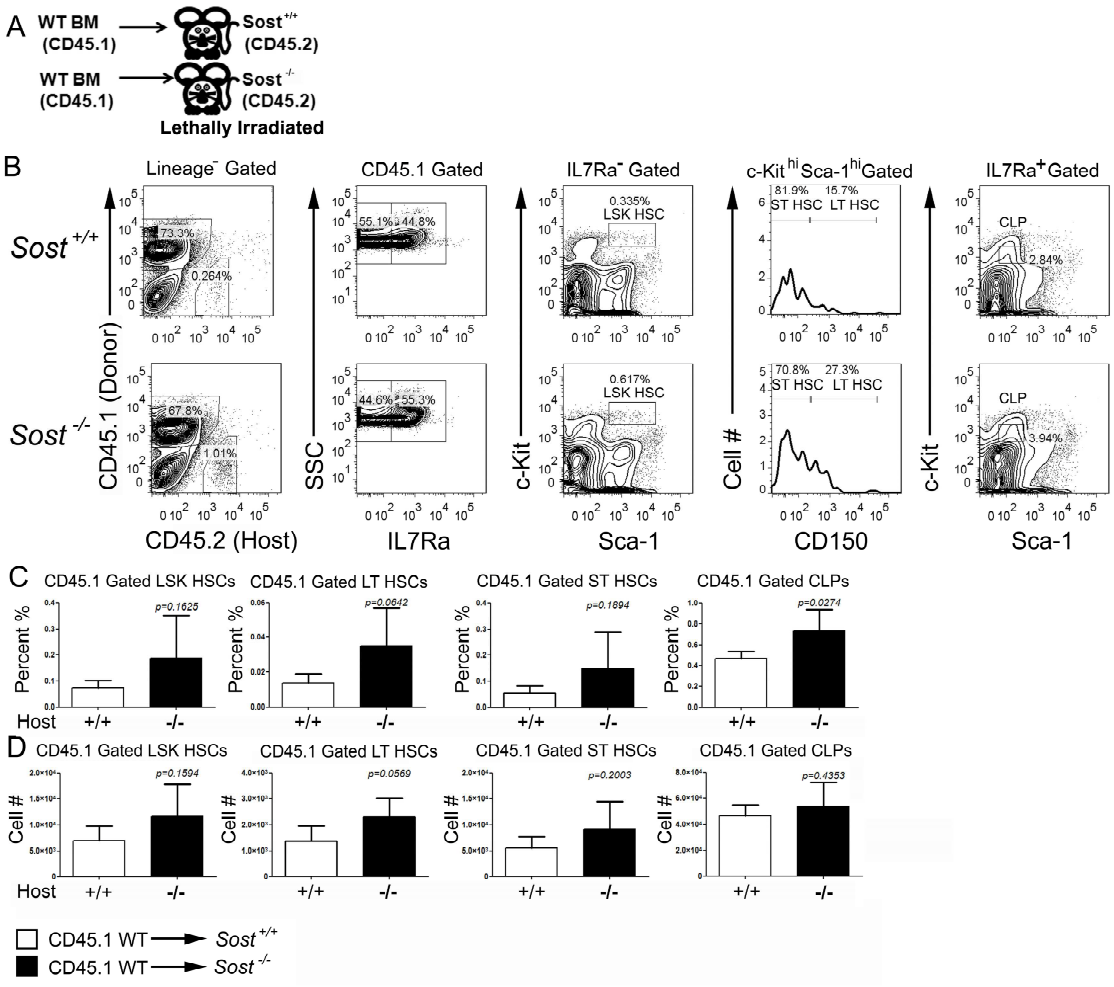
A
WT BM (CD45.1)
Sost+/+ (CD45.2)
WT BM (CD45.1)
Sost -/- (CD45.2)
Lethally Irradiated
B
Lineage- Gated
CD45.1 Gated
IL7Ra- Gated
c-Kit hi Sca-1 hi Gated
IL7Ra+ Gated
Sost +/+
Sost -/-
CD45.1 (Donor)
CD45.2 (Host)
IL7Ra
Sca-1
CD150
c-Kit
Cell #
SSC
73.3%
0.264%
67.8%
1.01%
55.1%
44.8%
44.6%
55.3%
0.335%
LSK HSC
0.617%
LSK HSC
81.9%
15.7%
ST HSC
LT HSC
70.8%
27.3%
ST HSC
LT HSC
CLP
2.84%
CLP
3.94%
C
CD45.1 Gated LSK HSCs
CD45.1 Gated LT HSCs
CD45.1 Gated ST HSCs
CD45.1 Gated CLPs
Percent %
p=0.1625
p=0.0642
p=0.1694
p=0.0274
Host
+/+
-/-
D
CD45.1 Gated LSK HSCs
CD45.1 Gated LT HSCs
CD45.1 Gated ST HSCs
CD45.1 Gated CLPs
Cell #
p=0.1594
p=0.0569
p=0.2003
p=0.4353
Host
+/+
-/-
CD45.1 WT → Sost+/+
CD45.1 WT → Sost -/-

Figure 4.5: Sost$^{-/-}$ bone marrow microenvironment does not influence HSC function in primary transplant. **(A)** Scheme of the bone marrow transplantation of CD45.1^{+} WT bone marrow into CD45.2^{+} WT (n=5) or *Sost*$^{-/-}$ (n=5) mice. **(B)** Representative FACS plots of hematopoietic stem and progenitor frequencies of WT (CD45.1)→WT (CD45.2) and WT (CD45.1)→*Sost*$^{-/-}$ (CD45.2) mice. **(C)** Total percentages of donor derived LSK HSCs (far left panel), LT HSCs (middle left panel), ST HSCs (middle left panel) and CLPs (far right panel). (**D)** Total cell numbers of donor derived LSK HSCs (far left panel), LT HSCs (middle left panel), ST HSCs (middle left panel) and CLPs (far right panel). Mean ± SD are shown from age and sex matched mice, and were considered to be statistically significant if $p < 0.05$, two-tailed Student's T-test.

There was a modest increase in the numbers of CLPs in CD45.1 → *Sost*$^{-/-}$ mice, but frequencies were unchanged between wild type controls. It was interesting that even though the increased bone phenotype is particularly dramatic in *Sost*$^{-/-}$ recipients, that there was no influence on hematopoietic stem cell engraftment after transplantation, given that other osteopetrotic murine models such as in mice with a constitutively active parathyroid hormone receptor under the control of the Col1a have marked decreases in HSCs [4]. This might be because the LSK HSC population that consists of LT-HSCs and ST-HSCs [1]. In order to determine if long term engraftment and LT HSC function was altered in *Sost*$^{-/-}$ mice, we performed serial transplantation, as well as competitive transplantation assays.

Competitive transplantations highlight subtle defects in WT HSC engraftment when exposed to a *Sost*$^{-/-}$ microenvironment

Primary transplantation assays can sometimes fail to expose subtle differences in HSC function. HSC that develop in a non-ideal bone marrow environment can harbor subtle differences in LT-HSC engraftment capacity, a feature that can be revealed by secondary transplantation or competitive transplantation. For instance, *Dkk-1-Tg* HSC displayed a subtle hematopoietic self renewal defect that was only observable after serial transplantation into WT hosts [62]. In contrast, *Sfrp-1*$^{-/-}$ and *Wif-1-Tg* HSC engraftment defects were more overt, and were detectable by primary transplantation into WT hosts [56,61]. To determine the role of *Sost* on LT-HSC function and engraftment efficiency, we performed a competitive transplant in which bone marrow cells from either *Sost*$^{-/-}$ mice or wildtype(both CD45.2^{+}) mice were transplanted at equal ratios with wildtype

$CD45.1^+CD45.2^+$ WT cells into lethally irradiated $CD45.1^+$ wildtype hosts (Figure 4.6A). When we compared the ratio of WT CD45.2 LSK HSCs to WT CD45.1 CD45.2 LSK HSCs, they were close to 50% as expected. However, the ratio of *Sost*$^{-/-}$ CD45.2 LSK to WT CD45.1 CD45.2 LSK HSCs was significantly higher, indicating increased engraftment efficiency in *Sost*$^{-/-}$ HSCs (Figure 4.6B-D). The same trend was also observed amongst CMP/MEP, GMP and CLP populations that originated from *Sost*$^{-/-}$ mice (Figure 4.6C-D). These results suggest that HSCs from *Sost*$^{-/-}$ mice are able to engraft and reconstitute hematopoietic lineages after transplantation at a superior level compared to that of their than wild-type counterparts.

Serial transplantations highlight subtle defects in long term engraftment when exposed to a *Sost*$^{-/-}$ microenvironment

Given the observed increase in LSK HSCs from the competitive transplantation experiments, we performed serial transplantations with WT CD45.1 cells that were first transplanted into WT or *Sost*$^{-/-}$ recipients (CD45.2) to detect any permanent self-renewal changes in LT-HSCs that developed in a *Sost*$^{-/-}$ microenvironment. If the hypothesis that *Sost*$^{-/-}$ phenotype has no effect on HSC engraftment was correct, we would expect a similar phenotype to that of our primary transplantations shown in Figure 4.5 (i.e. no changes in % HSPC, reduced cell numbers of all cell types, in particular CLP and B cells). Five weeks post-BMT, WT (CD45.1) → WT and WT (CD45.1) → *Sost*$^{-/-}$ chimeras were euthanized, and their BM was harvested. WT $CD45.2^+$ BM cells were also harvested from a non-transplanted donor at this time. Subsequently, $9.0x10^5$ BMCs

from the primary recipients (WT (CD45.1) → WT and WT (CD45.1) → *Sost*$^{-/-}$ chimeras) were co-transplanted with 3.0x10^5 WT CD45.2$^+$ BM cells into a secondary, healthy WT CD45.2$^+$ (Figure 4.7A) host. If the CD45.1$^+$ cells from the primary BMT could not reconstitute the secondary hosts efficiently, then we expected only the WT CD45.2$^+$ BM to rescue the secondary hosts. The % donor CD45.1$^+$ chimerism in the peripheral blood of primary recipients were not significantly different, however peripheral blood CD45.1$^+$ donor chimerism was increased in secondary CD45.2$^+$ recipients that received WT CD45.1$^+$ BM that developed in the *Sost*$^{-/-}$ primary host environment (Figure 4.7B, Recipient #2). When we analyzed bone marrow populations 5 weeks after secondary transplantation, we observed lower levels of CD45.1$^+$ LSK HSCs, LT HSCSs and ST HSCs that originated from the primary *Sost*$^{-/-}$ microenvironment, but these decreases did not reach statistical significance (likely due to the marked variability in the levels of CD45.1$^+$ cell engraftment observed in individual secondary recipients (Figures 4.7C and 4.7D)). However, after secondary transplantation, we observed a statistically significant decrease in the absolute number of CLPs that were derived from WT BM that first developed in the *Sost*$^{-/-}$ primary host (Figure 4.7D). This is interesting, as both the primary transplantation and competitive transplantations displayed reduced CLPs (Figures 4.5 and 4.6). Since the donor CD45.1$^+$ cells were transplanted with CD45.2$^+$ facilitator cells in our serial transplantation, (a situation that is similar to that of our competitive transplantation assays (Figure 4.6)), we examined the ratio of CD45.1$^+$ cells to the total hematopoietic cells present in the BM to determine if there were any overt differences in HSC populations in our serial transplantation recipients. Analysis of WT LSK HSCs, LT HSCs, ST HSC and CLPs ratios in serial transplant recipients did not

reveal any differences in WT cell that first developed in the *Sost*$^{-/-}$ primary host (Figure 4.7F). Under steady state conditions (i.e. non-transplanted mice), *Sost*$^{-/-}$ HSCs and CLPs from *Sost*$^{-/-}$ mice appear normal, however, the competitive and serial transplantation assays revealed subtle differences in these populations (Figures 4.1, 4.6 and 4.7). As *Sost* is not expressed in hematopoietic cells, the defects observed in *Sost*$^{-/-}$ HSCs are non-cell autonomous. The properties of *Sost*$^{-/-}$ HSCs described in this chapter appear to be permanent, as the increased engraftment efficiency persists, even when *Sost*$^{-/-}$ BM cells are transplanted into WT secondary hosts (Figures 4.6 and 4.7).

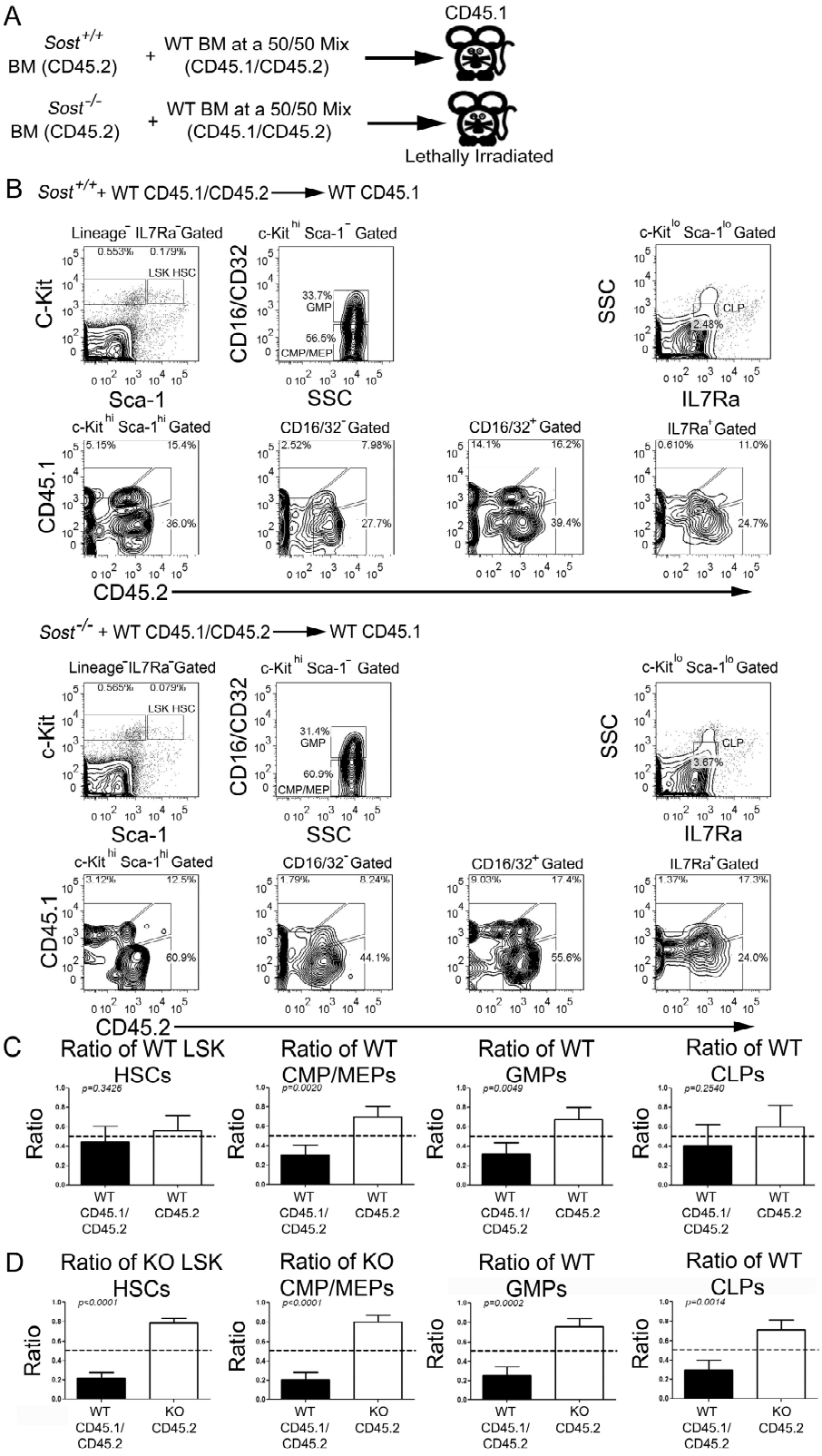
A
Sost+/+ BM (CD45.2)
+
WT BM at a 50/50 Mix (CD45.1/CD45.2)
CD45.1
Sost-/- BM (CD45.2)
+
WT BM at a 50/50 Mix (CD45.1/CD45.2)
Lethally Irradiated
B
Sost+/+ + WT CD45.1/CD45.2 → WT CD45.1
Lineage- IL7Ra- Gated
c-Kit
Sca-1
0.553%
0.179%
LSK HSC
c-Kit hi Sca-1- Gated
CD16/CD32
SSC
33.7%
GMP
56.6%
CMP/MEP
c-Kit lo Sca-1lo Gated
SSC
IL7Ra
CLP
2.48%
c-Kit hi Sca-1hi Gated
CD45.1
5.15%
15.4%
36.0%
CD16/32- Gated
2.52%
7.98%
27.7%
CD16/32+ Gated
14.1%
16.2%
39.4%
IL7Ra+ Gated
0.610%
11.0%
24.7%
CD45.2
Sost-/- + WT CD45.1/CD45.2 → WT CD45.1
Lineage- IL7Ra- Gated
0.565%
0.079%
LSK HSC
c-Kit hi Sca-1- Gated
31.4%
GMP
60.9%
CMP/MEP
c-Kit lo Sca-1lo Gated
CLP
3.67%
c-Kit hi Sca-1hi Gated
3.12%
12.5%
60.9%
CD16/32- Gated
1.79%
8.24%
44.1%
CD16/32+ Gated
9.03%
17.4%
55.6%
IL7Ra+ Gated
1.37%
17.3%
24.0%
C
Ratio of WT LSK HSCs
p=0.3426
Ratio of WT CMP/MEPs
p=0.0020
Ratio of WT GMPs
p=0.0049
Ratio of WT CLPs
p=0.2540
Ratio
WT CD45.1/ CD45.2
WT CD45.2
D
Ratio of KO LSK HSCs
p<0.0001
Ratio of KO CMP/MEPs
p<0.0001
Ratio of WT GMPs
p=0.0002
Ratio of WT CLPs
p=0.0014
Ratio
WT CD45.1/ CD45.2
KO CD45.2

Figure 4.6: HSC engraftment of WT and Sost$^{-/-}$ bone marrow cells is increased in competitive transplantation assays. **(A)** Scheme of the competitive bone marrow transplantation of *Sost*$^{+/+}$ (n=4) *Sost*$^{-/-}$ (n=4) mixed with WT (CD45.1 CD45.2) at a 50/50 mix and then transplanted into a lethally irradiated WT (CD45.1) recipient. **(B)** Representative FACS plots of hematopoietic stem and progenitor frequencies of WT(CD45.2) or Sost (CD45.2) mixed with WT(CD45.1 CD45.2) →WT Recipient (CD45.2) and **(C)** Ratios of donor derived CD45.2 WT vs. CD45.1 CD45.2 WT LSK HSCs (far left panel), CMP/MEPs (middle left panel), GMPs (middle left panel) and CLPs (far right panel). (**D)** Ratios of donor derived CD45.2 WT vs. CD45.1 CD45.2 LSK HSCs (far left panel), CMP/MEPs (middle left panel), GMPs (middle left panel) and CLPs (far right panel). Mean ± SD are shown from age and sex matched mice, and were considered to be statistically significant if $p < 0.05$, two-tailed Student's T-test.

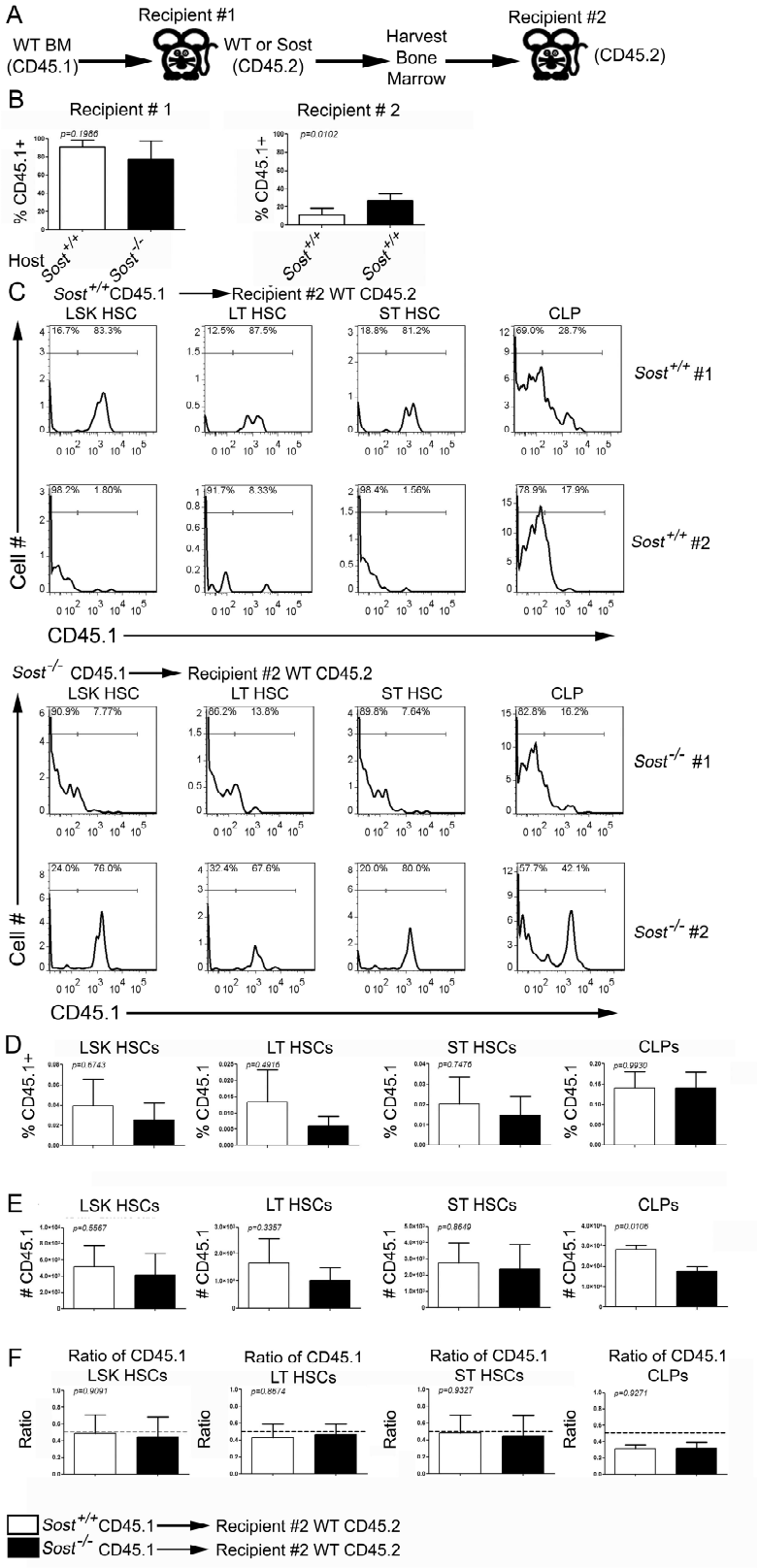
A
Recipient #1
WT BM
(CD45.1)
WT or Sost
(CD45.2)
Harvest
Bone
Marrow
Recipient #2
(CD45.2)
B
Recipient # 1
Recipient # 2
% CD45.1+
p=0.1966
p=0.0102
Host
Sost+/+
Sost-/-
C
Sost+/+CD45.1
Recipient #2 WT CD45.2
LSK HSC
LT HSC
ST HSC
CLP
Sost+/+ #1
Sost+/+ #2
Cell #
CD45.1
Sost-/- CD45.1
Recipient #2 WT CD45.2
Sost-/- #1
Sost-/- #2
D
LSK HSCs
LT HSCs
ST HSCs
CLPs
% CD45.1+
p=0.6743
p=0.4916
p=0.7476
p=0.9930
E
# CD45.1
p=0.5567
p=0.3357
p=0.8649
p=0.0106
F
Ratio of CD45.1
LSK HSCs
LT HSCs
ST HSCs
CLPs
Ratio
p=0.9091
p=0.8574
p=0.9327
p=0.9271
Sost+/+CD45.1
Recipient #2 WT CD45.2
Sost-/- CD45.1
Recipient #2 WT CD45.2

Figure 4.7: Sost$^{-/-}$ bone marrow microenvironment alters HSC function in secondary transplantation assays. **(A)** Scheme of the secondary bone marrow transplantation of CD45.1^{+} WT or *Sost*$^{-/-}$ bone marrow recipients that were euthanized and the bone marrow was transplanted into a second CD45.2^{+} WT recipient. **(B)** Percentages of CD45.1 Chimerism in the blood of Recipient #1 (WT CD45.1→ CD45.2 WT or Sost -/- hosts (n=5), left panel) and Recipient # 2 (Recipient #1 WT(CD45.1) or *Sost*$^{-/-}$ (CD45.1) BM → WT CD45.2 Recipient #2 (n=5), right panel) **(C)** Two Representative FACS plots of hematopoietic stem and progenitor frequencies of WT(CD45.1) (n=4) or *Sost*$^{-/-}$ (n=4) (CD45.1) BM →WT Recipient #2 (CD45.2). **(D)** Total percentages of donor derived LSK HSCs (far left panel), LT HSCs (middle left panel), ST HSCs (middle right panel) and CLPs (far right panel). (**E)** Total cell numbers of donor derived LSK HSCs (far left panel), LT HSCs (middle left panel), ST HSCs (middle right panel) and CLPs (far right panel). (**F)** Ratios of donor derived CD45.1 from WT (CD45.1) (n=4) or *Sost*$^{-/-}$ (n=4) (CD45.1) BM →WT Recipient #2 (CD45.2). LSK HSCs (far left panel), LT HSCs (middle left panel), ST HSCs (middle right panel) and CLPs (far right panel). Mean ± SD are shown from age and sex matched mice, and were considered to be statistically significant if $p < 0.05$, two-tailed Student's T-test.

4.4. Discussion:

Hematopoietic stem cells are sensitive to changes to their microenvironmental "niche" [81]. Wnt antagonists modulate Wnt signaling by controlling the osteoblast to osteocyte transition at the endosteum. Secretion of SOST by osteocytes negatively regulates bone growth and in *Sost*$^{-/-}$ mice, and in Chapter 3, we have revealed that there are alterations to B cell survival due to changes in the bone microenvironment [58]. In this study, *Sost*$^{-/-}$ mice displayed no alterations to BM LSK HSC, CMP/MEP, GMP and CLP populations. This finding was not entirely surprising, as *Dkk-1-Tg* mice did not show alterations to LSK HSC populations [62]. *Sost*$^{-/-}$ mice splenic CMP/MEP, GMP, and CLP populations were significantly higher that WT cohorts, which may be from migration from the BM, due to a lack of CXCL12 reported in Chapter 3 (Figure 4.2). Additionally, primary transplantation assays revealed a significant decrease in total CLP cell numbers from *Sost*$^{-/-}$ BM without influencing other HSPC populations. Interestingly, and in contrast, competitive and transplantation assays showed increases in the engraftment efficiency of *Sost*$^{-/-}$ LSK HSCs compared to WT controls (Figure 4.6D), but this engraftment efficiency was not observed in serial transplantation of WT HSC that developed in *Sost*$^{-/-}$ bone microenvironments (Figure 4.7F). Absence of *Sost* resulted in increased CLPs percentages in both primary and competitive transplantation assays (Figures 4.5 and 4.6), however, our serial transplantation assays had reduced CLPs (Figure 4.7). The differences observed in CLP populations in our transplantation assays indicates that CLPs are altered in the absence of *Sost*, but we have yet to identify the putative mechanism for the differences in our transplantation assays.

SOST can bind to both LRP5 and LRP6 proteins, and thus, could be a possible mechanism for regulating LSK HSC, CLP and CMP/MEP populations. WT LSK HSC and CMP/MEP populations both express *Lrp5*, while CLPs lack *Lrp5* expression, and WT LSK HSCs, CLPs, CMP/MEPs all express *Lrp6*. When we analyzed LSK HSC and CLP populations in *Lrp5*$^{-/-}$ mice, we observed significant differences to the total cell numbers of LSK HSC and CLP populations without significant differences to the frequencies of these populations. Two hypotheses can be proposed for the involvement of LRP5 and LRP6 in early HSC and CLP cell fate decisions. One hypothesis is that LRP6 is the chief receptor of SOST in CLPs (since CLPs do not express *Lrp5*) and that this interaction may be directly influencing CLP populations in *Lrp5*$^{-/-}$ mice. Although we have not yet tested this hypothesis directly in *Lrp6*$^{-/-}$ mice, the reduction of HSCs and CLPs in *Lrp5*$^{-/-}$ mice does not directly support this model. Instead, a more likely hypothesis is that LRP5 can influence both self renewal as well as HSC differentiation into CLPs, since Lrp5 is expressed in HSC, and we have observed reductions in both HSC and CLP populations in *Lrp5*$^{-/-}$mice. Analysis of *Lrp6* expression in *Lrp5*$^{-/-}$ mice will help to confirm whether or not this hypothesis is accurate.

In *Sost*$^{-/-}$ mice, osteocytes and osteoblasts are the stromal populations that are the most affected from the lack of SOST, however, the absence of *Sost* does not influence stromal cell function enough to change HSCs under normal homeostatic conditions[134]. The transgenes in the *Dkk-1-Tg* and *Wif-1-Tg* mice are under the control of the Col2.3 promoter, which specifically targets mature osteoblast populations [61,62]. Osteocytes are responsible for maintaining bone mass and control remodeling through by sensing stress induced by physical alterations and control osteoblast survival via the secretion of

SOST [144]. It is still not clear how the absence of *Sost* can alters osteoblast function as it pertains to hematopoietic stem cells engraftment and self renewal.

Another explanation as to how *Sost* deficiency increases HSC engraftment efficiency in competitive and serial transplantation assays is that the specific osteoblast population that supports HSCs is only moderately affected from the deletion of *Sost*. In *Sost*$^{-/-}$ mice, there is an overall increase in osteoblast activity, stemming from the increase in mature osteoblast function and transition from osteoblast to osteocytes [78,79]. It has recently been shown that OBs populations that express *Runx2*, an early marker of osteoblast fate, support hematopoietic stem cells better than those expressing *Osterix* [122]. We have shown in Chapter 2 that osteoblasts are more prone to mineralization, indicating a more mature osteoblastic phenotype, are less able to support hematopoiesis *in vitro*. While it's not known what specific osteoblast populations are involved in B cell development, our work indicates that there are two distinctly different osteoblast populations that are responsible for facilitating cell fate decisions in B cells (as was shown in Chapter 3), where as separate population of osteoblasts promotes self renewal of HSC populations in *Sost*$^{-/-}$ mice, as shown in the current chapter. Whether or not *Sost*$^{-/-}$ mice contain distinct osteoblast populations that could alter HSC populations in a non-cell autonomous manner is a question that remains to be answered.

The increased osteoblastic activity in *Sost*$^{-/-}$ mice may also originate from increased activity of MSC populations. Recently, Nestin^{+} MSCs were shown to be important the support of LT HSCs and establishing the HSC "niche". BM MSC populations are heterogeneous and contain tissue forming specific MSCs [8,147]. In

Sost$^{-/-}$ mice, we observed an increase in lineage^{-} B220^{-} IgM^{-} cells in *Sost*$^{-/-}$ mice, which include MSCs and other stromal populations (data not shown). Identification of the MSC populations that are altered from the absence of SOST may further help to identify the populations that are responsible for maintaining HSC populations in *Sost*$^{-/-}$ mice.

Osteoclasts are myeloid-derived cells responsible for bone resorption and also play a role in maintaining bone mass by altering endosteal osteoblasts. In *Sost*$^{-/-}$ mice, osteoclast function is not altered[78]. One model of osteopetrosis, the *op/op* murine model, display alterations in osteoclast function due to a point mutation in the M-CSF[148]. The *oc/oc* murine model (another model of osteopetrosis) displays osteoclast functional deficiencies due to a defect in *Tcirg1,* which is required for efficient osteoclast resorption function [148,149]. HSC and B cell development is reduced when osteoclast function is altered [80,149,150]. In the studies that used *Dkk-1-Tg, Wif-1-Tg* and *Sfrp-1*$^{-/-}$ mice osteoclast functional assays were not performed [56,61,62]. *Sost*$^{-/-}$ mice do not have overt deficiencies in osteoclast development, and functional assays using *Sost*$^{-/-}$ osteoclasts have yet to be performed, offering an alternative explanation as to why HSCs are only moderately altered in *Sost*$^{-/-}$ mice [78].

In summary, in this chapter, we have shown that HSCs in *Sost*$^{-/-}$ mice appear normal in frequency, cell number, and primary engraftment efficiency. However, using competitive and serial transplantation assays, we have revealed increased engraftment ability of HSCs that have resided in a *Sost*$^{-/-}$ BM environment. SOST antibody treatments are currently being developed as a treatment for osteoporosis due the fact that osteocytes are primarily responsible for SOST production and the dramatic increase to bone mass

observed in *Sost*$^{-/-}$ mice[144]. Our results in *Sost*$^{-/-}$ mice do not indicate any negative effects from the lack of *Sost* on HSCs, contrary to the effects on B cell development reported in Chapter 3. Future experiments to identify any detrimental phenotype to HSC populations in *Sost*$^{-/-}$ mice will help to determine the specific role of SOST and osteocytes on HSC and hematopoietic progenitor cell development in the bone marrow.

Chapter 5: Synthesis and Future Directions

Wnt signaling is required for efficient mineralization of osteoblasts and terminal differentiation into a mature osteocyte [134]. Although the contributions of Wnt signaling in hematopoiesis and osteoblast development are well understood, the regulation of Wnt antagonists in both of these processes is only beginning to be elucidated. Taken together, the studies presented in this dissertation have contributed to expanding current understanding in this area. In Chapter 2, we showed that mineralizing osteoblasts have reduced capacity to support hematopoiesis and that mineralizing MC3T3-E1 cells upregulate the Wnt antagonist SFRP-2. Further work on this project could focus on the role of SFRP-2 using different co-culture assays. For instance, OP9 cells have been shown to produce support both lymphoid and myeloid cells with the addition of IL-7 and Flt3 ligand. [107,151]. In addition, the OP9 cell line is now characterized as a mesenchymal stem cell line, given its expression of MSC cell surface markers and the capacity to differentiate into chondrocytes, osteoblasts, and adipocytes [152]. Addition of SFRP-2 to co-cultures using OP9 monolayers, instead of MC3T3-E1 cells might reveal what specific function SFRP-2 has in hematopoiesis. The capacity of OP9 to differentiate into osteoblasts can also reveal specific changes in Wnt antagonist signaling as mesenchymal stem cells differentiate into different terminal cell lineages, which could, in turn, can reveal more information about the dynamics of SFRP-2 in hematopoietic development *in vitro*. Corresponding studies using *Sfrp-2*$^{-/-}$ mice would add significantly to how this protein is relevant to both hematopoiesis and osteoblast development *in vivo* [68].

SFRPs are largely thought to inhibit Wnt signaling, however, there is evidence that supports that in some contexts, SFRPs can actually expand the range of Wnt signaling[121]. For instance, using Xenopus embryos, Mii and colleagues showed high levels of SFRPs expression throughout the embryo, while Wnt expression was limited to specialized areas in the same embryo[153]. SFRPs bound to Wnt proteins increased the area that Wnt proteins could travel, altering the gradient of Wnt signaling in these embryos. In our cultures, SFRP-2 could potentially increase the range of Wnt signaling which, in turn, could alter MC3T3-E1 support of granulocytes that we observed in Chapter 2 [121]. Wnt3a also binds to SFRPs and could possibly work in a similar manner to alter Wnt gradients in culture [63]. Using the MC3T3-E1 co-culture system, we could test if the addition of Wnt3a and SFRP-2 in different concentrations results in altered myeloid development. Furthermore, MC3T3-E1 co-culture systems could promote embryonic stem cell differentiation into hematopoietic stem cell populations, which opens the possibility of a new system that can promote differentiation of ESCs *in vitro* (Thompson and Manilay, unpublished data).

In Chapter 3, we found that the absence of *Sost* influences B cell lymphopoiesis. Currently, Amgen, Inc. is leading Phase 3 clinical trials for a sclerostin antibody as a potential treatment for osteoporosis [144]. Our findings that B cell survival is reduced in the absence of *Sost* suggests that this may be a possible side effect of altering the bone microenvironment using sclerostin-depleting antibodies. Although our data suggests that *Sost*$^{-/-}$ B cells respond normally to LPS stimulation, more exhaustive studies need to be completed to determine if B cell function is truly unaffected by the absence of *Sost*

[134,144]. Future work could focus on characterizing immunoglobulin titers and immune responses to more diverse antigens in $Sost^{-/-}$ mice, ultimately culminating in studies in which analysis of immune function in that mice with the sclerostin is performed.. No study of the immune system of human patients with Van Buchem's disease has been reported, and it would be interesting to investigate this further to see if the B cell phenotype extends to the Van Buchem's disease and to anti-sclerostin treated patients.

Another possible future direction of this work is to focus specifically on the stromal cell populations that are responsible for the reduction in B cell survival in *Sost*$^{-/-}$ mice. The identity of the stromal cell population that contains reduced CXCL12 expression in *Sost*$^{-/-}$ mice remains a mystery. Osteoblasts, osteoclasts and CXCL12 abundant reticular (CAR) cells have been shown to produce CXCL12 and regulate B cell survival. Currently, we hypothesize that osteoblasts are the only population that are affecting B cells in *Sost*$^{-/-}$ mice; however, there is a large population of Lin^{-} $CD45^{-}B220^{-}$ IgM^{-} cells in *Sost*$^{-/-}$ mice, which could contain MSC, OB, endothelial cells and other bone stromal cells that has yet to be characterized [90,136,154]. We assayed mRNA from digested bone samples in our studies, which should contain mostly osteoblasts but more extensive analysis on FACS-sorted osteoblast populations need to be completed.

Like the SFRPs, Wnt inhibitory factor (WIF) binds to Wnt ligands directly, but does not resemble SFRPs structurally (Figure 1.3A) [54]. WIF-1 was first characterized in *Xenopus* and was shown to be highly conserved from *Drosophila* to humans, and only one WIF has been identified to date in mammals [155]. WIF-1 contains a unique Wnt

inhibitory factor domain that lacks the CRD and NTR that is found in SFRPs [156,157]. In contrast to SFRPs, WIF-1 lacks the capacity to bind to Frizzled proteins [157]. Like SFRPs, WIF-1 can also block both canonical and non-canonical Wnt signaling. WIF-1 is expressed by mature OBs [158], although its role in hematopoiesis is only beginning to be elucidated [61,158].

Recently, Schaniel et al. showed that in WIF-1 transgenic mice (*Wif-1-Tg*), which over express WIF-1 in osteoblasts (under the control of the rat *Col2.3* promoter), no profound effect on their bone architecture was evident, but increased percentages of LT HSCs with reduced quiescence were present [61]. When *Wif-1-Tg* mice were injected with weekly doses of 5-fluorouracil (5-FU), which eliminates proliferating cells, *Wif-1-Tg* mice died by 12 weeks, where as all 5-FU-treated wild type mice survived past 12 weeks. This result indicated that *Wif-1-Tg* HSCs were more proliferative than wild type mice, or were unable to self-renew after treatment. Additionally, exhaustion of wild-type HSCs was observed only when they were transplanted into *Wif-1-Tg* hosts, demonstrating a non-cell autonomous effect of WIF-1 on hematopoiesis. Paradoxically, HSCs from *Wif-1-Tg* mice did not display reduced β-catenin signaling; rather, Wnt3a was dramatically increased, which could have led to overactive cycling of the HSCs. In line with this, Jagged-1, CXCL12, and N-cadherin, which are important for HSC self-renewal and maintenance, were all upregulated in osteoblasts in response to WIF-1 overexpression [81].

It is still unclear how WIF-1 is regulating LT-HSCs and their differentiated hematopoietic cell progeny. We have shown that *Sost*$^{-/-}$ mice have HSCs that are altered

through a non-cell autonomous mechanism. Although SOST and WIF-1 have different mechanisms to antagonize Wnt signaling, it is interesting that there are still pronounced defects in HSC in both *Sost*$^{-/-}$ and *Wif-1-Tg* mice. The experimental evidence indicates a non-cell autonomous role of WIF-1 on hematopoiesis, but there are no studies showing that WIF-1 can bind to HSCs directly. We also have not performed studies to see if *Sost*$^{-/-}$ can bind directly to HSCs or B cells, which could help to explain the differences observed in *Wif-1-Tg* mice and *Sost*$^{-/-}$ mice. Osteoblast-specific conditional WIF-1 knockout mice could also help to determine if WIF-1 serves a physiological role on hematopoiesis that is not compensated by some other Wnt antagonist in the bone marrow such as SOST, DKK-1 or SFRPs.

We know that *Dkk-1* is upregulated in *Sost*$^{-/-}$ mice, which in combination with the lack of Sclerostin may also be influencing B cell development (Loots et al. unpublished data). The Dickkopf (DKK) family consists of the secreted DKKs, which bind to the LRP4, LRP5 and LRP6 co-receptors [55,134] (Figure 1.3B). The first Dickkopf was identified in *Xenopus* as a modulator of head development [159]. There are 4 members in the DKK family of proteins, DKK-1, DKK-2, DKK-3 and DKK-4. In order for DKKs to effectively block Wnt signaling, the DKK receptor Kremen must be present. DKK proteins contain a cysteine rich domain (Cys1 domain) that is unique to the DKKs, and also contain a colipase domain (Cys2 domain) that may have a role in binding to LRP5/6 and Kremen [55,160]. Inhibition of Wnt signaling occurs with the binding of DKK proteins to both LRP5/6 co-receptors and Kremen, which is quickly internalized. To date, DKK-1 is the only DKK family protein that has been shown to influence hematopoiesis [62,161].

Fleming et al. discovered that transgenic mice expressing DKK-1 in osteoblasts under control of the rat *Col2.3* promoter (*Dkk-1-Tg*) showed a dysregulation in HSC quiescence, similar to that of *Wif-1-Tg* mice [61,62]. *Dkk-1-Tg* mice did not display differences in HSC, CMP, MEP and GMP populations, but there was a significant increase in CLPs in the bone marrow. β-catenin levels were reduced in both LT-HSC and ST-HSC, showing that the high levels of DKK1 secreted from endosteal osteoblasts could antagonize Wnt signaling in HSCs. HSCs from *Dkk-1-Tg* mice formed fewer CFUs *in vitro* and also resulted in higher lethality in recipients after secondary transplantation. Like in the *Wif-1-Tg* mice [61], this lethality was explained by exhaustion of *Dkk-1-Tg* HSCs, due to reduced quiescence, and this effect was found to be non-cell autonomous in nature by bone marrow transplantation studies. Interestingly, secondary and tertiary transplantation of bone marrow from WT→ *Dkk-1-Tg* mice back into WT recipients revealed a persistent HSC phenotype, even though the HSC were no longer in a *Dkk-1-Tg* environment. In our studies, we showed an increase in engraftment in both competitive and secondary transplantation in mice that were exposed to *Sost*$^{-/-}$ mouse BM environment. It has been postulated that this persistent non-quiescent phenotype in the transplanted HSCs may have resulted from permanent epigenetic programming in the HSC when they were exposed in the *Dkk-1-Tg* bone microenvironment. Similarly, epigenetic programming could explain our observed phenotype in *Sost*$^{-/-}$ HSCs, however, we still need to perform experiments to confirm this hypothesis.

In another study, TOP-GAL β-catenin reporter mice treated with exogenous DKK-1, displayed reduced β-catenin activation and increased RANKL signaling in endosteal osteoblasts (most likely due to inhibition of canonical Wnt signaling by DKK-1, which normally suppresses RANKL secretion)[161,162]. Mice treated with exogenous DKK-1 showed increased mobilization of hematopoietic stem and progenitor cells as well as vascular progenitors from the bone marrow to the blood [161]. This mobilization was only limited to that of progenitor cells, as there was no observed increase in mature granulocytes and monocytes in the blood. We still have yet to look at β catenin activation in *Sost*$^{-/-}$ mice. Crossing *Sost*$^{-/-}$ mice with TOP-GAL β-catenin reporter mice would show which hematopoietic populations are directly influenced from the deficiency in SOST.

It is interesting that exogenous DKK-1 mobilizes stem cells away from the bone marrow niche, as Fleming et al. noted no significant difference in the HSC and committed lineages in the peripheral blood in *Dkk-1-Tg* mice [62]. These different experimental results could be explained, in part, by the differences in the strategy used to identify LT-HSC, ST-HSC versus HSPCs in the two studies, or due to a quantitative difference between the levels of DKK-1 protein (and in turn, different thresholds of Wnt antagonism) in the different model systems. Recently, it has been suggested that analysis of vascular cells should be included in studies of hematopoiesis and Wnt antagonists, as vascular cells are important sources of Wnt ligands and intimately involved in HSC self renewal and subsequent development into hematopoietic progeny [3]. The changes in the vascular cells reported by Aicher et al. might indicate that vascular cells may contribute to HSC defects in *Dkk-1-Tg* mice.

In addition to the altered B cell development in *Sost*$^{-/-}$ mice, we observed a significant increase in splenic granulocytes. The consequence and the reason behind this increase require further investigation. *Sost* expression has not been observed in the spleen, however, in Chapter 4, we showed that the populations of CMP/MEP as well as GMP populations are higher in *Sost*$^{-/-}$ spleens compared to wild type cohorts. One hypothesis to explain this is that CMP/MEP/GMP progenitor cells migrate from the bone marrow to the spleen to compensate for the lack of space present in the bone marrow in Sost-/- mice. Injecting lethally irradiated mice with GFP^{+} HSPCs or using live animal tracking systems that can track fluorescently labeled progenitor cell migration are needed to test if CMP/MEP/GMP progenitor migration is occurring in *Sost*$^{-/-}$ mice [94]. Additionally, there may be altered chemokine levels (i.e. CXCL12) that extend beyond the BM in Sost-/- mice, such as the spleen or liver which could help to explain the altered progenitor populations present in the spleen. Identifying whether the increased myeloid populations in *Sost*$^{-/-}$ spleens are due to over proliferative CMP/MEP populations, or from the increased migration of CMP/MEP due to constrained space in the BM are some future studies would not only add significantly to understanding how bone microenvironments influence myeloid development and migration, but also identify a link for Wnt signaling and regulation of granulocytes.

It was surprising that the reduction in CXCL12 levels in *Sost*$^{-/-}$ BM in conjunction with the increase in osteoblast activity and *Dkk-1* expression observed in *Sost*$^{-/-}$ mice did not have a more dramatic phenotype on HSCs. One explanation for this might be that the levels of CXCL12 for LT-HSC and LSK HSC function are determined more by the

expression of CXCL12 in the bone marrow stromal cells, such as CAR cells and MSCs, than that of osteoblast cells [6,8]. CXCL12 is required to retain HSCs in the bone marrow, and excess Wnt signaling has recently been shown to reduce CXCL12 secretion in stromal cells [102,163]. Further analysis is required to determine how CXCL12 expression in osteoblasts and other osteolineage cell types modulate HSC cell fate decisions at the endosteum.

One of the most interesting aspects about SOST is how different it is functionally from the other Wnt antagonists in the context of hematopoietic stem cell development. SFRP-1 and SFRP-2 have demonstrated negative and positive influences on hematopoietic stem cells respectively [56,57]. Excess of osteoblast specific DKK-1 and WIF-1 were shown to decrease LT-HSC function, while SOST had no effect on hematopoietic stem cells [61,62]. All Wnt antagonists that have been studied in the context of hematopoiesis have been shown to influence hematopoiesis through non-cell autonomous mechanisms. The populations of osteoblasts populations that are changed due to alterations in Wnt antagonist modulation might explain the differences observed in hematopoietic stem and progenitor cell function. Further work to characterize Wnt antagonist knock out models (i.e., using *Sfrp-2*$^{-/-}$ of *Wif-1* $^{-/-}$) or transgenic mouse models would be helpful in determining how each of these Wnt antagonists contributes specifically to hematopoietic stem and progenitor cell biology.

REFERENCES

1. Seita J, Weissman IL (2010) Hematopoietic stem cell: self-renewal versus differentiation. Wiley Interdiscip Rev Syst Biol Med 2: 640-653.
2. Li L, Xie T (2005) Stem cell niche: structure and function. Annu Rev Cell Dev Biol 21: 605-631.
3. Ding L, Saunders TL, Enikolopov G, Morrison SJ (2012) Endothelial and perivascular cells maintain haematopoietic stem cells. Nature 481: 457-462.
4. Calvi LM, Adams GB, Weibrecht KW, Weber JM, Olson DP, et al. (2003) Osteoblastic cells regulate the haematopoietic stem cell niche. Nature 425: 841-846.
5. Zhang J, Niu C, Ye L, Huang H, He X, et al. (2003) Identification of the haematopoietic stem cell niche and control of the niche size. Nature 425: 836-841.
6. Sugiyama T, Kohara H, Noda M, Nagasawa T (2006) Maintenance of the hematopoietic stem cell pool by CXCL12-CXCR4 chemokine signaling in bone marrow stromal cell niches. Immunity 25: 977-988.
7. Kiel MJ, Morrison SJ (2006) Maintaining hematopoietic stem cells in the vascular niche. Immunity 25: 862-864.
8. Mendez-Ferrer S, Michurina TV, Ferraro F, Mazloom AR, Macarthur BD, et al. (2010) Mesenchymal and haematopoietic stem cells form a unique bone marrow niche. Nature 466: 829-834.
9. Porter RL, Calvi LM (2008) Communications between bone cells and hematopoietic stem cells. Arch Biochem Biophys 473: 193-200.

10. Pacifici R (2010) The immune system and bone. Arch Biochem Biophys 503: 41-53.

11. Bhandoola A, von Boehmer H, Petrie HT, Zuniga-Pflucker JC (2007) Commitment and developmental potential of extrathymic and intrathymic T cell precursors: plenty to choose from. Immunity 26: 678-689.

12. Yang L, Bryder D, Adolfsson J, Nygren J, Mansson R, et al. (2005) Identification of Lin(-)Sca1(+)kit(+)CD34(+)Flt3- short-term hematopoietic stem cells capable of rapidly reconstituting and rescuing myeloablated transplant recipients. Blood 105: 2717-2723.

13. Wilson A, Oser GM, Jaworski M, Blanco-Bose WE, Laurenti E, et al. (2007) Dormant and self-renewing hematopoietic stem cells and their niches. Ann N Y Acad Sci 1106: 64-75.

14. Ostrakhovitch EA, Li SS (2006) The role of SLAM family receptors in immune cell signaling. Biochem Cell Biol 84: 832-843.

15. Rossi L, Challen GA, Sirin O, Lin KK, Goodell MA (2011) Hematopoietic stem cell characterization and isolation. Methods Mol Biol 750: 47-59.

16. Yu M, Cantor AB (2012) Megakaryopoiesis and thrombopoiesis: an update on cytokines and lineage surface markers. Methods Mol Biol 788: 291-303.

17. Wilusz M, Majka M (2008) Role of the Wnt/beta-catenin network in regulating hematopoiesis. Arch Immunol Ther Exp (Warsz) 56: 257-266.

18. Sharma RP, Chopra VL (1976) Effect of the Wingless (wg1) mutation on wing and haltere development in Drosophila melanogaster. Dev Biol 48: 461-465.

19. Malhotra S, Baba Y, Garrett KP, Staal FJ, Gerstein R, et al. (2008) Contrasting responses of lymphoid progenitors to canonical and noncanonical Wnt signals. J Immunol 181: 3955-3964.

20. Rijsewijk F, Schuermann M, Wagenaar E, Parren P, Weigel D, et al. (1987) The Drosophila homolog of the mouse mammary oncogene int-1 is identical to the segment polarity gene wingless. Cell 50: 649-657.

21. Cadigan KM, Nusse R (1997) Wnt signaling: a common theme in animal development. Genes Dev 11: 3286-3305.

22. Yanagawa S, van Leeuwen F, Wodarz A, Klingensmith J, Nusse R (1995) The dishevelled protein is modified by wingless signaling in Drosophila. Genes Dev 9: 1087-1097.

23. Nemeth MJ, Bodine DM (2007) Regulation of hematopoiesis and the hematopoietic stem cell niche by Wnt signaling pathways. Cell Res 17: 746-758.

24. Malhotra S, Kincade PW (2009) Wnt-related molecules and signaling pathway equilibrium in hematopoiesis. Cell Stem Cell 4: 27-36.

25. Peifer M, Orsulic S, Sweeton D, Wieschaus E (1993) A role for the Drosophila segment polarity gene armadillo in cell adhesion and cytoskeletal integrity during oogenesis. Development 118: 1191-1207.

26. Riggleman B, Schedl P, Wieschaus E (1990) Spatial expression of the Drosophila segment polarity gene armadillo is posttranscriptionally regulated by wingless. Cell 63: 549-560.

27. Shitashige M, Hirohashi S, Yamada T (2008) Wnt signaling inside the nucleus. Cancer Sci 99: 631-637.

28. He X, Saint-Jeannet JP, Wang Y, Nathans J, Dawid I, et al. (1997) A member of the Frizzled protein family mediating axis induction by Wnt-5A. Science 275: 1652-1654.

29. Staal FJ, Luis TC, Tiemessen MM (2008) WNT signalling in the immune system: WNT is spreading its wings. Nat Rev Immunol 8: 581-593.

30. Kokolus K, Nemeth MJ (2010) Non-canonical Wnt signaling pathways in hematopoiesis. Immunol Res 46: 155-164.

31. Widelitz R (2005) Wnt signaling through canonical and non-canonical pathways: recent progress. Growth Factors 23: 111-116.

32. De A (2011) Wnt/Ca2+ signaling pathway: a brief overview. Acta Biochim Biophys Sin (Shanghai) 43: 745-756.

33. Timm A, Grosschedl R (2005) Wnt signaling in lymphopoiesis. Curr Top Microbiol Immunol 290: 225-252.

34. Austin TW, Solar GP, Ziegler FC, Liem L, Matthews W (1997) A role for the Wnt gene family in hematopoiesis: expansion of multilineage progenitor cells. Blood 89: 3624-3635.

35. Hausler KD, Horwood NJ, Chuman Y, Fisher JL, Ellis J, et al. (2004) Secreted frizzled-related protein-1 inhibits RANKL-dependent osteoclast formation. J Bone Miner Res 19: 1873-1881.

36. Liang H, Chen Q, Coles AH, Anderson SJ, Pihan G, et al. (2003) Wnt5a inhibits B cell proliferation and functions as a tumor suppressor in hematopoietic tissue. Cancer Cell 4: 349-360.

37. Ellett F, Lieschke GJ (2010) Zebrafish as a model for vertebrate hematopoiesis. Curr Opin Pharmacol 10: 563-570.

38. Clements WK, Kim AD, Ong KG, Moore JC, Lawson ND, et al. (2011) A somitic Wnt16/Notch pathway specifies haematopoietic stem cells. Nature 474: 220-224.

39. Stachura DL, Traver D (2011) Cellular dissection of zebrafish hematopoiesis. Methods Cell Biol 101: 75-110.

40. Held W, Kunz B, Lowin-Kropf B, van de Wetering M, Clevers H (1999) Clonal acquisition of the Ly49A NK cell receptor is dependent on the trans-acting factor TCF-1. Immunity 11: 433-442.

41. Staal FJ, Sen JM (2008) The canonical Wnt signaling pathway plays an important role in lymphopoiesis and hematopoiesis. Eur J Immunol 38: 1788-1794.

42. Reya T, Duncan AW, Ailles L, Domen J, Scherer DC, et al. (2003) A role for Wnt signalling in self-renewal of haematopoietic stem cells. Nature 423: 409-414.

43. Lu D, Zhao Y, Tawatao R, Cottam HB, Sen M, et al. (2004) Activation of the Wnt signaling pathway in chronic lymphocytic leukemia. Proc Natl Acad Sci U S A 101: 3118-3123.

44. Ranheim EA, Kwan HC, Reya T, Wang YK, Weissman IL, et al. (2005) Frizzled 9 knock-out mice have abnormal B-cell development. Blood 105: 2487-2494.

45. Reya T, O'Riordan M, Okamura R, Devaney E, Willert K, et al. (2000) Wnt signaling regulates B lymphocyte proliferation through a LEF-1 dependent mechanism. Immunity 13: 15-24.

46. Cobas M, Wilson A, Ernst B, Mancini SJ, MacDonald HR, et al. (2004) Beta-catenin is dispensable for hematopoiesis and lymphopoiesis. J Exp Med 199: 221-229.

47. Kirstetter P, Anderson K, Porse BT, Jacobsen SE, Nerlov C (2006) Activation of the canonical Wnt pathway leads to loss of hematopoietic stem cell repopulation and multilineage differentiation block. Nat Immunol 7: 1048-1056.

48. Xu Y, Banerjee D, Huelsken J, Birchmeier W, Sen JM (2003) Deletion of beta-catenin impairs T cell development. Nat Immunol 4: 1177-1182.

49. Castrop J, Verbeek S, Hofhuis F, Clevers H (1995) Circumvention of tolerance for the nuclear T cell protein TCF-1 by immunization of TCF-1 knock-out mice. Immunobiology 193: 281-287.

50. Germar K, Dose M, Konstantinou T, Zhang J, Wang H, et al. (2011) T-cell factor 1 is a gatekeeper for T-cell specification in response to Notch signaling. Proc Natl Acad Sci U S A 108: 20060-20065.

51. Okamura RM, Sigvardsson M, Galceran J, Verbeek S, Clevers H, et al. (1998) Redundant regulation of T cell differentiation and TCRalpha gene expression by the transcription factors LEF-1 and TCF-1. Immunity 8: 11-20.

52. Baba Y, Garrett KP, Kincade PW (2005) Constitutively active beta-catenin confers multilineage differentiation potential on lymphoid and myeloid progenitors. Immunity 23: 599-609.

53. Lane SW, Wang YJ, Lo Celso C, Ragu C, Bullinger L, et al. (2011) Differential niche and Wnt requirements during acute myeloid leukemia progression. Blood.

54. Chien AJ, Conrad WH, Moon RT (2009) A Wnt survival guide: from flies to human disease. J Invest Dermatol 129: 1614-1627.

55. Choi HY, Dieckmann M, Herz J, Niemeier A (2009) Lrp4, a novel receptor for Dickkopf 1 and sclerostin, is expressed by osteoblasts and regulates bone growth and turnover in vivo. PLoS One 4: e7930.

56. Renstrom J, Istvanffy R, Gauthier K, Shimono A, Mages J, et al. (2009) Secreted frizzled-related protein 1 extrinsically regulates cycling activity and maintenance of hematopoietic stem cells. Cell Stem Cell 5: 157-167.

57. Nakajima H, Ito M, Morikawa Y, Komori T, Fukuchi Y, et al. (2009) Wnt modulators, SFRP-1, and SFRP-2 are expressed in osteoblasts and differentially regulate hematopoietic stem cells. Biochem Biophys Res Commun 390: 65-70.

58. Cain CJ, Rueda R, McLelland B, Collette NM, Loots GG, et al. (2012) Absence of sclerostin adversely affects B cell survival. J Bone Miner Res 27: 1451-1461.

59. Yokota T, Oritani K, Garrett KP, Kouro T, Nishida M, et al. (2008) Soluble frizzled-related protein 1 is estrogen inducible in bone marrow stromal cells and suppresses the earliest events in lymphopoiesis. J Immunol 181: 6061-6072.

60. Oshima T, Abe M, Asano J, Hara T, Kitazoe K, et al. (2005) Myeloma cells suppress bone formation by secreting a soluble Wnt inhibitor, sFRP-2. Blood 106: 3160-3165.

61. Schaniel C, Sirabella D, Qiu J, Niu X, Lemischka IR, et al. (2011) Wnt-inhibitory factor 1 dysregulation of the bone marrow niche exhausts hematopoietic stem cells. Blood.

62. Fleming HE, Janzen V, Lo Celso C, Guo J, Leahy KM, et al. (2008) Wnt signaling in the niche enforces hematopoietic stem cell quiescence and is necessary to preserve self-renewal in vivo. Cell Stem Cell 2: 274-283.

63. Bovolenta P, Esteve P, Ruiz JM, Cisneros E, Lopez-Rios J (2008) Beyond Wnt inhibition: new functions of secreted Frizzled-related proteins in development and disease. J Cell Sci 121: 737-746.

64. Lopez-Rios J, Esteve P, Ruiz JM, Bovolenta P (2008) The Netrin-related domain of Sfrp1 interacts with Wnt ligands and antagonizes their activity in the anterior neural plate. Neural Dev 3: 19.

65. Bodine PV, Zhao W, Kharode YP, Bex FJ, Lambert AJ, et al. (2004) The Wnt antagonist secreted frizzled-related protein-1 is a negative regulator of trabecular bone formation in adult mice. Mol Endocrinol 18: 1222-1237.

66. Girnun GD, Smith WM, Drori S, Sarraf P, Mueller E, et al. (2002) APC-dependent suppression of colon carcinogenesis by PPARgamma. Proc Natl Acad Sci U S A 99: 13771-13776.

67. Moldes M, Zuo Y, Morrison RF, Silva D, Park BH, et al. (2003) Peroxisome-proliferator-activated receptor gamma suppresses Wnt/beta-catenin signalling during adipogenesis. Biochem J 376: 607-613.

68. Satoh W, Gotoh T, Tsunematsu Y, Aizawa S, Shimono A (2006) Sfrp1 and Sfrp2 regulate anteroposterior axis elongation and somite segmentation during mouse embryogenesis. Development 133: 989-999.

69. Satoh W, Matsuyama M, Takemura H, Aizawa S, Shimono A (2008) Sfrp1, Sfrp2, and Sfrp5 regulate the Wnt/beta-catenin and the planar cell polarity pathways during early trunk formation in mouse. Genesis 46: 92-103.

70. Cheng YH, Chitteti BR, Streicher DA, Morgan JA, Rodriguez-Rodriguez S, et al. (2010) Impact of osteoblast maturational status on their ability to enhance the hematopoietic function of stem and progenitor cells. J Bone Miner Res.

71. Roux S (2010) New treatment targets in osteoporosis. Joint Bone Spine 77: 222-228.

72. van Bezooijen RL, ten Dijke P, Papapoulos SE, Lowik CW (2005) SOST/sclerostin, an osteocyte-derived negative regulator of bone formation. Cytokine Growth Factor Rev 16: 319-327.

73. Semenov M, Tamai K, He X (2005) SOST is a ligand for LRP5/LRP6 and a Wnt signaling inhibitor. J Biol Chem 280: 26770-26775.

74. Kamiya N, Ye L, Kobayashi T, Mochida Y, Yamauchi M, et al. (2008) BMP signaling negatively regulates bone mass through sclerostin by inhibiting the canonical Wnt pathway. Development 135: 3801-3811.

75. Bilezikian JP, Raisz LG, Martin TJ (2008) Principles of bone biology. San Diego, Calif.: Academic Press/Elsevier. 2 v. (xxiv, 1942, liv p. + 1922 p. of plates) p.

76. Kramer I, Loots GG, Studer A, Keller H, Kneissel M (2010) Parathyroid hormone (PTH)-induced bone gain is blunted in SOST overexpressing and deficient mice. J Bone Miner Res 25: 178-189.

77. Loots GG, Kneissel M, Keller H, Baptist M, Chang J, et al. (2005) Genomic deletion of a long-range bone enhancer misregulates sclerostin in Van Buchem disease. Genome Res 15: 928-935.

78. Li X, Ominsky MS, Niu QT, Sun N, Daugherty B, et al. (2008) Targeted deletion of the sclerostin gene in mice results in increased bone formation and bone strength. J Bone Miner Res 23: 860-869.

79. Krause C, Korchynskyi O, de Rooij K, Weidauer SE, de Gorter DJ, et al. (2010) Distinct modes of inhibition by sclerostin on bone morphogenetic protein and Wnt signaling pathways. J Biol Chem 285: 41614-41626.

80. Tagaya H, Kunisada T, Yamazaki H, Yamane T, Tokuhisa T, et al. (2000) Intramedullary and extramedullary B lymphopoiesis in osteopetrotic mice. Blood 95: 3363-3370.

81. Kiel MJ, Morrison SJ (2008) Uncertainty in the niches that maintain haematopoietic stem cells. Nat Rev Immunol 8: 290-301.

82. Elford PR, Felix R, Cecchini M, Trechsel U, Fleisch H (1987) Murine osteoblastlike cells and the osteogenic cell MC3T3-E1 release a macrophage colony-stimulating activity in culture. Calcif Tissue Int 41: 151-156.

83. Taichman RS, Emerson SG (1994) Human osteoblasts support hematopoiesis through the production of granulocyte colony-stimulating factor. J Exp Med 179: 1677-1682.

84. Marie PJ (2008) Transcription factors controlling osteoblastogenesis. Arch Biochem Biophys 473: 98-105.

85. Hartmann C (2009) Transcriptional networks controlling skeletal development. Curr Opin Genet Dev 19: 437-443.

86. Wiktor-Jedrzejczak WW, Ahmed A, Szczylik C, Skelly RR (1982) Hematological characterization of congenital osteopetrosis in op/op mouse. Possible mechanism for abnormal macrophage differentiation. J Exp Med 156: 1516-1527.

87. Xie Y, Yin T, Wiegraebe W, He XC, Miller D, et al. (2009) Detection of functional haematopoietic stem cell niche using real-time imaging. Nature 457: 97-101.

88. Horowitz MC, Coleman DL, Ryaby JT, Einhorn TA (1989) Osteotropic agents induce the differential secretion of granulocyte-macrophage colony-stimulating factor by the osteoblast cell line MC3T3-E1. J Bone Miner Res 4: 911-921.

89. Nelissen JM, Torensma R, Pluyter M, Adema GJ, Raymakers RA, et al. (2000) Molecular analysis of the hematopoiesis supporting osteoblastic cell line U2-OS. Exp Hematol 28: 422-432.

90. Wu JY, Purton LE, Rodda SJ, Chen M, Weinstein LS, et al. (2008) Osteoblastic regulation of B lymphopoiesis is mediated by Gs{alpha}-dependent signaling pathways. Proc Natl Acad Sci U S A 105: 16976-16981.

91. Nagasawa T (2006) Microenvironmental niches in the bone marrow required for B-cell development. Nat Rev Immunol 6: 107-116.

92. Calvi LM, Bromberg O, Rhee Y, Weber JM, Smith JN, et al. (2012) Osteoblastic expansion induced by parathyroid hormone receptor signaling in murine osteocytes is not sufficient to increase hematopoietic stem cells. Blood 119: 2489-2499.

93. Visnjic D, Kalajzic Z, Rowe DW, Katavic V, Lorenzo J, et al. (2004) Hematopoiesis is severely altered in mice with an induced osteoblast deficiency. Blood 103: 3258-3264.

94. Lo Celso C, Fleming HE, Wu JW, Zhao CX, Miake-Lye S, et al. (2009) Live-animal tracking of individual haematopoietic stem/progenitor cells in their niche. Nature 457: 92-96.

95. Schroeder TM, Jensen ED, Westendorf JJ (2005) Runx2: a master organizer of gene transcription in developing and maturing osteoblasts. Birth Defects Res C Embryo Today 75: 213-225.

96. Rauner M, Sipos W, Pietschmann P (2008) Age-dependent Wnt gene expression in bone and during the course of osteoblast differentiation. Age (Dordr) 30: 273-282.

97. Westendorf JJ, Kahler RA, Schroeder TM (2004) Wnt signaling in osteoblasts and bone diseases. Gene 341: 19-39.

98. Li X, Zhang Y, Kang H, Liu W, Liu P, et al. (2005) Sclerostin binds to LRP5/6 and antagonizes canonical Wnt signaling. J Biol Chem 280: 19883-19887.

99. Sawakami K, Robling AG, Ai M, Pitner ND, Liu D, et al. (2006) The Wnt co-receptor LRP5 is essential for skeletal mechanotransduction but not for the anabolic bone response to parathyroid hormone treatment. J Biol Chem 281: 23698-23711.

100. Nteliopoulos G, Marley SB, Gordon MY (2009) Influence of PI-3K/Akt pathway on Wnt signalling in regulating myeloid progenitor cell proliferation. Evidence for a role of autocrine/paracrine Wnt regulation. Br J Haematol 146: 637-651.

101. Glass DA, 2nd, Karsenty G (2006) Canonical Wnt signaling in osteoblasts is required for osteoclast differentiation. Ann N Y Acad Sci 1068: 117-130.

102. Tamura M, Sato MM, Nashimoto M (2011) Regulation of CXCL12 expression by canonical Wnt signaling in bone marrow stromal cells. Int J Biochem Cell Biol 43: 760-767.

103. Malhotra S, Kincade PW (2009) Canonical Wnt pathway signaling suppresses VCAM-1 expression by marrow stromal and hematopoietic cells. Exp Hematol 37: 19-30.

104. Sudo H, Kodama HA, Amagai Y, Yamamoto S, Kasai S (1983) In vitro differentiation and calcification in a new clonal osteogenic cell line derived from newborn mouse calvaria. J Cell Biol 96: 191-198.

105. Quarles LD, Yohay DA, Lever LW, Caton R, Wenstrup RJ (1992) Distinct proliferative and differentiated stages of murine MC3T3-E1 cells in culture: an in vitro model of osteoblast development. J Bone Miner Res 7: 683-692.

106. Wang D, Christensen K, Chawla K, Xiao G, Krebsbach PH, et al. (1999) Isolation and characterization of MC3T3-E1 preosteoblast subclones with distinct in vitro and in vivo differentiation/mineralization potential. J Bone Miner Res 14: 893-903.

107. Schmitt TM, de Pooter RF, Gronski MA, Cho SK, Ohashi PS, et al. (2004) Induction of T cell development and establishment of T cell competence from embryonic stem cells differentiated in vitro. Nat Immunol 5: 410-417.

108. Gravano DM, Manilay JO (2010) Inhibition of proteolysis of Delta-like-1 does not promote or reduce T-cell developmental potential. Immunol Cell Biol 88: 746-753.

109. Sheehan DC, Hrapchak BB (1980) Theory and practice of histotechnology. St. Louis: Mosby. xiii, 481 p., 481 leaf of plates p.

110. Gravano DM, McLelland BT, Horiuchi K, Manilay JO (2010) ADAM17 deletion in thymic epithelial cells alters aire expression without affecting T cell developmental progression. PLoS One 5: e13528.

111. Wu JY, Scadden DT, Kronenberg HM (2009) The Role of the Osteoblast Lineage in the Bone Marrow Hematopoietic Niches. J Bone Miner Res.

112. Nilsson SK, Johnston HM, Whitty GA, Williams B, Webb RJ, et al. (2005) Osteopontin, a key component of the hematopoietic stem cell niche and regulator of primitive hematopoietic progenitor cells. Blood 106: 1232-1239.

113. Jung Y, Wang J, Havens A, Sun Y, Jin T, et al. (2005) Cell-to-cell contact is critical for the survival of hematopoietic progenitor cells on osteoblasts. Cytokine 32: 155-162.

114. Jung Y, Wang J, Schneider A, Sun YX, Koh-Paige AJ, et al. (2006) Regulation of SDF-1 (CXCL12) production by osteoblasts; a possible mechanism for stem cell homing. Bone 38: 497-508.

115. Chan CK, Chen CC, Luppen CA, Kim JB, DeBoer AT, et al. (2009) Endochondral ossification is required for haematopoietic stem-cell niche formation. Nature 457: 490-494.

116. Boiret N, Rapatel C, Veyrat-Masson R, Guillouard L, Guerin JJ, et al. (2005) Characterization of nonexpanded mesenchymal progenitor cells from normal adult human bone marrow. Exp Hematol 33: 219-225.

117. Horowitz MC, Fretz JA, Lorenzo JA (2010) How B cells influence bone biology in health and disease. Bone 47: 472-479.

118. Long F (2012) Building strong bones: molecular regulation of the osteoblast lineage. Nat Rev Mol Cell Biol 13: 27-38.

119. Yazid MD, Ariffin SH, Senafi S, Razak MA, Wahab RM (2010) Determination of the differentiation capacities of murines' primary mononucleated cells and MC3T3-E1 cells. Cancer Cell Int 10: 42.

120. Duncan AW, Rattis FM, DiMascio LN, Congdon KL, Pazianos G, et al. (2005) Integration of Notch and Wnt signaling in hematopoietic stem cell maintenance. Nat Immunol 6: 314-322.

121. Mii Y, Taira M (2011) Secreted Wnt "inhibitors" are not just inhibitors: regulation of extracellular Wnt by secreted Frizzled-related proteins. Dev Growth Differ 53: 911-923.

122. Chitteti BR, Cheng YH, Streicher DA, Rodriguez-Rodriguez S, Carlesso N, et al. (2010) Osteoblast lineage cells expressing high levels of Runx2 enhance hematopoietic progenitor cell proliferation and function. J Cell Biochem 111: 284-294.

123. Nakahama K (2010) Cellular communications in bone homeostasis and repair. Cell Mol Life Sci 67: 4001-4009.

124. Williams BO, Insogna KL (2009) Where Wnts went: the exploding field of Lrp5 and Lrp6 signaling in bone. J Bone Miner Res 24: 171-178.

125. Yu Q, Quinn WJ, 3rd, Salay T, Crowley JE, Cancro MP, et al. (2008) Role of beta-catenin in B cell development and function. J Immunol 181: 3777-3783.

126. Quarto N, Behr B, Longaker MT (2010) Opposite spectrum of activity of canonical Wnt signaling in the osteogenic context of undifferentiated and differentiated

mesenchymal cells: implications for tissue engineering. Tissue Eng Part A 16: 3185-3197.

127. Takada I, Mihara M, Suzawa M, Ohtake F, Kobayashi S, et al. (2007) A histone lysine methyltransferase activated by non-canonical Wnt signalling suppresses PPAR-gamma transactivation. Nat Cell Biol 9: 1273-1285.

128. Baksh D, Tuan RS (2007) Canonical and non-canonical Wnts differentially affect the development potential of primary isolate of human bone marrow mesenchymal stem cells. J Cell Physiol 212: 817-826.

129. Brunkow ME, Gardner JC, Van Ness J, Paeper BW, Kovacevich BR, et al. (2001) Bone dysplasia sclerosteosis results from loss of the SOST gene product, a novel cystine knot-containing protein. Am J Hum Genet 68: 577-589.

130. Leupin O, Kramer I, Collette NM, Loots GG, Natt F, et al. (2007) Control of the SOST bone enhancer by PTH using MEF2 transcription factors. J Bone Miner Res 22: 1957-1967.

131. Otero DC, Rickert RC (2003) CD19 function in early and late B cell development. II. CD19 facilitates the pro-B/pre-B transition. J Immunol 171: 5921-5930.

132. Hardy RR, Carmack CE, Shinton SA, Kemp JD, Hayakawa K (1991) Resolution and characterization of pro-B and pre-pro-B cell stages in normal mouse bone marrow. J Exp Med 173: 1213-1225.

133. Shih TA, Roederer M, Nussenzweig MC (2002) Role of antigen receptor affinity in T cell-independent antibody responses in vivo. Nat Immunol 3: 399-406.

134. Moester MJ, Papapoulos SE, Lowik CW, van Bezooijen RL (2010) Sclerostin: current knowledge and future perspectives. Calcif Tissue Int 87: 99-107.

135. Semerad CL, Christopher MJ, Liu F, Short B, Simmons PJ, et al. (2005) G-CSF potently inhibits osteoblast activity and CXCL12 mRNA expression in the bone marrow. Blood 106: 3020-3027.

136. Tokoyoda K, Egawa T, Sugiyama T, Choi BI, Nagasawa T (2004) Cellular niches controlling B lymphocyte behavior within bone marrow during development. Immunity 20: 707-718.

137. Zhu J, Garrett R, Jung Y, Zhang Y, Kim N, et al. (2007) Osteoblasts support B-lymphocyte commitment and differentiation from hematopoietic stem cells. Blood 109: 3706-3712.

138. Vallespinos M, Fernandez D, Rodriguez L, Alvaro-Blanco J, Baena E, et al. (2011) B Lymphocyte commitment program is driven by the proto-oncogene c-Myc. J Immunol 186: 6726-6736.

139. de Alboran IM, Baena E, Martinez AC (2004) c-Myc-deficient B lymphocytes are resistant to spontaneous and induced cell death. Cell Death Differ 11: 61-68.

140. Mansour A, Anginot A, Mancini SJ, Schiff C, Carle GF, et al. (2011) Osteoclast activity modulates B-cell development in the bone marrow. Cell Res.

141. Miyaura C, Onoe Y, Inada M, Maki K, Ikuta K, et al. (1997) Increased B-lymphopoiesis by interleukin 7 induces bone loss in mice with intact ovarian function: similarity to estrogen deficiency. Proc Natl Acad Sci U S A 94: 9360-9365.

142. Li Y, Toraldo G, Li A, Yang X, Zhang H, et al. (2007) B cells and T cells are critical for the preservation of bone homeostasis and attainment of peak bone mass in vivo. Blood 109: 3839-3848.

143. Nie Y, Waite J, Brewer F, Sunshine MJ, Littman DR, et al. (2004) The role of CXCR4 in maintaining peripheral B cell compartments and humoral immunity. J Exp Med 200: 1145-1156.

144. Papapoulos SE (2011) Targeting sclerostin as potential treatment of osteoporosis. Ann Rheum Dis 70 Suppl 1: i119-122.

145. Chapel H, Cunningham-Rundles C (2009) Update in understanding common variable immunodeficiency disorders (CVIDs) and the management of patients with these conditions. Br J Haematol 145: 709-727.

146. Nilsson SK, Bertoncello I (1994) Age-related changes in extramedullary hematopoiesis in the spleen of normal and perturbed osteopetrotic (op/op) mice. Exp Hematol 22: 377-383.

147. Park D, Spencer JA, Koh BI, Kobayashi T, Fujisaki J, et al. (2012) Endogenous bone marrow MSCs are dynamic, fate-restricted participants in bone maintenance and regeneration. Cell Stem Cell 10: 259-272.

148. Kodama H, Yamasaki A, Nose M, Niida S, Ohgame Y, et al. (1991) Congenital osteoclast deficiency in osteopetrotic (op/op) mice is cured by injections of macrophage colony-stimulating factor. J Exp Med 173: 269-272.

149. Blin-Wakkach C, Wakkach A, Sexton PM, Rochet N, Carle GF (2004) Hematological defects in the oc/oc mouse, a model of infantile malignant osteopetrosis. Leukemia 18: 1505-1511.

150. Lymperi S, Ersek A, Ferraro F, Dazzi F, Horwood NJ (2011) Inhibition of osteoclast function reduces hematopoietic stem cell numbers in vivo. Blood 117: 1540-1549.

151. Kitajima K, Tanaka M, Zheng J, Sakai-Ogawa E, Nakano T (2003) In vitro differentiation of mouse embryonic stem cells to hematopoietic cells on an OP9 stromal cell monolayer. Methods Enzymol 365: 72-83.

152. Gao J, Yan XL, Li R, Liu Y, He W, et al. (2010) Characterization of OP9 as authentic mesenchymal stem cell line. J Genet Genomics 37: 475-482.

153. Mii Y, Taira M (2009) Secreted Frizzled-related proteins enhance the diffusion of Wnt ligands and expand their signalling range. Development 136: 4083-4088.

154. Mansour A, Anginot A, Mancini SJ, Schiff C, Carle GF, et al. (2011) Osteoclast activity modulates B-cell development in the bone marrow. Cell Res 21: 1102-1115.

155. Hsieh JC, Kodjabachian L, Rebbert ML, Rattner A, Smallwood PM, et al. (1999) A new secreted protein that binds to Wnt proteins and inhibits their activities. Nature 398: 431-436.

156. Kawano Y, Kypta R (2003) Secreted antagonists of the Wnt signalling pathway. J Cell Sci 116: 2627-2634.

157. Malinauskas T, Aricescu AR, Lu W, Siebold C, Jones EY (2011) Modular mechanism of Wnt signaling inhibition by Wnt inhibitory factor 1. Nat Struct Mol Biol 18: 886-893.

158. Vaes BL, Dechering KJ, van Someren EP, Hendriks JM, van de Ven CJ, et al. (2005) Microarray analysis reveals expression regulation of Wnt antagonists in differentiating osteoblasts. Bone 36: 803-811.

159. Glinka A, Wu W, Delius H, Monaghan AP, Blumenstock C, et al. (1998) Dickkopf-1 is a member of a new family of secreted proteins and functions in head induction. Nature 391: 357-362.

160. Niehrs C (2006) Function and biological roles of the Dickkopf family of Wnt modulators. Oncogene 25: 7469-7481.

161. Aicher A, Kollet O, Heeschen C, Liebner S, Urbich C, et al. (2008) The Wnt antagonist Dickkopf-1 mobilizes vasculogenic progenitor cells via activation of the bone marrow endosteal stem cell niche. Circ Res 103: 796-803.

162. Spencer GJ, Utting JC, Etheridge SL, Arnett TR, Genever PG (2006) Wnt signalling in osteoblasts regulates expression of the receptor activator of NFkappaB ligand and inhibits osteoclastogenesis in vitro. J Cell Sci 119: 1283-1296.

163. Broxmeyer HE (2008) Chemokines in hematopoiesis. Curr Opin Hematol 15: 49-58.